

Mitochondria and Disease:
**Mutation and expression landscape of mitochondria-associated
genes in different disease types**

Dissertation der Fakultät für Biologie der Ludwigs-Maximilians-
Universität München

zur Erlangung des Doktorgrades der
Naturwissenschaften Dr. rer. nat.

durchgeführt im
Max-Planck-Institut für Biochemie
Martinsried

vorgelegt von
Prasanna S Koti
aus Indien

München, September 2015

Erstgutachter: Prof. Dr. Barbara Conradt

Zweitgutachter: Prof. Dr. John Parsch

Tag der Einreichung: 24. 10. 2016

Tag der mündlichen Prüfung: 18. 10. 2016

Curriculum vitae

Prasanna S Koti

0091 80 23636825 (Land line phone)
prasanskoti@googlemail.com

COMPUTER SKILLS

Languages

· Perl, python, JavaScript, php, HTML, R, MySQL, Linux

Software

· FastQ toolkit, GATK software, Integrated genome viewer, Microsoft office suite

EXPERIENCE

- | | |
|----------------------------------|--|
| April 2010 -
June 2010 | Research Assistant, Max Planck Institute for Plant Breeding
Research, Germany |
| | · Analysis of biologically significant sequence motifs in <i>Colletotrichum higginsianum</i> genome |
| December
2009 - April
2010 | Member of <i>Blumeria</i> genome sequencing consortium, Max Planck
Institute for Plant Breeding Research, Germany |
| | · Computational prediction and annotation of function regions in the genome. |

EDUCATION

- | | |
|------------------------------|---|
| January 2011 -
Current | PhD (Computational Biology), Ludwig Maximilian University of Munich and Max
Planck Institute of Biochemistry, Germany |
| October 2007 -
March 2010 | Master of Science in Life Science informatics, Bonn Aachen International center
for Information technology, Bonn University, Germany |

PUBLICATIONS

- Villaveces JM, Koti P, Habermann BH. Tools for visualization and analysis of molecular networks, pathways, and -omics data. *Adv Appl Bioinform Chem.* 2015;8:11-22
- Spanu PD et al. (2010) Genome expansion and gene loss in powdery mildew fungi reveal tradeoffs in extreme parasitism. *Science* 330: 1543 - 1546.

Eidesstattliche Erklärung

Ich, Prasanna. S. Koti versichere hiermit an Eides statt, dass die vorgelegte Dissertation von mir selbständig und ohne unerlaubte Hilfe angefertigt ist.

Erklärung

Hiermit erkläre ich, dass die Dissertation nicht ganz oder in wesentlichen Teilen einer anderen Prüfungskommission vorgelegt worden ist und dass ich mich anderweitig einer Doktorprüfung ohne Erfolg **nicht** unterzogen habe.

München, den 17. 09. 2015

.....

(Prasanna. S. Koti)

ABSTRACT

Mitochondria are indispensable organelles of eukaryotic cells, takes part in the efficient generation of energy required for the cellular activities. They also converge to accomplish various functions such as intrinsic apoptotic pathway, fatty acid beta oxidation, cellular balance of reactive oxygen species (ROS), iron sulphur cluster biogenesis and so-forth which are necessary for the viability of the cell.

Ominous diseases may arise of incompetent mitochondrial function activity, for example, cardiomyopathy, optic atrophy and diabetes mellitus. Mitochondrial disorders may emerge as a result of mutations not only in the mitochondria DNA (mtDNA) but also in the nuclear DNA (nDNA) encoding proteins, which forms part of the mitochondrial proteome.

The advent of next generation sequencing (NGS) data has hugely accelerated the generation of millions of DNA sequences and opened up avenues to study diseases at a rapid pace. NGS enables transcriptome sequencing of both the normal and the disease samples realised by the RNA sequencing (RNA-seq) technology. This facilitate the measure of the gene expression in the diseases compared to their normal samples, in addition to the capture of disease specific mutations. In this thesis, workflows to extract mutation and expression data from the RNAseq samples using well developed bioinformatics tools have been achieved.

Mitochondria encompassing crucial cellular functions are fulfilled by protein coding genes encoded by both mtDNA and nDNA. In this thesis, an overall model termed as mitochondrial model (MitoModel) is developed, which at present includes 17 mitochondria specific processes with 659 genes further grouped into functional clusters. The MitoModel forms a network model with genes connected not only within a single function but also across functions. It is an interactive model with an

option to map mutation and expression data and further the MitoModel provide users several information including enrichment analysis of most affected mitochondrial function and a downloadable variants file.

The usage of MitoModel has proved the efficiency of the approach to understand the behaviour of the mitochondria from the RNA-seq data in HCT116 5/4, RPE1 5/3 12/3 and RPE1H2B 21/3 aneuploidy cell lines generated by collaborators. It also throws light on the differences in the mitochondrial metabolism and physiology in the extreme stress reactivity mice from the expression data. Finally, MitoModel was successfully used to emphasize on the representative mitochondrial genes that were consistently affected in the RNA-seq data of 16 samples of primary colorectal cancer and corresponding liver metastases samples.

CONTENTS

LIST OF TABLES.....	xv
LIST OF FIGURES.....	xxiii

1 Introduction

1.1.1	Anatomy of mitochondria.....	1
1.1.2	Mitochondrial genome.....	2
1.1.3	Mitochondria and nuclear genome interaction.....	3
1.1.4	Homoplasmy and heteroplasmy.....	3
1.1.5	Mitochondria and diseases.....	4
1.1.6	Mitochondria in cancer and aneuploidy.....	5
1.1.7	Mitochondria in major depression.....	6
1.1.8	Goals of the thesis.....	7
1.1.9	Outline of this thesis.....	8

1.2 Mitochondria and their functions

1.2.1	Mitochondria associated functions.....	11
1.2.1.1	Electron transport chain.....	12
1.2.1.2	Glycolysis.....	12
1.2.1.3	Pyruvate transfer.....	13
1.2.1.4	Formation of Acetyl CoA.....	13
1.2.1.5	Tricarboxylic acid cycle.....	13
1.2.1.6	Beta oxidation of fatty acids.....	14
1.2.1.7	ROS defence.....	14
1.2.1.8	Apoptosis.....	15
1.2.1.9	Import and sorting.....	15
1.2.1.10	Mitochondrial dynamics.....	16
1.2.1.11	Iron sulphur cluster biosynthesis.....	17
1.2.1.12	Replication and transcription.....	18

1.2.1.13	Translation.....	18
1.2.1.14	Calcium transport.....	19
1.2.1.15	Heme biosynthesis.....	19
1.2.1.16	Cardiolipin biosynthesis.....	20
1.2.1.17	Urea cycle.....	20

2 Methods and Implementation

2.1	RNA-sequencing.....	23
2.2	Illumina sequencing.....	24
2.3	Base call accuracy.....	24
2.4	Trim Galore.....	25
2.5	Alignment.....	25
2.6	Mapping quality.....	28
2.7	Picard tools.....	28
2.8	The genome analysis toolkit.....	29
2.9	SNPiR filtration.....	32
2.10	Oncotator.....	32
2.11	Mitowheel.....	32
2.12	Cufflinks package.....	32
2.13	Variant discovery workflow.....	33
2.14	Mitochondrial model.....	40

3 Results

3.1 Gene expression and mutation analysis using MitoModel in three different aneuploidy cell lines

3.1.1	Task description.....	52
3.1.2	Data analysis.....	52
3.1.3	MitoModel of the HCT116 5/4 cell line	52
	3.1.3.1 Summary for HCT116 5/4 MitoModel.....	72
3.1.4	MitoModel of the RPE1 5/3 12/3 cell line.....	72
	3.1.4.1 Summary for RPE1 5/3 12/3 MitoModel.....	90

3.1.5	MitoModel of the RPE1H2B 21/3 cell line	91
3.1.5.1	Summary for RPE1H2B 21/3 MitoModel.....	100
3.1.6	Comparison between HCT116 5/4, RPE1 5/3 12/3 and RPE1H2B 21/3 MitoModels.....	101
3.2	Analysis of expression difference between LR and HR stress reactivity mice: impact of mitochondrial function	
3.2.1	Data analysis.....	104
3.2.2	LR vs. HR MitoModel.....	104
3.3	Representative MitoModel in 16 samples of primary colorectal cancer and liver metastases	
3.3.1	Task description.....	130
3.3.2	Data analysis.....	130
3.3.3	Clustering analysis.....	130
3.3.4	Representative MitoModels.....	131
3.3.5	Characterizing representative genes.....	132
4	Discussion.....	145
5	Conclusion and future perspectives	
<hr/>		
5.1	Conclusion.....	153
5.2	Future perspective.....	154
	Appendix A Bibliography.....	157
	Appendix B Acknowledgements.....	171
	Appendix C Mitochondria associated genes, functions and their references.....	173

LIST OF TABLES

Table 1: An example of expression input file.....	51
Table 2: An example of mutation input file.....	51
Table 3: An example of MitoModel variant output file.....	50
Table 4: Up-regulated genes in the electron transport chain of HCT116 5/4 cell line.....	55
Table 5: Down-regulated genes in the electron transport chain of HCT116 5/4 cell line.....	56
Table 6: Mutated genes in the electron transport chain of the HCT116 5/4 cell line...	56
Table 7: Up-regulated genes in fatty acid beta-oxidation of HCT116 5/4 cell line.....	57
Table 8: Down-regulated genes in the fatty acid beta-oxidation of HCT116 5/4 cell line.....	57
Table 9: Up-regulated genes in the apoptosis of HCT116 5/4 cell line.....	58
Table 10: Down-regulated genes in the apoptosis of HCT116 5/4 cell line.....	58
Table 11: Mutated genes in the apoptosis of the HCT116 5/4 cell line.....	59
Table 12: Up-regulated genes in the heme biosynthesis of HCT116 5/4 cell line.....	59
Table 13: Down-regulated genes in the heme biosynthesis of HCT116 5/4 cell line...	60
Table 14: Up-regulated genes in the glycolysis of HCT116 5/4 cell line.....	60
Table 15: Down-regulated genes in the glycolysis of HCT116 5/4 cell line.....	61
Table 16: Up-regulated genes in the TCA cycle of HCT116 5/4 cell line.....	61
Table 17: Up-regulated genes in the pyruvate transfer of HCT116 5/4 cell line.....	62
Table 18: Up-regulated genes in the Fe-S cluster biosynthesis of HCT116 5/4 cell line.....	62
Table 19: Down-regulated genes in the Fe-S cluster biosynthesis of HCT116 5/4 cell line.....	62
Table 20: Up-regulated genes in the mitochondrial dynamics of the HCT116 5/4 cell line.....	63
Table 21: Down-regulated genes in the mitochondrial dynamics of the HCT116 5/4	

cell line.....	64
Table 22: Mutated genes in the mitochondrial dynamics of HCT116 5/4 cell line.....	64
Table 23: Up-regulated genes in the import and sorting of HCT116 5/4 cell line.....	64
Table 24: Down-regulated genes in the import and sorting of HCT116 5/4 cell line...	65
Table 25: Mutated genes in the import and sorting of the HCT116 5/4 cell line.....	65
Table 26: Up-regulated genes in the replication and transcription of the HCT116 5/4 cell line.....	66
Table 27: Down-regulated genes in the replication and transcription of the HCT116 5/4 cell line.....	67
Table 28: Mutated genes in the replication and transcription of the HCT116 5/4 cell line.....	67
Table 29: Up-regulated genes in the translation of HCT116 5/4 cell line.....	68
Table 30: Down-regulated genes in the translation of HCT116 5/4 cell line.....	69
Table 31: Mutated genes in the translation of HCT116 5/4 cell line.....	69
Table 32: Up-regulated genes in the calcium transport of the HCT116 5/4 cell line...	70
Table 33: Down-regulated genes in the calcium transport of the HCT116 5/4 cell line.....	70
Table 34: Down-regulated genes in the cardiolipin biosynthesis of the HCT116 5/4 cell line.....	70
Table 35: Up-regulated genes in the ROS defence of the HCT116 5/4 cell line.....	71
Table 36: Down-regulated genes in the ROS defence of the HCT116 5/4 cell line.....	71
Table 37: Up-regulated genes in the electron transport chain of RPE1 5/3 12/3 cell line.....	76
Table 38: Down-regulated genes in the electron transport chain of RPE1 5/3 12/3 cell line.....	76
Table 39: Up-regulated genes in the fatty acid beta oxidation of RPE1 5/3 12/3 cell line.....	77
Table 40: Down-regulated genes in the fatty acid beta oxidation of RPE1 5/3 12/3 cell line.....	77
Table 41: Up-regulated genes in the apoptosis of RPE1 5/3 12/3 cell line.....	78
Table 42: Down-regulated genes in the apoptosis of RPE1 5/3 12/3 cell line.....	78

Table 43: Up-regulated genes in the heme biosynthesis of RPE1 5/3 12/3 cell line.....	79
Table 44: Down-regulated genes in the heme biosynthesis of RPE1 5/3 12/3 cell line.....	79
Table 45: Up-regulated genes in the glycolysis of RPE1 5/3 12/3 cell line.....	80
Table 46: Down-regulated genes in the glycolysis of RPE1 5/3 12/3 cell line.....	80
Table 47: Up-regulated genes in the formation of Acetyl CoA function of RPE1 5/3 12/3 cell line.....	81
Table 48: Up-regulated genes in the TCA cycle of RPE1 5/3 12/3 cell line.....	81
Table 49: Down-regulated genes in the TCA cycle of RPE1 5/3 12/3 cell line.....	81
Table 50: Up-regulated genes in the Fe-S cluster biosynthesis of RPE1 5/3 12/3 cell line.....	82
Table 51: Up-regulated genes in the mitochondrial dynamics of the RPE1 5/3 12/3 cell line.....	83
Table 52: Down-regulated genes in the mitochondrial dynamics of the RPE1 5/3 12/3 cell line.....	83
Table 53: Up-regulated genes in the import and sorting of the RPE1 5/3 12/3 cell line.....	84
Table 54: Down-regulated genes in the import and sorting of the RPE1 5/3 12/3 cell line.....	84
Table 55: Mutated gene in the import and sorting of the RPE1 5/3 12/3 cell line.....	84
Table 56: Up-regulated genes in the replication and transcription of the RPE1 5/3 12/3 cell line.....	85
Table 57: Down-regulated genes in the replication and transcription of the RPE1 5/3 12/3 cell line.....	85
Table 58: Up-regulated genes in the translation of the RPE1 5/3 12/3 cell line.....	87
Table 59: Down-regulated genes in the translation of the RPE1 5/3 12/3 cell line.....	87
Table 60: Up-regulated genes in the calcium transport of the RPE1 5/3 12/3 cell line.....	87
Table 61: Down-regulated genes in the calcium transport of the RPE1 5/3 12/3 cell line.....	88

Table 62: Up-regulated genes in the cardiolipin biosynthesis of the RPE1 5/3 12/3 cell line.....	88
Table 63: Up-regulated genes in the ROS defence of the RPE1 5/3 12/3 cell line.....	89
Table 64: Down-regulated genes in the ROS defence of the RPE1 5/3 12/3 cell line....	89
Table 65: Up-regulated genes in the electron transport chain of the RPE1H2B 21/3 cell line.....	93
Table 66: Down-regulated genes in the fatty acid beta oxidation function of the RPE1H2B 21/3 cell line.....	94
Table 67: Up-regulated genes in the apoptosis function of the RPE1H2B 21/3 cell line.....	94
Table 68: Down-regulated genes in the glycolysis function of the RPE1H2B 21/3 cell line.....	95
Table 69: Up-regulated gene in the Fe-S cluster biosynthesis function of the RPE1H2B 21/3 cell line.....	95
Table 70: Down-regulated gene in the Fe-S cluster biosynthesis function of the RPE1H2B 21/3 cell line.....	96
Table 71: Up-regulated genes in the mitochondrial dynamics of the RPE1H2B 21/3 cell line.....	96
Table 72: Down-regulated genes in the mitochondrial dynamics of the RPE1H2B 21/3 cell line.....	97
Table 73: Down-regulated genes in the import and sorting function of the RPE1H2B 21/3 cell line.....	97
Table 74: Up-regulated genes in the replication and transcription function of the RPE1H2B 21/3 cell line.....	98
Table 75: Down-regulated genes in the replication and transcription of the RPE1H2B 21/3 cell line.....	98
Table 76: Up-regulated genes in the translation of the RPE1H2B 21/3 cell line.....	99
Table 77: Down-regulated genes in the translation of the RPE1H2B 21/3 cell line.....	99
Table 78: Up-regulated genes in the ROS defence function of the RPE1H2B 21/3 cell line.....	99
Table 79: Down-regulated genes in the ROS defence function of the	

RPE1H2B 21/3 cell line.....	100
Table 80: The top 5 up-regulated genes of the TCA cycle, in the LR vs. HR Comparison.....	108
Table 81: The top 5 down-regulated genes of the TCA cycle, in the LR vs. HR Comparison.....	108
Table 82: The top up-regulated genes of the cardiolipin biosynthesis, in the LR vs. HR comparison.....	109
Table 83: The top down-regulated genes of the cardiolipin biosynthesis, in the LR vs. HR comparison.....	109
Table 84: The top 5 up-regulated genes of the ETC, in the LR vs. HR comparison.....	110
Table 85: The top 5 down-regulated genes of the ETC, in the LR vs. HR comparison....	111
Table 86: The top 5 up-regulated genes of the mitochondrial dynamics, in the LR vs. HR comparison.....	112
Table 87: The top 5 down-regulated genes of the mitochondrial dynamics, in the LR vs. HR comparison.....	112
Table 88: The top 5 up-regulated genes of the glycolysis, in the LR vs. HR comparison.....	113
Table 89: The top 5 down-regulated genes of the glycolysis, in the LR vs. HR comparison.....	113
Table 90: The top 5 up-regulated genes of the ROS defence, in the LR vs. HR comparison.....	115
Table 91: The top 5 down-regulated genes of the ROS defense, in the LR vs. HR comparison.....	115
Table 92: The top up-regulated genes of the heme biosynthesis, in the LR vs. HR comparison.....	116
Table 93: The top down-regulated genes of the heme biosynthesis, in the LR vs. HR comparison.....	116
Table 94: The Top 5 up-regulated genes of the apoptosis, in the LR vs. HR comparison.....	117
Table 95: The top 5 down-regulated genes of the apoptosis, in the LR vs. HR comparison.....	117

Table 96: The top down-regulated gene of the pyruvate transfer, in the LR vs. HR comparison.....	118
Table 97: The top up-regulated genes of the import and sorting, in the LR vs. HR comparison.....	119
Table 98: The top 5 down-regulated genes of the import and sorting, in the LR vs. HR comparison.....	119
Table 99: Top 5 up-regulated genes of the Fe-S cluster biosynthesis, in the LR vs. HR comparison.....	120
Table 100: The top 5 down-regulated genes of the Fe-S cluster biosynthesis, in the LR vs. HR comparison.....	121
Table 101: The top 5 up-regulated genes of the replication and transcription, in the LR vs. HR comparison.....	122
Table 102: The top 5 down-regulated genes of the replication and transcription, in the LR vs. HR comparison.....	122
Table 103: The up-regulated gene of the 'formation of acetyl CoA', in the LR vs. HR comparison.....	123
Table 104: The down-regulated gene of the 'formation of acetyl CoA', in the LR vs. HR comparison.....	123
Table 105: The top 5 up-regulated genes of the translation, in the LR vs. HR comparison.....	124
Table 106: Top 5 down-regulated genes of the translation, in the LR vs. HR comparison.....	124
Table 107: The top 5 up-regulated genes of the beta-oxidation of fatty acids, in the LR vs. HR comparison.....	125
Table 108: The top 5 down-regulated genes of the beta-oxidation of fatty acids, in the LR vs. HR comparison.....	125
Table 109: The top up-regulated genes of the Calcium transport, in the LR vs. HR comparison.....	126
Table 110: The top down-regulated gene of the Calcium transport, in the LR vs. HR comparison.....	127
Table 111: The top down-regulated gene of the Urea cycle, in the	

LR vs. HR comparison.....	127
Table 112: Differentially expressed, representative genes observed in both primary CRC and liver metastases of all the clusters in the electron transport chain function.....	132
Table 113: Representative genes with mutation sites observed in both the primary CRC and the liver metastases of all the clusters in the electron transport chain function.....	133
Table 114: Differentially expressed, representative genes observed in both primary CRC and liver metastases of all the clusters in the beta oxidation of fatty acids function.....	135
Table 115: Representative genes with mutation sites observed in both the primary CRC and the liver metastases of all the clusters in the beta oxidation of fatty acids function.....	135
Table 116: Differentially expressed, representative genes observed in both primary CRC and liver metastases of all the clusters in the glycolytic function.....	137
Table 117: Representative genes with mutation sites observed in both the primary CRC and the liver metastases of all the clusters in the glycolysis function.....	137
Table 118: Differentially expressed, representative genes observed in both primary CRC and liver metastases of all the clusters in the Urea cycle function.....	138
Table 119: Representative genes with mutation sites observed in both the primary CRC and the liver metastases of all the clusters in the Urea cycle function.....	138
Table 120: Differentially expressed, representative genes observed in both primary CRC and liver metastases of all the clusters in the mitochondrial dynamics function.....	139
Table 121: Representative genes with mutation sites observed in both the primary CRC and the liver metastases of all the clusters in the mitochondrial dynamics function.....	140
Table 122: Differentially expressed, representative genes observed in both	

primary CRC and liver metastases of all the clusters in the apoptosis function.....140

Table 123: Representative genes with mutation sites observed in both the primary CRC and the liver metastases of all the clusters in the apoptosis function.....141

Table 124: Differentially expressed, representative genes observed in both primary CRC and liver metastases of all the clusters in the replication and transcription function.....142

Table 125: Representative genes with mutation sites observed in both the primary CRC and the liver metastases of all the clusters in the replication and transcription function.....142

Table 126: Differentially expressed, representative genes observed in both primary CRC and liver metastases of all the clusters in the ROS defence function.....143

Table 127: Representative genes with mutation sites observed in both the primary CRC and the liver metastases of all the clusters in the ROS defence function.....143

LIST OF FIGURES

Figure 1: Structure of mitochondria.....	2
Figure 2: The human mitochondrial genome.....	3
Figure 3: Variant discovery workflow.....	34
Figure 4: Overview of variants analysis workflow depicting the levels of data handling (input, manipulation and output).....	35
Figure 5: Visual representation of MitoModel with functions as clusters annotated with their names.....	42
Figure 6: A simple depiction of the interactive ability brandished by the MitoModel.....	44
Figure 7: An instance of Percentage (%) affected functions observed on the MitoModel.....	45
Figure 8: Graphical visualization of overall expression changes in MitoModel.....	46
Figure 9: A further graphical representaiton of the MitoModel's overall expression pattern.....	49
Figure 10: An overview of the interaction architecture between user and MitoModel server.....	47
Figure 11: Visual display of the HCT 116 5/4 MitoModel.....	53
Figure 12: Percentage (%) of affected functions observed on the HCT116 5/4 MitoModel.....	54
Figure 13: Number of affected genes observed on all the functions of HCT116 5/4 MitoModel.....	72
Figure 14: Visual display of the RPE1 5/3 12/3 MitoModel.....	73
Figure 15: Percentage (%) of affected functions observed on the RPE1 5/3 12/3 MitoModel.....	74
Figure 16: Number of affected genes observed on all the functions of RPE1H2B 21/3 MitoModel.....	90
Figure 17: A visual representation of the RPE1H2B 21/3 MitoModel.....	91

Figure 18: Percentage (%) of affected functions observed on the RPE1H2B 21/3 MitoModel.....	92
Figure 19: Number of affected genes observed on all the functions of RPE1H2B 21/3MitoModel.....	101
Figure 20: Comparison of HCT116 5/4, RPE1 5/3 12/3 and RPE1H2B 21/3 MitoModels.....	102
Figure 21: Visual representation of LR vs. HR mouse MitoModel with functions as clusters annotated with their names	105
Figure 22: Percentage (%) of affected functions observed on the mouse MitoModel...	106
Figure 23: Graphical display of model parameters, two horizontal lines describing log2fold change cutoff values (up: 1.50 and down -1.50) and a vertical line describing p-value cutoff (0.05).....	107
Figure 24: Dendrogram showing 4 distinct clusters derived from 16 primary CRC samples and liver metastases samples.....	131

CHAPTER 1

Introduction

Mitochondria are ubiquitous organelles present in eukaryotic cells with the major function of energy production in the form of ATP through oxidative phosphorylation. Acquired several billion years ago by eubacterial invasion through symbiosis, they have immensely impacted the metabolism and homeostasis of eukaryotes [Dyall et al., 2004].

1.1.1 ANATOMY OF MITOCHONDRIA:

Anatomically mitochondria are enclosed by two membranes designated as outer and inner mitochondrial membranes, which are separated by the so-called intermembrane space (Figure 1). Both the membranes have specific functions. The inner membrane houses the complete electron transport chain and ATP synthase complex for the generation of energy. The outer membrane accommodates channels and multi-protein translocase complexes which aid the import of molecules and proteins into mitochondria, respectively. In the living cells, mitochondrial shape varies and range from punctuate structures to tubular networks [Anesti & Scorrano, 2006].

The inner membrane forms several folds called cristae, which enclose the main mitochondrial area, which is referred to as the mitochondrial matrix. This matrix contains the mitochondrial DNA (mtDNA) and enzymes that take part in many critical functions of the organelle (see for instance:

<http://www.ncbi.nlm.nih.gov/books/NBK9896/> , accessed July 28, 2015).

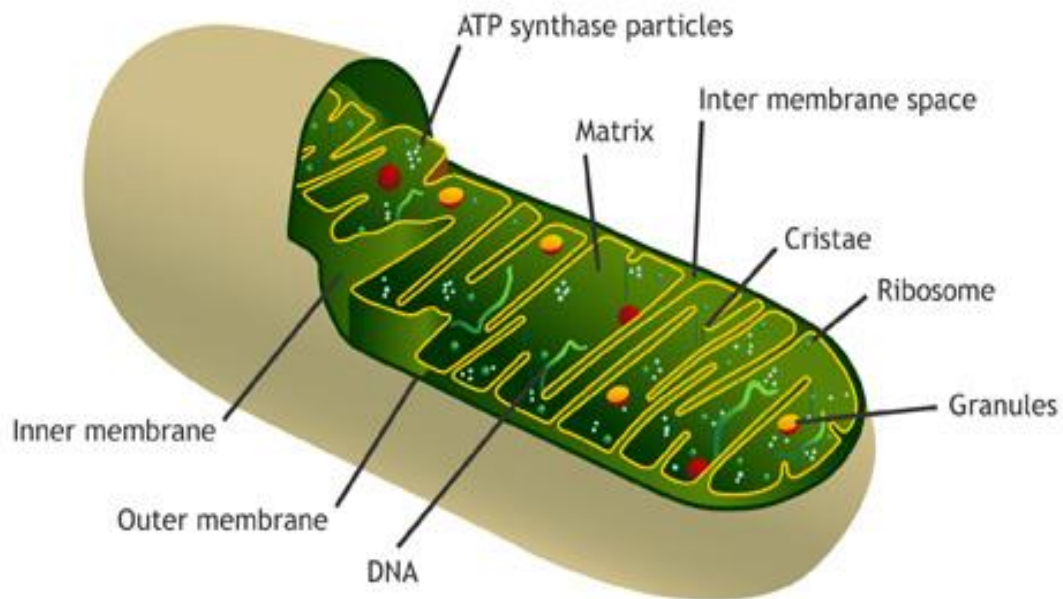


Figure 1: Structure of mitochondria. Figure taken from:

[http://biotechlearn.org.nz/themes/barcoding life/images/diagram of a mitochondrion](http://biotechlearn.org.nz/themes/barcoding%20life/images/diagram%20of%20a%20mitochondrion)
accessed July 28, 2015

1.1.2 MITOCHONDRIAL GENOME:

Mitochondria have their own genome, which is composed of a single, circular DNA molecule. The human mitochondrial genome consists of 16569 bases. It contains 37 genes encoding for 13 polypeptides mostly involved in oxidative phosphorylation, 22 tRNAs and 2 rRNAs required for mitochondrial protein translation. It also contains two non-coding regions necessary for replication start, one for the heavy and one for light strand depicted as OH and OL (Figure 2). Each mitochondria contains several copies of its DNA enclosed into specialized structures called nucleoids, which form the vehicles of transmission and inheritance [Taylor & Turnbull, 2005].

Homoplasmy is referred to the presence of identical copies of the mitochondrial genome in a cell, whereas heteroplasmy refers to the habitation of two or more mitochondrial genotypes in a single eukaryotic cell.

These terms are frequently used to define the mtDNA mutations leading to diseases. For instance, a homoplasmic mutation is present in all the copies of the genome and heteroplasmic mutation is present in only few copies of the mitochondrial genome. In case of heteroplasmic mutations, there is a minimum threshold level for the disease to develop and manifest clinical symptoms [Rossignol et al., 2003].

The mtDNA is inherited maternally and transmission of mtDNA mutations also occur maternally. Homoplasmic mtDNA mutations are transmitted to all the offsprings, for example patients with LEBER HEREDITARY OPTIC NEUROPATHY (LHON) have homoplasmic mtDNA mutations and all the offsprings inherit the mutation. Even though all the offsprings inherit the mutation, only few develop the disease [Man et al., 2003], which points out that not only mtDNA factors but also nuclear genetic factors are important for the development of this disease.

Transmission of a heteroplasmic mutation is more complicated due to the fact that there is a genetic bottleneck during development and the amount of mutated mtDNA transmitted to offspring is variable [Brown et al., 2001]. Hence both, nuclear genetic [Battersby et al., 2003] and environmental factors affect the development of a disease caused by a heteroplasmic, mitochondrial mutation. [Taylor & Turnbull, 2005].

1.1.5 MITOCHONDRIA AND DISEASES:

Mitochondrial diseases are effectively disorders that result from the dysfunction of the electron transport chain. Furthermore, there are other crucial functions converging in mitochondria, such as the apoptotic pathway, fatty acid beta

oxidation, cellular balance of reactive oxygen species (ROS) and iron sulphur cluster biogenesis, which could directly or indirectly affect the efficient operational activity of mitochondria.

Mitochondrial disorders may arise from mutations not only in the mtDNA but also in the nuclear DNA encoding mitochondrial proteins. For example, individuals with external ophthalmoplegia display a diverse variation pattern: some patients have large deletions in mtDNA, others have a single nucleotide variation, and still others have heterozygous variants of nuclear encoded, mitochondrial genes [Chinnery, 2014].

Some of the most common disorders associated either with the mtDNA encoded genes or nuclear encoded mitochondrial genes include ptosis, external ophthalmoplegia, proximal myopathy and exercise intolerance, cardiomyopathy, sensorineural deafness, optic atrophy, pigmentary retinopathy, and diabetes mellitus (see: <http://www.ncbi.nlm.nih.gov/books/NBK1224/>, accessed on 28 July 2015).

1.1.6 MITOCHONDRIA IN CANCER AND ANEUPLOIDY:

Deriving energy by cells, from glycolysis rather than a highly efficient oxidative phosphorylation was termed 'Warburg effect' [Zheng, 2012]. This effect was formulated by the observation from Otto Warburg that the tumour cells yield more lactate in the presence of oxygen, which he termed "aerobic glycolysis" resulting from impairment of the oxidative phosphorylation machinery in mitochondria. However, several investigations found that defects of mitochondrial OXPHOS are not common in spontaneous tumors and is intact in most cancers [Zheng, 2012].

mtDNA mutations have been reported in a variety of cancers, including renal adenocarcinoma, colon cancer cells, head and neck tumours, astrocytic tumours, thyroid tumours, breast tumours, ovarian tumours, prostate and bladder cancer, neuroblastomas and oncocytomas [Wallace, 2012]. These mutations belong to two classes: mutations that assist the neoplastic transformation, and those that aid the cancer cell adaptation to the changing bioenergetic environments. Next to mutations in the mitochondrial genome, many mutations in the nuclear encoded mitochondrial genes have been observed in specific cancers [Wallace, 2012].

Mitochondrial ROS are not only signalling molecules, but also potent mutagens and an increase in the ROS production along with dysfunctional apoptosis, could lead to neoplastic transformation [Wallace, 2012].

Mitochondrial activity and misregulations has been observed in the Down's syndrome (DS) or trisomy 21. It is one of the most common aneuploidies resulting in intellectual disability disorder caused by three copies of chromosome 21. Increased oxidative stress due to decreased regulation of several mitochondrial components have been observed in the DS [Coskun & Busciglio, 2012]. It was also suggested that mitochondrial biogenesis was up-regulated in trisomy 21: mitochondrial superoxide production and oxidative stress were observed to be 3 times higher in DS fibroblasts [Coskun & Busciglio, 2012].

1.1.7 MITOCHONDRIA IN MAJOR DEPRESSION:

Misregulations associated with mitochondrial functions in major depression (MD) are differences in the translation, decreased gene expression of mtDNA encoded genes and nuclear encoded genes, decreased complex I activity and low ATP production rates [Gardner & Boles, 2011].

Patients suffering from major depression have been reported to have dysregulations in the hypothalamus-pituitary-adrenocortical (HPA) axis and deficits in cognitive processes caused by hippocampal and prefrontal cortex (PFC) malfunction. Three mouse lines were selectively bred for high (HR), intermediate (IR), and low (LR) stress reactivity, determined by the corticosterone response to a psychological stressor, probing the behavioural and functional consequences of increased vs. decreased HPA axis reactivity on the hippocampus and PFC. The hippocampal proteomic analysis identified several proteins differentially expressed in HR and LR mice, those including proteins involved in the energy metabolism pathway [Knapman et al., 2012].

1.1.8 GOALS OF THE THESIS:

There are a large scale availability of sequence data for several diseases from various data sources, which can be utilized to generate gene expression and mutation data. The main aim of this study is to understand the mitochondrial contribution in diseases. Thus the work is aimed at the development and deployment of a mitochondrial model (MitoModel) that would operate in an inclusive manner with both mtDNA encoded and nuclear encoded mitochondrial genes. The mapping of the gene expression and mutation data on to the MitoModel will be an efficient approach to disclose the metabolic and physiological variations carried by mitochondria in a disease state.

GOAL-1: Functional classification of mitochondrial genes and brief annotation of gene function in the respective mitochondrial function [see Chapter 1.2].

GOAL-2: Development and deployment of a user-friendly, interactive MitoModel [see Chapter 2].

GOAL-3: Development of workflows to analyse RNA-sequencing data, extracting mutational and gene expression data in different disease types.

GOAL-4: Utilising the MitoModel to understand three different disease phenotypes:

- a. Gene expression and mutation analysis using the MitoModel in three different aneuploidy cell lines: the HCT 116 cell line tetrasomic for chromosome 5 (HCT116 5/4), the RPE1 cell line trisomic for chromosome 5 and chromosome 12 (RPE1 5/3 12/3) and finally, the RPE1H2B cell line trisomic for chromosome 21 (RPE1H2B 21/3) [see Chapter 3.1].
- b. Using the MitoModel to understand the expression difference between the HR and LR stress reactivity mice to elucidate potential malfunctions of mitochondria [see chapter 3.2].
- c. Retrieval of representative mitochondrial genes consistently afflicted in the MitoModel, in 16 samples of colorectal cancer and corresponding liver metastasis [see chapter 3.3].

1.1.9 OUTLINE OF THIS THESIS:

Chapter 1.2 provides a brief introduction to the methodology followed by the collection of mitochondria-associated genes and their functional classification.

Chapter 2 describes the methods utilized for the development of the analysis pipeline to deduce mutation and expression data; it also gives information about the construction and deployment of the MitoModel.

Chapter 3.1 discusses the application of expression and mutation data on the MitoModel for the three aneuploidy cell lines to analyse a potential mitochondrial involvement.

Chapter 3.2 describes the employment of MitoModel on the two extreme stress reactivity (LR vs. HR) mice to elucidate the contrasting behaviour with respect to mitochondrial metabolism and physiology.

Chapter 3.3 provides details on the application of MitoModel and extraction of the most representative MitoModel genes in 16 colorectal cancer samples and its corresponding liver metastases

Chapter 4 provides conclusions and outlook onto future perspectives of this work.

CHAPTER 1.2

Mitochondria and their functions

Mitochondria are the power houses of the cell, efficiently producing ATP for cellular functions and activities. In addition, they are involved in diverse functions such as beta oxidation of fatty acids, apoptosis, biosynthesis of heme, FE-S cluster biosynthesis and calcium signalling. The human mitochondrial genome encodes only 13 polypeptides; the remaining 99% of mitochondrial proteins are synthesized at cytosolic ribosomes and then imported into mitochondria. Efforts to compile the mitochondrial proteome have been done and Pagliarini et al in 2008 came up with MitoCarta, a list of nearly 1100 genes coding for mouse mitochondrial genome [Pagliarini et al., 2008].

A seemingly quarter proportion of the mouse mitochondrial proteome have no known biological functions [Meisinger et al., 2008]. In this chapter, an approach is taken to organize mitochondria associated genes, including all mtDNA- and nuclear encoded mitochondrial genes into groups based on their function. This is accomplished by a comprehensive literature survey, specifically pinpointing the role of a gene in mitochondria-associated functions.

1.2.1 MITOCHONDRIA ASSOCIATED FUNCTIONS:

In this section, the approach was to bring all mitochondria associated genes together, specifically focussing on the functions that are well defined through decades of experimental research. These functions included until now are briefly defined below and the genes with their roles and their references are catalogued in the Appendix C.

1.2.1.1 ELECTRON TRANSPORT CHAIN:

Situated in the inner mitochondrial membrane, the electron transport chain consists of a series of enzyme complexes reducing oxygen to water resulting in protons (H⁺) being pumped across the inner mitochondrial membrane from the matrix. This gives rise to an electrochemical proton gradient across the inner membrane which is later utilized by the ATP synthase complex to synthesize ATP from ADP and inorganic phosphate [Schaffer & Suleiman, 2010].

The gene information of all the complexes involved and the gene symbols were downloaded from the Hugo gene nomenclature committee (HGNC) under the gene group “Mitochondrial respiratory chain complexes” (available at: <http://www.genenames.org/cgi-bin/genefamilies/set/639> , accessed August 4, 2015). Respiratory chain assembly factors were also downloaded from the HGNC under the gene group “Mitochondrial respiratory chain complex assembly factors” (available at: <http://www.genenames.org/cgi-bin/genefamilies/set/645> , accessed August 4, 2015). There are a total of 131 genes included in the electron transport chain function (1 until 131 in Appendix C).

1.2.1.2 GLYCOLYSIS:

All cells crave for energy not only for their homeostasis but also for growth and division. The major source of cellular energy is glucose, which is assimilated by its breakdown via glycolysis to pyruvate. The pyruvate then enters mitochondria where it is further broken down by the tricarboxylic acid cycle (TCA) and oxidative phosphorylation to produce large amounts of ATP.

Glycolysis is capable of producing ATP but to a much lesser extent as compared to oxidative phosphorylation in the mitochondria. Glycolytic ATP generation for a molecule of glucose results in only 2 ATP molecules compared to 36 ATP molecules generated by oxidative phosphorylation. Even though the energy generation

efficiency is low, the pace of energy production is faster [Lunt & Vander heiden, 2011].

Glycolysis in its entirety takes place in the cytoplasm of the cell. Inclusion of the genes taking part in this process is deliberate to take into account changed mitochondrial functions in a disease state, which depend primarily on the glycolytic fuel. Furthermore, glycolysis is tightly linked to the TCA cycle. There are in total 31 genes catalogued in this function (132 until 163 in Appendix C).

1.2.1.3 PYRUVATE TRANSFER:

Pyruvate is formed by the breakdown of glucose in the glycolytic pathway. It is further taken up as a major substrate by the TCA cycle in mitochondria. The process of transferring pyruvate is yielded by the formation of the complex between two proteins Mpc1 and Mpc2 (BRP44 and BRP44L in humans) in the inner mitochondrial membrane [Bricker et al., 2012]. Only two genes were catalogued for this function (164 until 165 in Appendix C).

1.2.1.4 FORMATION OF ACETYL COA:

Irreversible conversion of pyruvate to acetyl CoA is performed before it is taken up by the TCA cycle. At this point the carbon atoms from the glycolysis are either transformed into energy or further stored as lipids. The oxidative decarboxylation of pyruvate to acetyl CoA is performed by the pyruvate dehydrogenase complex, which is a multi enzyme complex in the mitochondrial matrix (available at:

<http://www.ncbi.nlm.nih.gov/books/NBK22347/>, accessed on August 5, 2015).

There were 5 genes catalogued in this section (166 until 170 in Appendix C).

1.2.1.5 TRICARBOXYLIC ACID (TCA) CYCLE:

Tricarboxylic acid (TCA) cycle also known as Krebs cycle or citric acid cycle takes place inside mitochondria. The major function of the TCA cycle is reaping high

energy electrons from acetyl CoA. The cycle includes a series of oxidation reduction reactions giving rise to two molecules of CO₂, one molecule of GTP and high energy electrons in the form of NADH and FADH₂(available at:

<http://www.ncbi.nlm.nih.gov/books/NBK21163/>, accessed on August 6, 2015).

There were 18 genes catalogued in this function (171 until 189 in Appendix C).

1.2.1.6 BETA OXIDATION OF FATTY ACIDS:

Fatty acid metabolism is one of the major metabolic functions that play an important role in the energy homeostasis of an organism. Though peroxisomes harbors a machinery for fatty acid metabolism, it is the mitochondrial beta oxidation of fatty acids, which is the primary pathway in the degradation of the fatty acids. Defects in fatty acid metabolism have harmful consequences that include hypoglycaemia, hypertrophic cardiomyopathy, myopathy and rhabdomyolysis [Houten & Wanders, 2010]. There are 53 genes catalogued in this function (190 until 243 in Appendix C).

1.2.1.7 ROS DEFENCE:

Efficient energy manufacturing is conducted by the mitochondrial electron transport chain. Misregulations in transport activity of electrons from one to another complex may lead to direct interaction of the electrons with the O₂, leading to the generation of superoxide, a free radical. These reactive oxygen species (ROS) can act under normal conditions as signalling molecules. In pathophysiological conditions, they contribute to critical disease phenotypes including cancer.

The antioxidant defence machinery inside mitochondria as well as the cytoplasm can target ROS molecules and limit their oxidative damage capacity. A failure in controlling ROS by antioxidant enzymes or excessive ROS generation can significantly damage lipids, proteins and DNA and eventually disrupting cellular

functions [Sabharwal & Schumacker, 2014]. There were 23 genes catalogued in this function (244 until 267 in Appendix C).

1.2.1.8 APOPTOSIS:

Apoptosis is a well-orchestrated set of cellular processes that will lead to the death of the cell. It is as important as cell division and development due of the fact that it contributes to proper cellular homeostasis. In vertebrate cells, there are two apoptotic pathways, the extrinsic and the intrinsic pathway. Both converge at the point of activating the death caspases.

Mitochondria can activate the intrinsic pathway through the inception of mitochondrial outer membrane permeabilization. This leads to the release of Cytochrome C from the inter membrane space further activating caspases and in turn apoptosis [Tait & Green, 2010]. There were 35 genes catalogued in this function (268 until 303 in Appendix C).

1.2.1.9 IMPORT AND SORTING:

The endosymbiotic theory confers that mitochondria lost most of its genetic material to the nuclear genome. As a result the nuclear genome encodes almost 99% of the mitochondrial proteins that were transferred from the endosymbiont during eukaryotic evolution [Dolezal et al., 2006]. Mitochondria with its own replication, transcription and translation machinery encodes only 1% of the mitochondrial proteins which forms a part of the respiratory chain complexes [Schmidt et al., 2010].

Mitochondria not only possess a central role in energy conversion, but also have crucial roles in multiple metabolic and signalling pathways. A well-established protein import machinery is necessary and is present in all eukaryotic cells, including the last common ancestor to all eukaryotes [Dolezal et al., 2006].

Proteins entering mitochondria through the import machinery contain special targeting signals that are recognized by mitochondrial receptors. Depending on their signals and import route, they are transported to different mitochondrial sub compartments. There are several types of targeting signals. The best known signal is the N-terminal mitochondrial targeting peptide, which is cleaved off after mitochondrial import. This signal targets proteins to the mitochondrial matrix. Several other internal targeting signals exist. Internal signals remain within the mature protein [Schmidt et al., 2010, Dolezal et al., 2006]. There were 32 genes catalogued in this function (304 until 336 in Appendix C).

1.2.1.10 MITOCHONDRIAL DYNAMICS:

In eukaryotic cells, mitochondria do not form a static organelle. They are rather highly dynamic and constantly change via fusion with other mitochondria or fission, dividing to equip cells with new mitochondria. Mitochondria thus form a highly interconnected network in the cell [Palmer et al., 2011]. The viability of a cell is highly dependent on the proper functioning of this network and the regulation of the mitochondrial network depends on proper coordination between fusion and fission events [Hales, 2010].

Fusion or joining of two mitochondria forms the fundamental process of the mitochondrial dynamics [Ranieri et al., 2013]. The mechanism is essential to maintain the organelle population in the cell homogeneously [Palmer et al., 2011]. It also provides an opportunity to exchange the mitochondrial contents between the fused mitochondria, and aides damaged and aged mitochondria, prolonging their survivability [Ranieri et al., 2013].

Fission or division of mitochondria in a cell is essential for many reasons: it is necessary to maintain sufficiently high numbers of mitochondria so that a full

complement of mitochondria are inherited by daughter cells during cell division; it is also required for segregating old and damaged mitochondria through mitophagy. Finally, fission is also required for the remodelling and rearrangement of the mitochondrial network [Palmer et al., 2011, Hales, 2010 and Ranieri et al., 2013].

Mitophagy is the autophagic clearance of the mitochondria and it is tightly linked to both, fusion and fission events. The selection of impaired mitochondria is established based on their membrane potential and the ones with reduced membrane potential are selected, enclosed in autophagosomes and subsequently broken down by lysosomes [Thomas & Gustafsson, 2013].

Mitochondrial movement plays an important role in reaching the mitochondria in highly polarized cells such as neurons. Impaired fission and fusion dynamics have been suggested to reduce mitochondrial motility, though the relationship is yet to be established [Chen & Chan, 2009]. There were 40 genes catalogued in this function (583 until 623 in Appendix C).

1.2.1.11 Iron Sulphur (FE-S) CLUSTER BIOSYNTHESIS:

Fe-S cluster proteins are important cofactors involved in crucial cellular activities like electron transfer reactions, catalytic and regulatory processes. They serve as the main donors of sulphur during the biosynthesis of lipoic acid and biotin. There are several forms of Fe-S clusters, the simplest form being [2Fe-2S]; [4Fe-4S] and [3Fe-4S] are more complex clusters with an additional heavy metal ion.

The pathway for the synthesis for Fe-S clusters initiates in the mitochondria with a complex called the mitochondrial iron sulphur cluster (ISC) assembly machinery. The core of this machinery is not only required for the biosynthesis of Fe-S proteins in mitochondria but also for the maturation of the same proteins in the cytoplasm by the cytosolic iron-sulphur protein assembly (CIA) machinery. Defects in Fe-S

cluster biogenesis can severely affect other cellular functions like the electron transport chain, the TCA cycle and other cofactor biosynthesis processes including heme biosynthesis [Rouault & Tong, 2005] & [Lill, 2009]. There were 25 genes catalogued in this function (337 until 362 in Appendix C).

1.2.1.12 REPLICATION AND TRANSCRIPTION:

The mitochondrial genome only encodes a few polypeptides and RNA molecules required for mitochondrial translation processes. The genome itself is a double stranded circular molecule. Mitochondrial genes are devoid of introns. It also consist of non-coding regions on both the heavy and light strands, which are important blocks in the genome and contain essential elements for the transcription and replication.

Transcription from the mitochondrial genome gives rise to polycistronic precursor RNAs later processed to yield mRNA, rRNA and tRNA molecules. The replication process and its regulation in mitochondria are complex and efforts are ongoing to identify enzymatic activities during the replication process. There are also intense debates about the models of mitochondrial replication. Currently there are two documented models. In the strand-asymmetric model, the transcription of the light strand promoter provides primers for the heavy strand replication and once the leading strand replication has reached two thirds of the genome, the light strand replication is initiated in the opposite direction resulting in new mtDNA molecules of both strands. In the symmetric replication model, both the leading and the lagging strand replicates symmetrically from multiple replication forks in the genome [Falkenberg et al., 2007]. There are 73 genes catalogued in this function (363 until 435 in Appendix C).

1.2.1.13 TRANSLATION:

Mitochondria contain their own translation machinery. The human mitochondrial genome itself encodes the 22 tRNAs and 2 mitochondrial rRNAs required for translation. For an efficient translation process to take place, the mtDNA has to be transcribed and a sizable number of nuclear encoded translational regulators must be imported into the mitochondria.

The mitochondrial translation machinery includes the mtDNA encoded tRNAs and rRNAs as well as nuclear encoded initiation, elongation and termination factors, mitochondrial ribosomal proteins, aminoacyl-tRNA synthetases and methionyl-tRNA transformylase. The translation process includes initiation, elongation and termination followed by quality control and protein insertion into the inner mitochondrial membrane [Smits et al., 2010]. There are 146 genes catalogued in this function (436 until 582 in Appendix C).

1.2.1.14 CALCIUM TRANSPORT:

Calcium signalling is a process which coordinates several extracellular stimuli and triggers several important functions within a cell. Cells respond differentially to the increase or decrease of calcium concentration. It has been shown that the membrane potential difference generated within the mitochondria acts as a major driving force for calcium accumulation in mitochondria. The mitochondria are also in close proximity of Endoplasmic reticulum (ER) and the sarcoplasmic reticulum, which serves as the important intracellular calcium stores.

Calcium in mitochondria regulates several crucial cellular functions. Calcium inside mitochondria regulates the ATP production by oxidative phosphorylation, cell death pathways, intrinsic apoptosis and autophagy [Rizzuto et al., 2012]. There were 15 genes catalogued in this function (624 until 639 in Appendix C).

1.2.1.15 HEME BIOSYNTHESIS:

Heme is a non-protein chemical compound, which becomes part of a protein by binding to it. For instance, it is a cofactor of crucial proteins such as haemoglobin, myoglobin and cytochrome proteins. Heme consists of central ferrous ion with four nitrogen atoms binding to it in porphyrin compounds, such as hemoproteins.

Hemeproteins play a central role in the many cellular activities such as electron transport, apoptosis, detoxification, protection against oxygen radicals, nitrogen monoxide synthesis and oxygen transport [Dailey, 1997]. There are 8 genes catalogued in this function (640 until 648 in Appendix C).

1.2.1.16 CARDIOLIPIN BIOSYNTHESIS:

Phospholipids form the basic component of the lipid bilayer that surrounds cells as well as organelles present inside cells. Cardiolipin is a phospholipid, which is almost exclusively present in the mitochondrial inner membrane [Kiebish et al., 2008]. The uniqueness of the cardiolipin is its structure, which is formed by diphosphatidylglycerol together with four acyl chains giving it its dimeric nature. This dimer in turn gives rise to a highly specific conical structure favouring the hexagonal H_{II} phase of the membrane and is implicated in the membrane fusion [Cullis et al., 1986].

By adopting the hexagonal H_{II} phase, cardiolipin in mitochondria can form contact sites between the inner and outer mitochondrial membrane [Ardail et al., 1990]. There are 5 genes catalogued in this function (649 until 653 in Appendix C).

1.2.1.17 UREA CYCLE:

Ammonium ions are formed during the breakdown of amino acids and are used for the biosynthesis of nitrogen compounds. The excess free NH_4^+ ions is however toxic and is thus quickly converted into the more tolerable form called urea. In this form, it can then be secreted. The synthesis of urea is conducted through the urea cycle

and any defects in this cycle will result in the build-up of NH_4^+ in the blood in humans (available at: <http://www.ncbi.nlm.nih.gov/books/NBK22450/> , accessed on August 6, 2015). There are 6 genes catalogued in this function (654 until 659 in Appendix C).

CHAPTER 2

Methods And Implementation

Sequencing is a technique to capture the whole array of nucleotides present in a DNA or RNA molecule. One of the major achievement of the sequencing technology is the human genome sequencing project, concluded in 2003 [Grada & Weinbrecht, 2013]. The human genome project was realized by the first generation sequencing technology, dominated by Sanger sequencing [Sanger et al., 1977].

With the availability of the human genome, the demand for faster and much cheaper alternatives lead to the development of second or next generation sequencing (NGS) technology. The major advancements in NGS compared to its predecessor are the higher pace and the lower cost of sequencing. There are a number of NGS platforms which deliver low cost, high throughput data such as Illumina, Roche 454, Ion torrent and SOLiD sequencing [Grada & Weinbrecht, 2013]. In this thesis, the sequencing data used for the analysis was RNA-sequencing generated by the Illumina sequencing technology.

2.1 RNA-SEQUENCING (RNA-seq):

Transcriptome analysis reveals a thorough understanding of functional elements of the genome and is an effective approach to recognize transcriptional changes during development and diseases. It provides an insight into the complete set of transcripts, transcriptional structures of the genes and the changing expression levels of the transcripts under different conditions. The NGS based approach to determine the complete transcriptome, termed RNA-seq, has revolutionized the manner in which transcriptomes are analysed.

In RNA-seq, total RNA is sheared into a collection of cDNA fragments with adapters attached to one or both ends. These fragments are deep sequenced to obtain either single end reads or paired end reads based on the protocol [Wang et al., 2009].

2.2 ILLUMINA SEQUENCING:

The Illumina sequencing technology provides a wide variety of applications in genomics, transcriptomics and epigenomics. Input samples to be sequenced are sheared into smaller sections and attached to slides using adapters. These fragments are PCR-amplified on the slide, creating several copies of the same read.

Single strands from the read to be sequenced are retained on the slides. In the next step, the slides are flooded with the fluorescently labelled nucleotides, DNA polymerase and a terminator to allow only a single base addition at a time. A fluorescent image of the slide indicating the base is recorded. In the next cycle, terminator and the fluorescent signal are removed and the addition of the following base and imaging process is further continued. Consequently, all signals of an Illumina run are recorded on a computer and used to construct the sequence [available at: <https://www.ebi.ac.uk/training/online/course/ebi-next-generation-sequencing-practical-course/what-next-generation-dna-sequencing/illumina->, accessed August 17, 2015].

2.3 BASE CALL ACCURACY:

The base call accuracy from NGS is determined by the phred quality score, which determines the quality of the base call during the sequencing [Ewing & Green, 1998]. A base call is assigned a quality value q which is logarithmically related to the estimated error probability p of that base call.

$$q = -10 \times \log_{10}(p)$$

If the quality score of a base is 30 then the error probability of that base call is 1/1000. The higher the quality value, the lower is the error probability of that base call and vice versa.

2.4 TRIM GALORE:

Trim Galore (available at:

http://www.bioinformatics.babraham.ac.uk/projects/trim_galore/, accessed June 14, 2015) accomplishes both, the removal of the adapter sequences and subsequent quality control of the raw RNA-seq reads in a single pass. For adapter sequence removal the default 13 bp standard Illumina adapters ('AGATCGGAAGAGC') suitable for both single and paired end libraries are used with the option for the provision of other adapter sequences. Trim Galore specifically uses Cutadapt [Martin, 2011] to remove adapter sequences from the raw sequencing reads. It removes the reads that are too short after the trimming process. However for paired end reads, there is an option to retain the best quality partner read, if one of the reads in the read pair becomes too short during the trimming process. For the quality control, the phred quality value of the base calls can be specified. The processed raw RNA-seq reads are output in the form of FastQ files which are quality checked with FastQC (available at: <http://www.bioinformatics.bbsrc.ac.uk/projects/fastqc/>, accessed June 21, 2015).

2.5 ALIGNMENT:

Alignment is the process of arranging the sequences of DNA, RNA, or protein to identify regions of similarity that may be a consequence of functional, structural, or evolutionary relationships between the sequences [available at: https://en.wikipedia.org/wiki/Sequence_alignment, accessed July 20, 2015]. With the advent of NGS data, aligning millions of short to long reads to the reference genome is the primary and critical task after the sequencing process. For RNA-seq

data, there are a number of aligners that are capable of aligning the reads with high accuracy. A brief discussion of the aligners used in this thesis are put forth below:

2.5.1 BWA ALIGNER:

Burrows-Wheeler Alignment tool (BWA) is a fast short read aligner based on backward search with Burrows-Wheeler Transform [Li and Durbin, 2009]. It supports both single and paired-end reads, and is also capable of allowing mismatches and gaps while aligning reads against a reference sequence.

Performance is reduced with long reads because BWA seeks a global alignment from first to last base of the read and long reads may inherently contain structural variations or there might be misassemblies in the reference genome.

2.5.2 STAR ALIGNER:

Spliced Transcripts Alignment to a Reference (STAR) is an ultrafast universal RNA-seq reads aligner [Dobin et al., 2013]. It has the ability to map both long and short RNA-seq reads to the reference sequences. It is provided as a C++ standalone code capable of running parallel threads on multicore systems.

It aligns the RNA-seq reads to the genome in a twostep process:

a. Seed search

In this step, the STAR algorithm discovers for each read the longest substring or maximum mappable prefix (MMP) that matches exactly to one or more substrings in the genomic sequences. These MMPs serve as the foundations in the genome, where the reads are aligned to with allowed mismatches.

The advantage of this step is that the algorithm recognizes splice junction information for each read without previous information of splice junction location.

b. Clustering, stitching and scoring:

In this step, the algorithm takes the log of all MMPs defined for the whole genome in the first phase and builds alignments for the entire read sequence. In case of paired end reads, seeds of the mates are clustered and stitched or aligned concurrently.

The alignment is validated by the local alignment scoring scheme, which is user controlled for defining the penalties for matches, mismatches, insertions, deletions and splice junction gaps.

The ability of the STAR algorithm to identify the splice junction information for the entire read sequences in the first pass alignment (PASS 1) provides an option to accurately align the entire read sequence to the genome in the second pass alignment (PASS 2). Alternatively, STAR can also be provided with possible splice junction information from an annotation file.

2.5.3 TOPHAT2 ALIGNER:

The TopHat aligner [Trapnell et al., 2009] is one of the most popular aligners used for the RNA-seq experiments. TopHat2 [Kim et al., 2013] is a significant extension of TopHat with several important enhancements. It can align both single and also paired-end reads with varying lengths. TopHat2 is also enhanced to align reads across fusion break events occurring as a consequence of genomic translocations.

Provided with transcriptome annotation file, TopHat2 aligns the reads across the known transcriptome with significant speed, sensitivity and accuracy. The

unmapped reads that remain after the mapping are realigned to identify novel exons and novel introns based on the known junction signals (GT-AG, GC-AG, and AT-AC). Some of the reads are remapped with Bowtie2 [Langmead et al., 2012] by splitting them into smaller non overlapping segments (25 bp each by default).

2.6 MAPPING QUALITY

Mapping quality is the post alignment probability that a read aligned belongs to its assigned position [Li et al., 2008]. The probability p is calculated as:

$$p = 10^{-q/10}$$

Where q is the mapping quality. If for instance, mapping quality value $q = 20$ then

$$p = 10^{-20/10}$$

$$p = 10^{-2} = 0.01$$

Which means there is 0.01 percent chance that the read aligned is erroneous.

2.7 PICARD TOOLS

The Picard tools (available at: <http://broadinstitute.github.io/picard/index.html>, accessed July 13, 2015) are a set of java command line tools used in the manipulation of next generation sequencing data. The tools are implemented in the HTSJDK (available at: <http://samtools.github.io/htsjdk/>, accessed July 13, 2015) java library and supports both SAM and BAM formats retrieved during NGS data analysis.

2.7.1 MARK DUPLICATES

During the sequencing process DNA molecules are sequenced several times resulting in the accumulation of duplicate reads, which would distort the calling of putative variants during SNP analysis.

MarkDuplicates (available at: <http://broadinstitute.github.io/picard/command-line-overview.html#MarkDuplicates> , accessed July 13, 2015) is a Picard command line tool which inspects the alignments to locate and subsequently flag duplicate reads, such that they will be ignored in downstream SNP calling steps.

2.8 THE GENOME ANALYSIS TOOLKIT (GATK):

GATK is a software package developed for the analysis of next generation DNA sequencing data [Mckenna et al., 2010], emphasizing principally on variant discovery and genotyping [Depristo et al., 2011].

The toolkit maintains a stable and most upto date version of tools called “walkers”, that can be used individually or in combination eventuating into pipelines for the analysis of data. It is built to be highly generic and can be used for multiple organisms including humans.

It is proficient in handling whole genome, exome and also RNA-seq data and for each kind of data, best practices recommendations for variant calling are provided and updated frequently [Van der Auwera, 2013].

2.8.1 SPLIT'N'TRIM:

This step includes the removal of the sequences overhanging into intronic regions. The process involves slicing the reads into exonic segments by hard clipping the part mapped to the intronic region. This is achieved by GATK's SplitNCigarReads tool (available at:

https://www.broadinstitute.org/gatk/guide/tooldocs/org_broadinstitute_gatk_tools_walkers_RNA-seq_SplitNCigarReads.php, accessed July 19, 2015). It is mainly focussed on reducing false calls generated by the reads mapping to intronic regions.

2.8.2 REASSIGN MAPPING QUALITIES:

STAR aligner assigns a mapping quality value of 255 for good alignments, which technically means “UNKNOWN” and would be rejected by GATK during the variant calling step.

This is circumvented by reassigning the mapping quality value of 255 to 60, which is acceptable by GATK. Reassigning mapping qualities is accomplished by the tool, ReassignOneMappingQualityFilter (available at: https://www.broadinstitute.org/gatk/gatkdocs/org_broadinstitute_gatk_engine_filters_ReassignOneMappingQualityFilter.php, accessed July 19, 2015).

2.8.3 REALIGNMENT AROUND INDELS:

Mapping artifacts around indels often are miscalled as SNPs. To avoid this, a realignment process is done, which identifies the region for reads around indels to eliminate these artifacts.

Realignment is achieved in two steps:

- a. In the first step, genomic intervals that require realignment are identified. This task is achieved by RealignerTargetCreator tool (available at: https://www.broadinstitute.org/gatk/guide/tooldocs/org_broadinstitute_gatk_tools_walkers_indels_RealignerTargetCreator.php , accessed July 20, 2015).
- b. In the second step, realignment of reads is performed after identifying the optimal consensus sequence. Local realignment of reads around indels is performed by IndelRealigner tool (available at: https://www.broadinstitute.org/gatk/guide/tooldocs/org_broadinstitute_gatk_tools_walkers_indels_IndelRealigner.php, accessed July 20, 2015).

2.8.4 BASE RECALIBRATION:

Variant calling algorithms use base quality score as a criteria to call variants in the genomic data. Quality scores assigned to individual bases in the sequencing read are subjected to various sources of systematic errors. These systemic errors could lead

to the erroneous base calls. Base quality score recalibration adjusts the base quality scores in the data based on a model of covariation calculated based on a list of already known SNPs, such as dbSNP [Sherry et al., 2001]. This step is accomplished by the tool BaseRecalibrator (available at: https://www.broadinstitute.org/gatk/guide/tooldocs/org_broadinstitute_gatk_tools_walkers_bqsr_BaseRecalibrator.php, accessed July 20, 2015).

2.8.5 VARIANT CALLING AND FILTERING:

This step involves the identification of variant sites corresponding to the reference genome and calculates the genotypes of each sample at that site. The major challenge is to establish a balance between sensitivity (minimize false negatives: inability of the model to predict real variants) and specificity (minimize false positives: failure of the model to recognize false variants). This balance is achieved by dividing this process into two steps:

- a. The variant calling step: This step aims to maximize sensitivity by conducting local de-novo assembly of reads in the active region to identify SNPs and indels simultaneously. This is accomplished by the tool HaplotypeCaller (available at: https://www.broadinstitute.org/gatk/guide/tooldocs/org_broadinstitute_gatk_tools_walkers_haplotypecaller_HaplotypeCaller.php. accessed July 20, 2015).
- b. The variant filtering step: This step aims to achieve maximum specificity and can be customizable by users based on the data. Here the output generated by the HaplotypeCaller is subjected to hard filtering such as minimum base quality, strand bias, clustered SNPs and many more. This step is accomplished by the tool VariantFiltration (available at: https://www.broadinstitute.org/gatk/guide/tooldocs/org_broadinstitute_gatk_tools_walkers_filters_VariantFiltration.php. accessed July 20, 2015).

2.9 SNPiR FILTRATION:

To further process and minimize false positives from the filtered data obtained from GATK's VariantFiltration step, several filtering steps are defined in the study "Reliable identification of genomic variants from RNA-seq data" [Piskol et al., 2013]. These include the removal of false calls in the repetitive regions of the genome, in homopolymer regions, removal of variants close to splice junctions and finally filtering known RNA editing sites.

2.10 ONCOTATOR:

Oncotator is a tool which annotates point mutations and indels integrating cancer relevant information to the annotations [Ramos et al., 2015]. It is available as a web server [available at: <http://www.broadinstitute.org/oncotator> , accessed July 21, 2015], which restricts the amount of data submission. However a standalone version can be used in case of large amounts of data.

2.11 MITOWHEEL:

MitoWheel is a web based visual representation of the human mitochondrial genome [Zsurka and Csordás, 2009]. It displays the revised Cambridge reference sequence and has several components to browse upon (available at: <http://mitowheel.org/mitowheel.html> . accessed July 21, 2015).

The mitochondrial genome is represented in a circular manner which can be spinned to view specific components of the genome such as its genes. It also consists of a search box to specifically select a region of interest. One important feature of the tool is its ability to map mutations to understand the genes affected and the functional consequences.

2.12 CUFFLINKS PACKAGE:

Cufflinks [Trapnell et al., 2012] works with TopHat alignment files of each condition and is designed to address the issue of alternative splicing events in the genes. Cufflinks [Trapnell et al., 2012] collects a transcriptome assembly and then reports full length transcript fragments or transfrags, which explains all the splicing events in the input data. Post assembly, expression abundance of each transfrag is quantified in the data using a rigorous statistical model of RNA-seq and is reported as Fragments Per Kilobase of transcript per Million fragments mapped (FPKM) [Trapnell et al., 2010].

2.12.1 CUFFMERGE:

For all the samples in the experiment, Cuffmerge performs a meta assembly of the transfrags which were put forth by the Cufflinks process. Provided a reference genome annotation file, it integrates the reference transcripts into a merged assembly producing a single annotation file to be used for differential analysis [Trapnell et al., 2012].

2.12.2 CUFFDIFF:

Cuffdiff [Trapnell et al., 2012] calculates the expression difference between two or more samples in an experiment and tests the statistical significance of the observed change in expression between them. Multiple replicates, either biological or technical can be provided per condition and Cuffdiff learns for each gene the variation among the replicates to calculate the significance of expression change [Trapnell et al., 2012].

2.13 VARIANT DISCOVERY WORKFLOW:

The discovery of the variants in the form of mutation sites and expression difference between two samples (Normal vs. Disease) is conducted by following the workflow depicted in the Figure 3.

The fasta files generated from the RNA-seq forms the input, which then proceeds into the mutation sites analysis workflow (see section 2.13.1) and subsequently into the expression analysis workflow (see section 2.13.2). Final output of this step is the generation of two files: one output file contains the mutation sites and the second one the expression difference specific to the disease state.

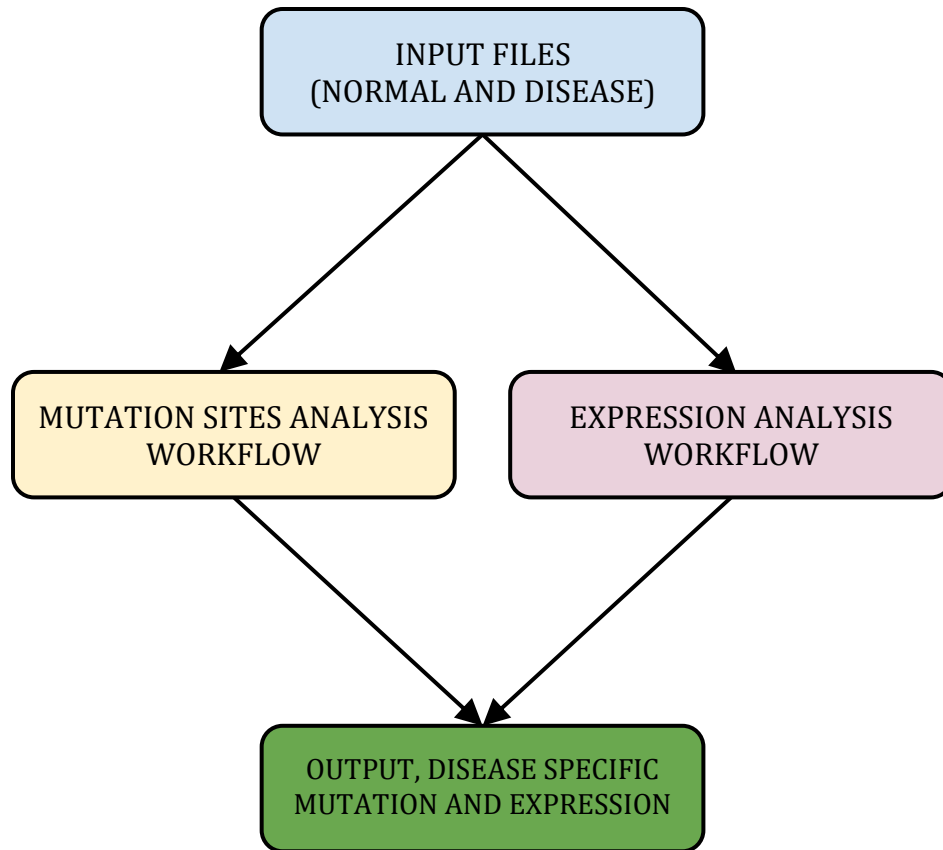


Figure 3: Variant discovery workflow

2.13.1 MUTATION SITES ANALYSIS WORKFLOW:

To discover mutation sites in both the nuclear and mitochondrial genomes, specific workflows were designed. In this section a general overview of the variants workflow is briefly discussed.

In each experiment, the workflow (Figure 4) begins with the FASTQ files of each sample as the input file. Reads may be single- or paired-end depending on the design of the experiment. The input file then enters individually into the nuclear genome variant analysis workflow (see section 2.13.1.1) and mitochondrial genome variant analysis workflow (see section 2.13.1.2), the results of which are subsequently manipulated by several analytical processes. Finally, an output file with the list of mutations and its annotations giving information about the gene harboring the mutation, as well as its potential effect on the protein function is returned.

After obtaining the mutation sites and its annotations for both samples (usually Normal vs. Disease), disease-specific data is extracted by comparing it with the normal data.

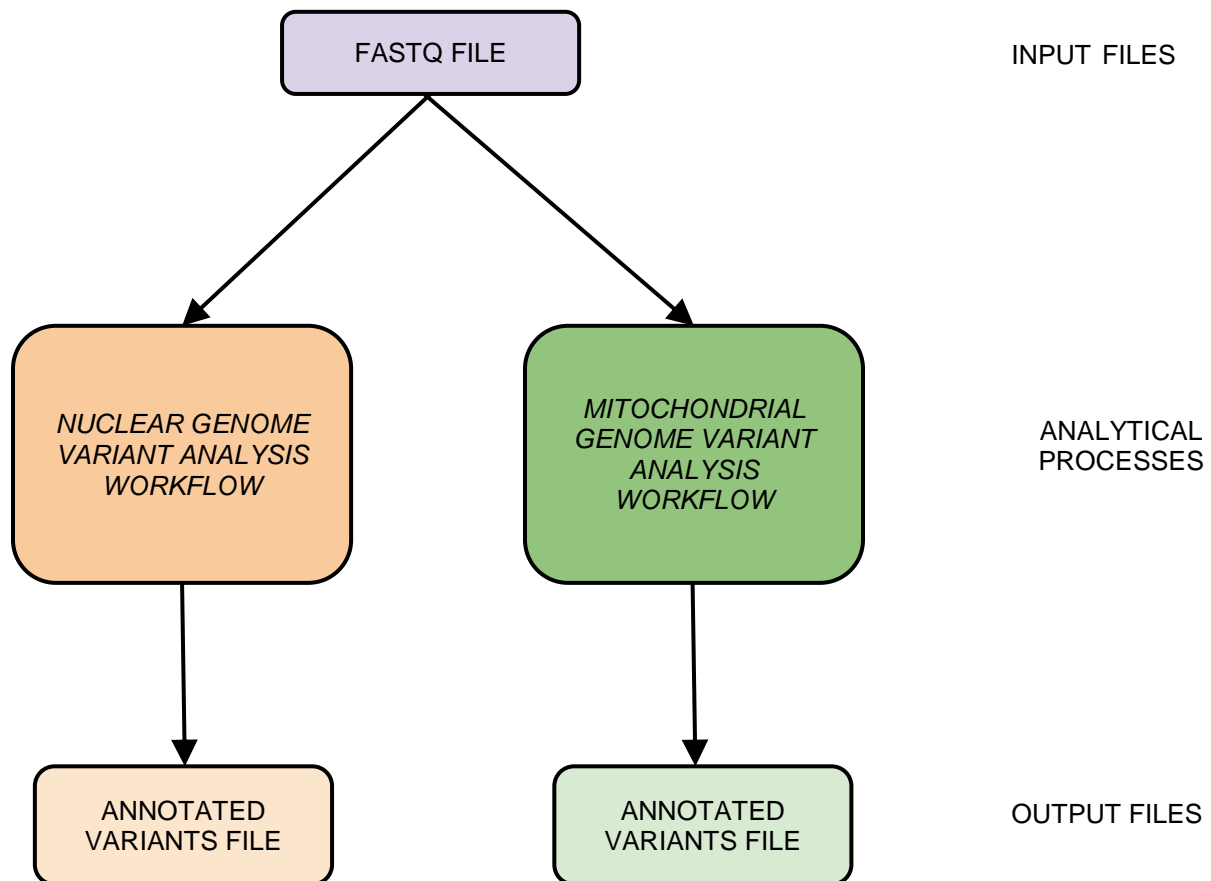


Figure 4: Overview of variants analysis workflow depicting the levels of data handling (input, manipulation and output).

2.13.1.1 NUCLEAR GENOME VARIANT ANALYSIS WORKFLOW:

For each sample in the experiment, identification of variants in RNA-seq data is achieved by following the best practice recommendations provided by GATK (available at: <https://www.broadinstitute.org/gatk/guide/best-practices?bpm=RNAseq> . accessed on July 21, 2015).

Module I. Pre-processing RNA-seq reads:

This module pre-processes raw RNA-seq reads, which includes removal of adapter sequences and quality control. This is achieved by processing the raw RNA-seq reads using Trim Galore (see section 2.4) with selecting default adapter sequence for illumina reads and a quality cutoff score of 20 on phred scale.

The processed FastQ reads move over to module II, and here they are mapped to the reference genome.

Module II. Map to the Reference genome:

This module maps pre-processed RNA-seq reads to the human genome version 19. This is accomplished by the STAR aligner (see section 2.5.2) using the 2-PASS approach, wherein the first pass (1-PASS) identifies the splice junctions and then guides the second pass (2-PASS) towards the final alignment.

MarkDuplicates (see section 4.3a), a command line tool belonging to the Picard tool (see section 4.3) is used to remove duplicate reads.

The final alignment file in BAM format further pre-processed (module III) for subsequent variant detection using the variant calling and filtering module (module IV).

Module III. Pre-processing alignment file:

Module III pre-processes the alignment file for variant calling by removing overhanging reads in intronic regions. This is accomplished by the tool Split'N'Trim (see section 2.8.1) available in the GATK (see section 2.8) package.

Furthermore, the mapping quality value of the alignment file is adjusted using a tool called ReassignOneMappingQualityFilter (see section 2.8.2) offered in the GATK package.

Finally, local realignment around indels is performed (see section 2.8.3) and base score recalibration is done using the tool BaseRecalibrator (see section 2.8.4) provided by GATK package.

The alignment file in BAM format is next submitted to variant calling and filtering (module IV).

Module IV. Variant calling and filtering:

In this module the critical task of variant calling (see section 2.8.5) is performed. Identified variants are subsequently filtered to obtain the *bona fide* variants present in a sample.

Filtering of the variants is done using the SNPiR pipeline (see section 2.9). In this step, false calls are removed in repetitive regions of the genome, homopolymer regions, around splice junctions and known RNA editing sites. Finally, one is left with the most likely, genomic SNPs.

Module V. Annotation of filtered variants:

The final annotation of identified variants is achieved by the Oncotator tool (see section 2.10).

2.13.1.2 MITOCHONDRIAL GENOME VARIANT ANALYSIS:

In this section, the prediction of variants in the form of homoplasmic or heteroplasmic sites in the mitochondrial genome is described. The workflow to decode heteroplasmic sites in mitochondrial genome was adapted from the work of [Goto et al., 2011] and was integrated in a Galaxy workflow [available at: <https://usegalaxy.org/u/aun1/p/heteroplasmy>, accessed on July 21, 2015], which is an open, web based platform to do biomedical research [Giardine et al., 2005]. The workflow is divided into several modules as detailed below.

Module I. Pre-processing RNA-seq reads:

This module pre-processes raw RNA-seq reads, which includes removal of adapter sequences and quality control. Trim Galore (see section 2.4) was used with selecting default adapter sequence for illumina reads and a quality cutoff score of 20 on phred scale.

The processed FastQ reads are in the next step mapped to the reference genome (module II).

Module II. Map to the Reference genome:

The filtered reads are mapped to the human mitochondrial revised Cambridge reference sequence [Andrews et al., 1999]. Since the mitochondrial genome is a circular molecule, the genome has to be extended on both ends by the length of the input reads -1. Reads are mapped to this extended genome using the BWA aligner (see section 2.5.1) with the default settings.

The alignment file in BAM format is further used for calling variant sites (module III).

Module III. Segregating the alignment file:

In this module reads mapped to the plus strand are separated from reads mapped to the minus strand of the genome.

Both resulting read files are investigated for variant sites with a minimum coverage of 100 reads and the base quality value of 20. Only variant sites passing this filter are retained for further processing.

Module IV. Applying conservative filter settings:

For mitochondrial variant calling, a conservative variant detection setting of at least 5 % coverage and base quality value of 20 on the phred scale is applied to call the variants. Variant calling is done for all reads in plus and minus direction separately.

Module V. Calling variant sites:

Variants present in the plus and minus strand files are merged and those sites which are common to both the files are chosen and retained as *bona fide* variant sites. This process eliminates the variants present on only strand, which are most likely due to technical issues during sequencing.

The variant sites are further manually analysed for their hetero- and homoplasmic nature. Further annotation information is extracted for the variants by mapping them on MitoWheel (see section 2.11).

2.13.2 EXPRESSION ANALYSIS WORKFLOW:

Differential gene expression analysis for two conditions (Normal and Disease) is done in a workflow described below:

Module I. Pre-processing RNA-seq reads:

Pre-processing of reads is done as described in *section 2.13.1.1 Module I*,

Module II. Map to the Reference genome:

Pre-processed RNA-seq reads for the 2 conditions to be compared are individually mapped to the reference genome using TopHat2 (see section 2.5.3) with default settings. The alignment files is then submitted to transcriptome assembly and merging (module III).

Module III. Transcriptome assembly and merging:

For both conditions, Cufflinks assembles full length transcripts for all the genes expressed and provides an expression value in form of a metric called FPKM (see section 2.12).

The transcriptomes of both conditions are merged by Cuffmerge (see section 2.12.1) and further annotated using a provided annotation file.

Module IV. Differential expression of genes:

Keeping the merged transcriptomes as background gene models, Cuffdiff (see section 2.12.2) calculates the expression difference between two conditions and provides the statistical significance of the expression change between two samples.

2.14 MITOCHONDRIAL MODEL (*MitoModel*):

The MitoModel is a web-based application that was developed for analysing mitochondrial contributions in diseases. The main aim is to map analysed expression and/or mutation data from NGS studies onto MitoModel. By this, we can identify the mitochondria specific metabolic and physiological changes in the disease state compared to the normal condition.

2.14.1 MITOMODEL CONSTRUCTION:

MitoModel is an amalgamation consisting of 659 human genes, which are functionally associated with mitochondria (see Appendix C). It represents a closely connected network, with interactions among 659 genes being fetched from string database [Szklarczyk et al. 2015] with a medium confidence score of 0.40 and above for each interaction. In summary, the human and mouse MitoModel illustrates 659 genes with 10985 and 12571 interactions among them respectively.

A similar MitoModel for mouse was constructed by deriving 659 mouse orthologous genes from the human gene set, using the HCOP's human orthology prediction [Eyre et al., 2007]. MitoModel is classified in 17 mitochondria-specific processes (Figure 5).

MitoModel considers the following parameters for the differentially expressed genes: A gene is observed as up-regulated if its log₂fold change is greater than 1.5 and second, p-value is less than 0.05. A gene is observed as a down-regulated gene if its log₂fold change less than -1.5 and its p-value is less than 0.05.

MitoModel uses different visual cues for displaying gene expression. A circular node corresponds to a gene that is neither up- or down-regulated. An up-triangle and down-triangle nodes correspond to genes, which are up-regulated or down-regulated, respectively. Mutation sites mapped on the MitoModel are depicted as cross nodes and finally a diamond-shaped node represents a gene that is mis-regulated (up- or down-regulated) and also harbors a mutation.

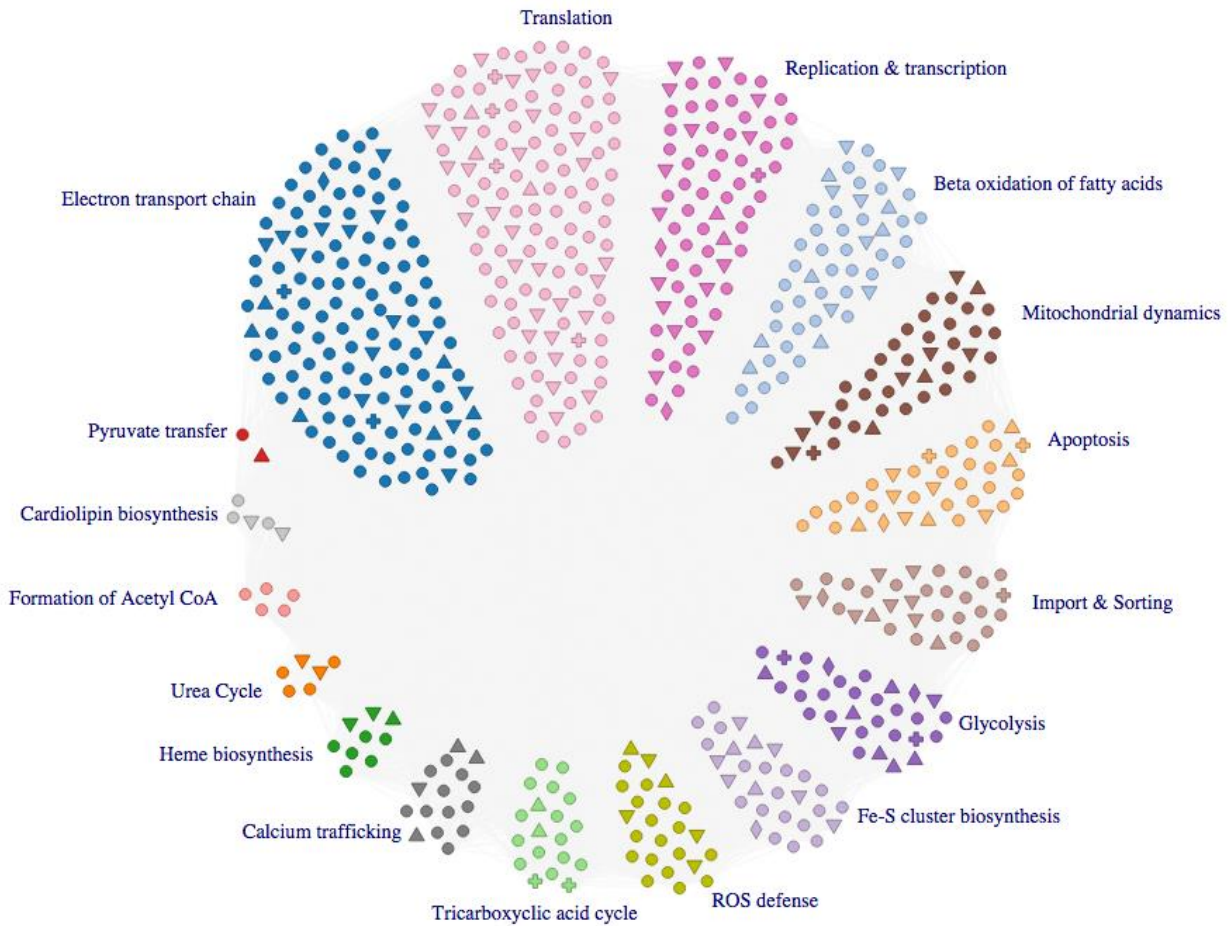


Figure 5: Visual representation of MitoModel with functions as clusters annotated with their names

One of the major advantage of the MitoModel is the fact that it is highly interactive. If the cursor moves on to a single node, a small window pops up with information on the selected gene, such as its name, function, expression values of the normal and disease samples, its p-value and finally, information on observed mutations in the samples (Figure 6). In addition to gene-relevant information, all interactions of the gene to partners within and across functions are shown.

The design and concept of the MitoModel was derived from the work developed by Jim Vallandingham (available at: <http://flowingdata.com/2012/08/02/how-to->

[make-an-interactive-network-visualization/](#), accessed July 23, 2015) and restructured by us to fulfil our specific requirements.

The MitoModel is complemented by an enrichment analysis, identifying the most affected functions based on the percentage changed genes [Percentage = (number of affected genes in the function / total genes in the function) X 100].

Analysed functional categories are represented as clusters, whereby each node corresponds to a gene (Figure 7). The size of the node corresponds to the log₂fold change value, where higher log₂fold change corresponds to bigger circle and vice versa. The colour corresponds to the gene regulation, where blue corresponds to up-regulation, green corresponds to no differential regulation and red corresponds to down-regulation. The nodes with dark borders represents genes containing mutations.

Differentially regulated genes in MitoModel (Figure 8) are also displayed as a graph briefly described below: two horizontal lines describe log₂fold change cutoff values (up: 1.50 and down: -1.50) and a vertical line describes the p-value cutoff (0.05). The overall expression pattern is printed, giving an idea about the number of up-regulated and down-regulated genes. In Figure 9, for example, there is a higher number of down-regulated genes compared to up-regulated genes.

The design and concept, for the display of enrichment analysis were adapted from the work by Shan Carter (available at:

<http://www.nytimes.com/interactive/2012/02/13/us/politics/2013-budget-proposal-graphic.html>, accessed July 23, 2015) and restructured (kindly provided by José Villaveces, Computational Biology group, Max Planck Institute of Biochemistry) to our specific needs.

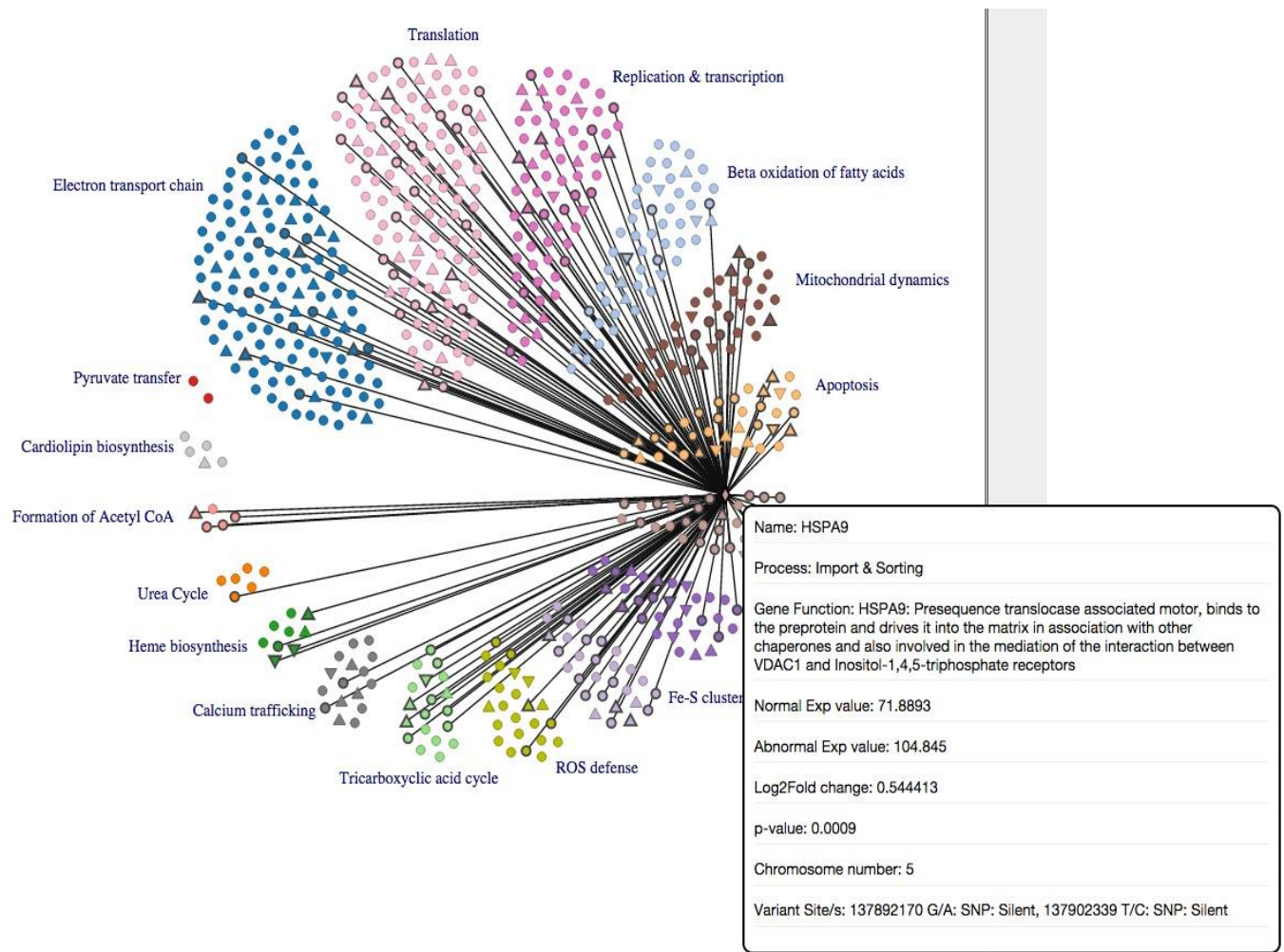
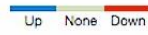


Figure 6: A simple depiction of the interactive ability brandished by the MitoModel

Color shows gene regulation



Dark Borders show mutations



Size shows Log2 fold change

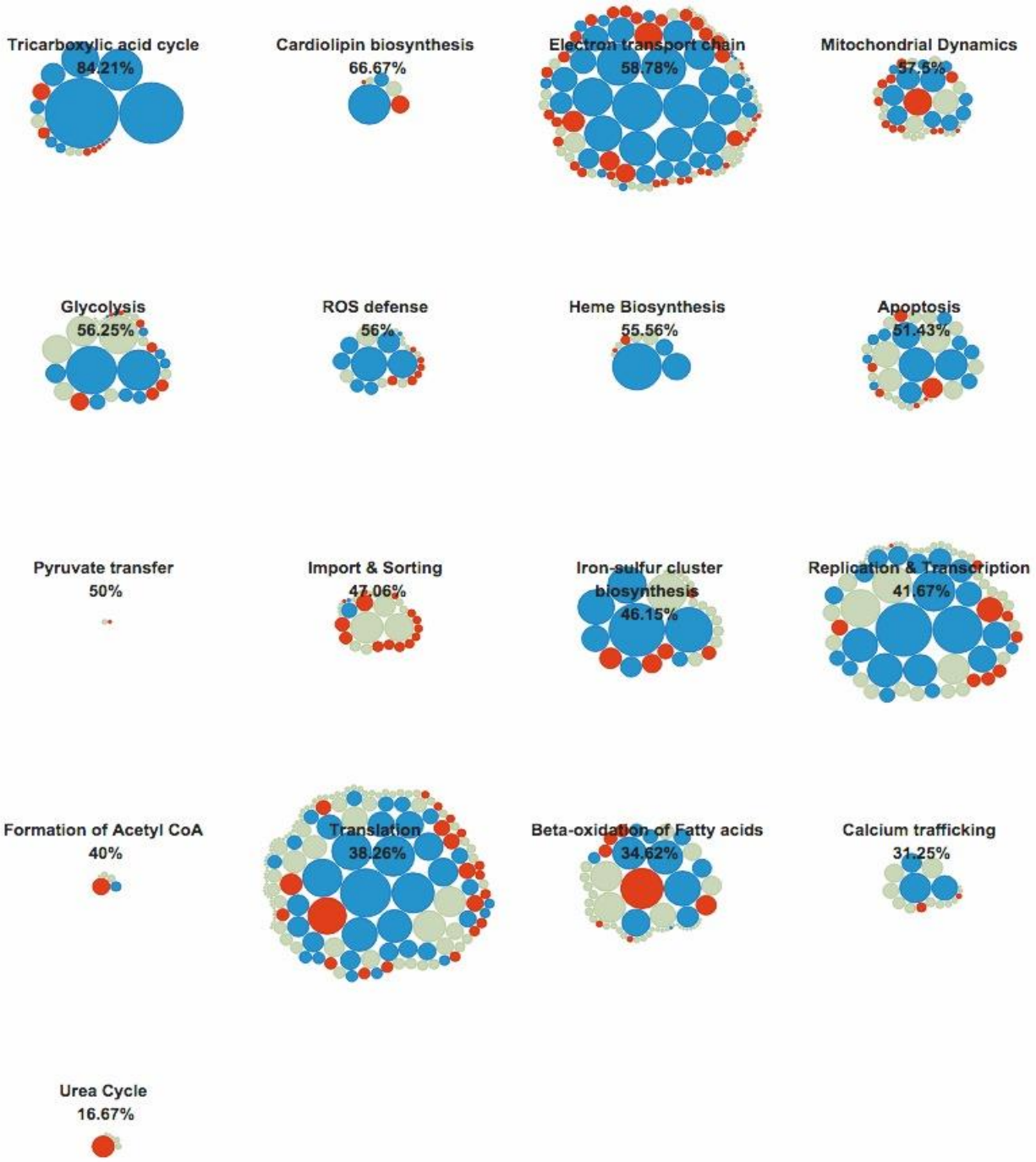
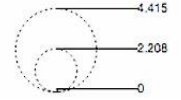


Figure 7: An instance of Percentage (%) affected functions observed on the MitoModel

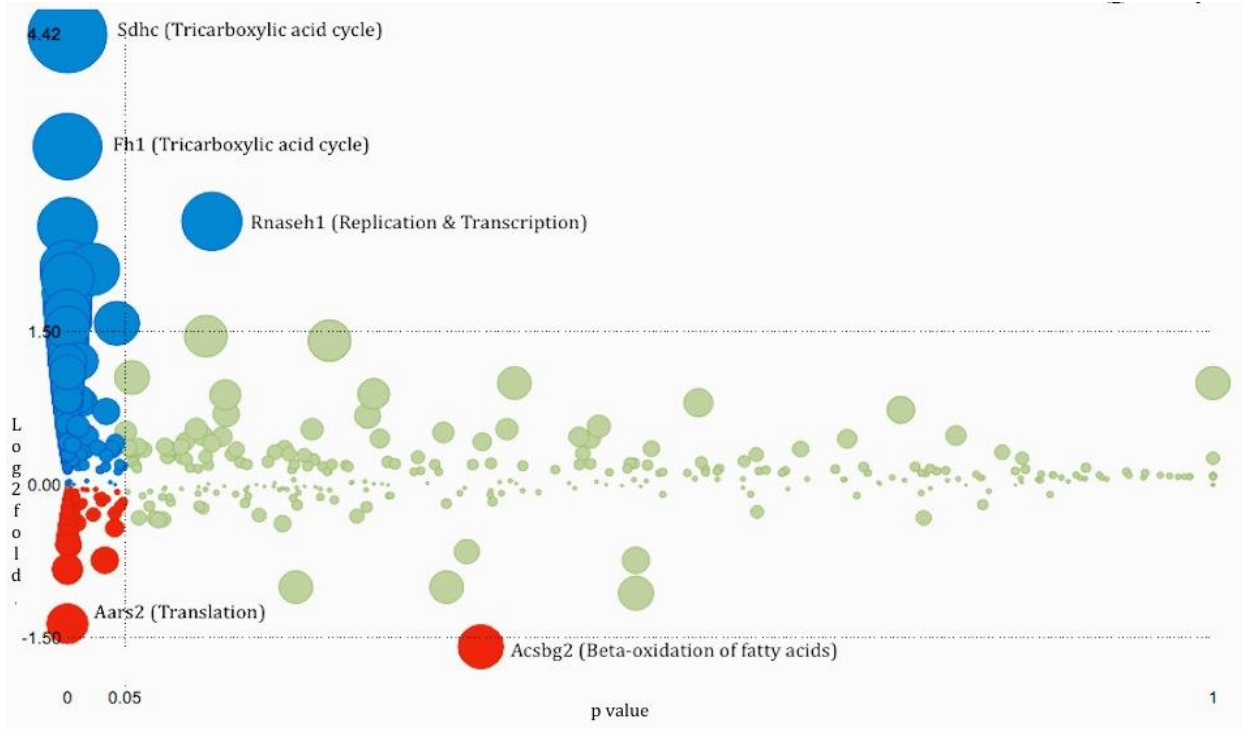


Figure 8: Graphical visualization of overall expression changes in MitoModel

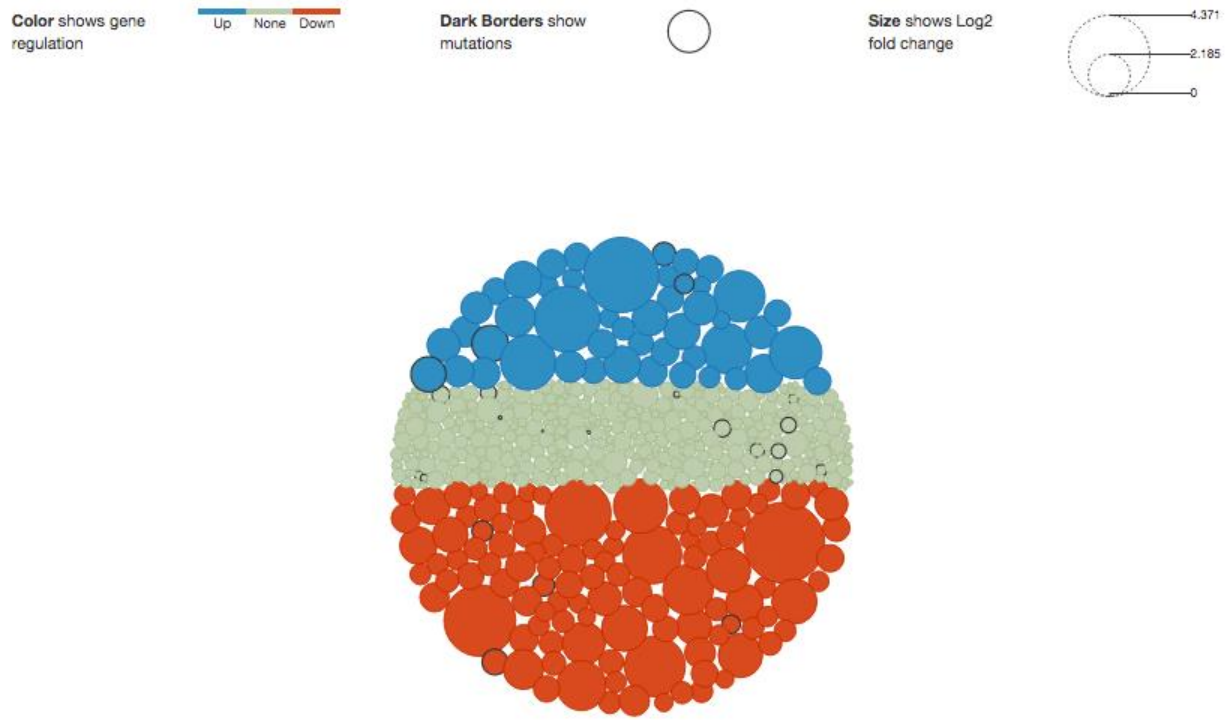


Figure 9: A further graphical representaiton of the MitoModel’s overall expression pattern

2.14.2 MITOMODEL IMPLEMENTATION:

MitoModel is implemented in the form of a web-server, which can be accessed by users for analysing their own data. An overview of the architecture is shown in Figure 10. The interaction between the users and the web-server takes place in three simple steps.

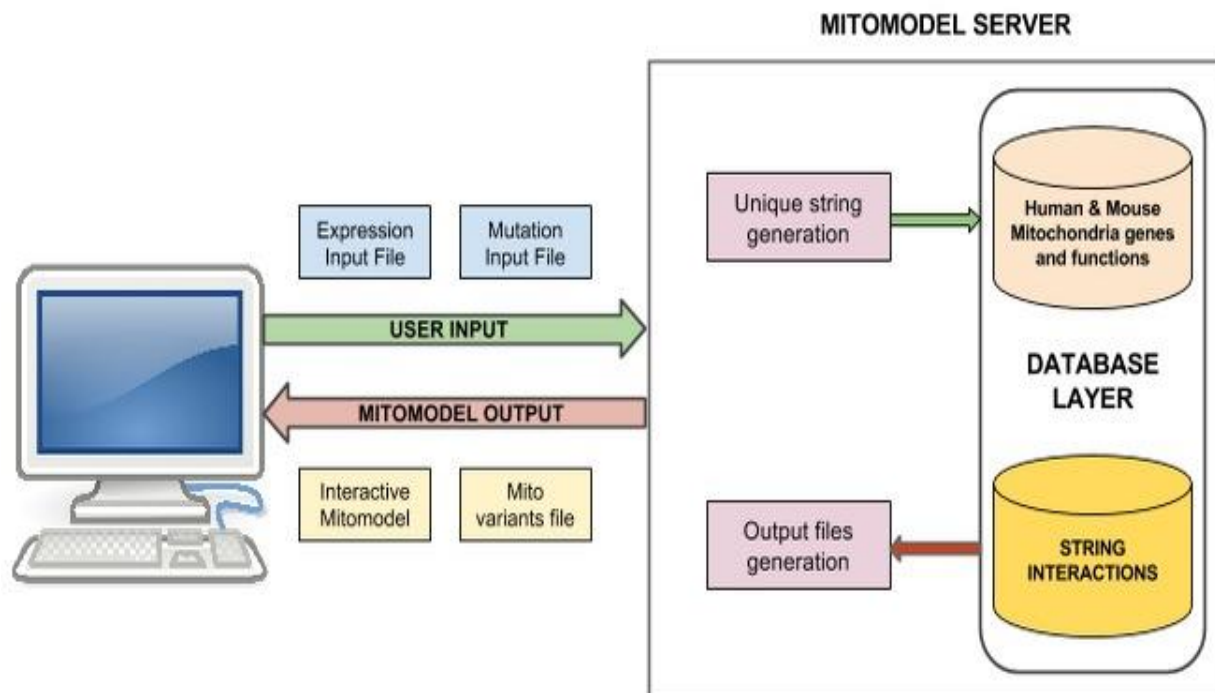


Figure 10: An overview of the interaction architecture between user and MitoModel server

Step 1. User submission of input data:

The MitoModel server is designed to accept both, expression and the mutation data at once and map them on to MitoModel simultaneously. Users with only expression or mutation data can also submit these data individually to obtain mapped results on MitoModel. Both the expression (Table 1) and the mutation (Table 2) input files are accepted as tab-separated files.

Gene Name	Condition 1	Condition 2	Log2fold	p-value
SIC25A34	5.14185	0.525591	-3.29027	0.04165
EPHB2	21.6398	77.9794	1.84941	0.03615
CD52	113.979	24.01	-2.24706	0.14155
MFSD2A	2.671	16.7198	2.64611	0.0318

Table 1: An example of a tab-separated expression input file

The expression input file has 5 columns, including gene name in form of the official gene symbol (presently only NCBI gene symbols are recognized), condition 1 with = expression values of the control (normal) condition, condition 2 with expression values of the disease state, the Log2fold with the log2fold changes observed between condition 1 and 2 and finally the p-value stating the statistical significance of the observed differential expression.

Gene Name	Chromosome	Position	Reference allele	Variant allele	Mutation type	Consequence
MT-CO2	M	8159	T	C	SNP	Missense
AGO1	1	36391661	TGAA	T	DEL	3'UTR
ITIH1	3	52825585	T	C	SNP	Silent
GPR35	2	241566012	G	A	SNP	Intron

Table 2: An example of a tab-separated mutation input file

The mutation input file has 7 columns, which are Gene Name (again the official gene symbol offered by NCBI), Chromosome, giving the chromosome number the mutated gene is located on, position with the chromosomal position of the mutation, reference allele with the base observed in the reference genome, variant allele with the observed mutation from the dataset, mutation type, interpreted as the type of mutation, and finally consequence, predicting the functional consequence of the mutation in the specific gene.

Step 2. Web-server interaction:

Once the data is submitted, a unique session-string is created, which represents the input data of the user and will keep the session exclusive for that user.

The MitoModel server comprises a database layer which is created using MySQL (available at: <http://www.mysql.com/> . accessed July 26, 2015) database. It includes two components, mitochondrial genes and their function layers and the interaction among the mitochondria genes.

Immediately after the input data is received by the MitoModel server, the expression or mutation data or both are extracted and mapped to the genes that are present in the mitochondria gene and function layer from the database. The integrated data along with all the interactions from the interaction layer are bound together as a JSON file (available at: <http://www.json.org/>, accessed July 26, 2015) to be displayed on the webpage.

Step3. MitoModel server output:

The MitoModel server output consists of two elements. The first one is the interactive webpage, which gives the user a glimpse of the mapped MitoModel, including a brief information of the gene function, its interactors, expression related values and mutation information. In addition to the visual enrichment analysis described above, the user can also download a tab-separated file with (Table 3) information about the up-regulated, down-regulated and mutated genes, all clustered according to their respective mitochondrial processes.

OUTPUT FOR YOUR DATA:

UP-REGULATED GENES:

GENE NAME PROCESS LOG2FOLD P-VALUE
NDUFA7 Electron transport chain 1.50887 0.12765
SLC27A5 Fatty acid beta-oxidation 3.37316 0.04555
ACSL1 Fatty acid beta-oxidation 1.8343 0.0498
PMAIP1 Apoptosis 1.9635 0.1193
CDK1 Apoptosis 2.01598 0.04185

DOWN-REGULATED GENES:

GENE NAME PROCESS LOG2FOLD P-VALUE
COX6B2 Electron transport chain -2.64248 0.11955
SLC27A6 Fatty acid beta-oxidation -3.0519 0.12155
ACSM1 Fatty acid beta-oxidation -3.00877 0.08585
BCL2 Apoptosis -3.11932 0.0147
BCL2L11 Apoptosis -2.23847 0.03105
SLC2A5 Glycolysis -1.99308 0.1512

MUTATED GENES:

GENE NAME CHROMOSOME PROCESS VARIANT DESCRIPTION
MT-ND3 M Electron transport chain 10233 G/A: SNP: Missense_mutation
MT-ND5 M Electron transport chain 13366 G/A: SNP: Nonsense_mutation
ACSL6 5 Fatty acid beta-oxidation 131288468 G/A: SNP: 3'UTR
GFER 16 Fe-S cluster biosynthesis 2035868 C/T: SNP: Splice_Site

Table 3: An example of MitoModel variant output file

CHAPTER 3

RESULTS

3.1 Gene expression and mutation analysis using MitoModel in three different aneuploidy cell lines

Aneuploidy refers to an abnormal chromosome count in a cell, whose chromosome numbers are either greater or smaller than its wild type on the level of the whole genome or part of it [Griffiths et al., 2000]. These extra copies of chromosomes are detrimental to eukaryotic cells. In humans, chromosomal abnormalities are often detected in cancer [Gordon et al., 2012], developmental growth, mental retardation and multiple congenital malformations. The elementary process of how aneuploidy is formed and what its consequences are to the cell remain illusive to date [Biancotti & Benvenisty, 2011].

To further our knowledge on the underlying mechanisms of aneuploidy, aneuploid cell lines were created in the lab of Zuzana Storchova. Three cell lines were created in this project: tetrasomic derivatives of HCT116 carrying 4 additional copies of chromosome 5 (HCT116 5/4), trisomic derivatives of RPE1 carrying 3 additional copies of chromosome 5 and 12 (RPE1 5/3 12/3) and trisomic derivatives of RPE1 carrying 3 additional copies of chromosome 21 (RPE1H2B 21/3) [Stingele et al., 2012]. Cell lines were further investigated by Dürrbaum et al in 2014, revealing that complex aneuploidy exhibits the same pathway changes as simple trisomy and tetrasomy [Dürrbaum et al., 2014].

3.1.1 TASK DESCRIPTION:

The data used for this task was generated at Max Planck institute of Biochemistry by Milena Dürrbaum and Zuzana Storchová and provided for us for further analysis of mitochondrial functions. The data included RNA-seq samples of HCT116 5/4, RPE1 5/3 12/3 and RPE1H2B 21/3 with their corresponding wild types. All sample were provided with 3 biological replicates.

Our task was to deduce the differential expression and the mutation data specific for each cell line and map them on to MitoModel to identify mitochondrial variations in each cell line.

3.1.2 DATA ANALYSIS:

The mutation and expression data for each cell line and for each replicate were generated by comparing aneuploidy cell lines with their wild type cell lines by following the workflow defined in the section 2.13. Subsequently, only aneuploidy specific variants were recorded and input files specifics for MitoModel were prepared. The input files were prepared following the MitoModel format specification described in the section 2.14.2.

The MitoModel input files for each cell line were then mapped to the MitoModel to obtain individual MitoModels for each cell line.

3.1.3 MitoModel of the HCT116 5/4 cell line:

A simple depiction of the HCT116 5/4 MitoModel, after mapping the mutation and expression input files, describes the nodes with mutations, as well as nodes, which were up-regulated and down-regulated in respective functions (Figure 11).

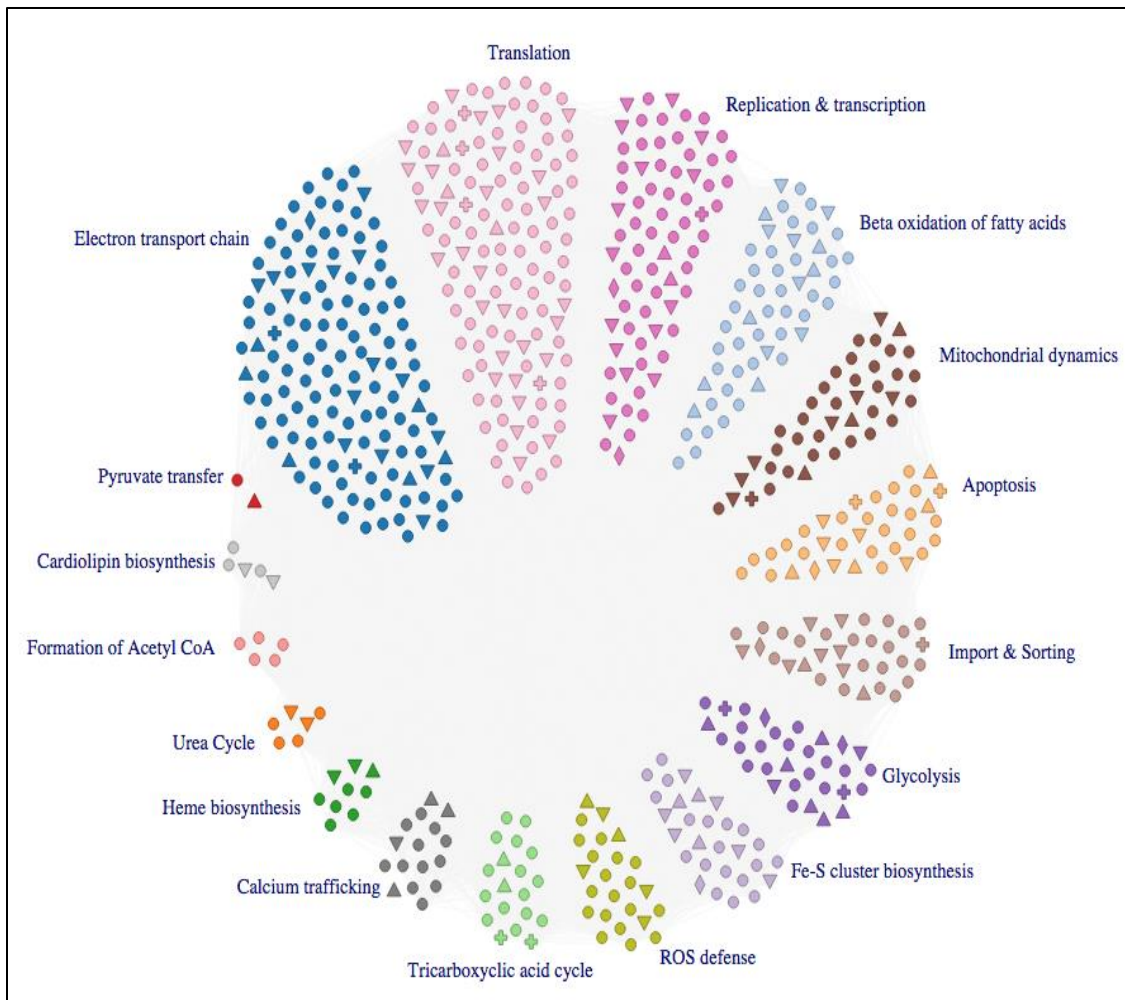


Figure 11: Visual display of the HCT 116 5/4 MitoModel

Crucial functions that were observed to be affected based on the percentage are: Pyruvate transfer with 50%; Cardiolipin biosynthesis with 40%; Fe-S cluster biosynthesis with 34.48%; Heme biosynthesis with 33.33%, and so on (Figure 12).

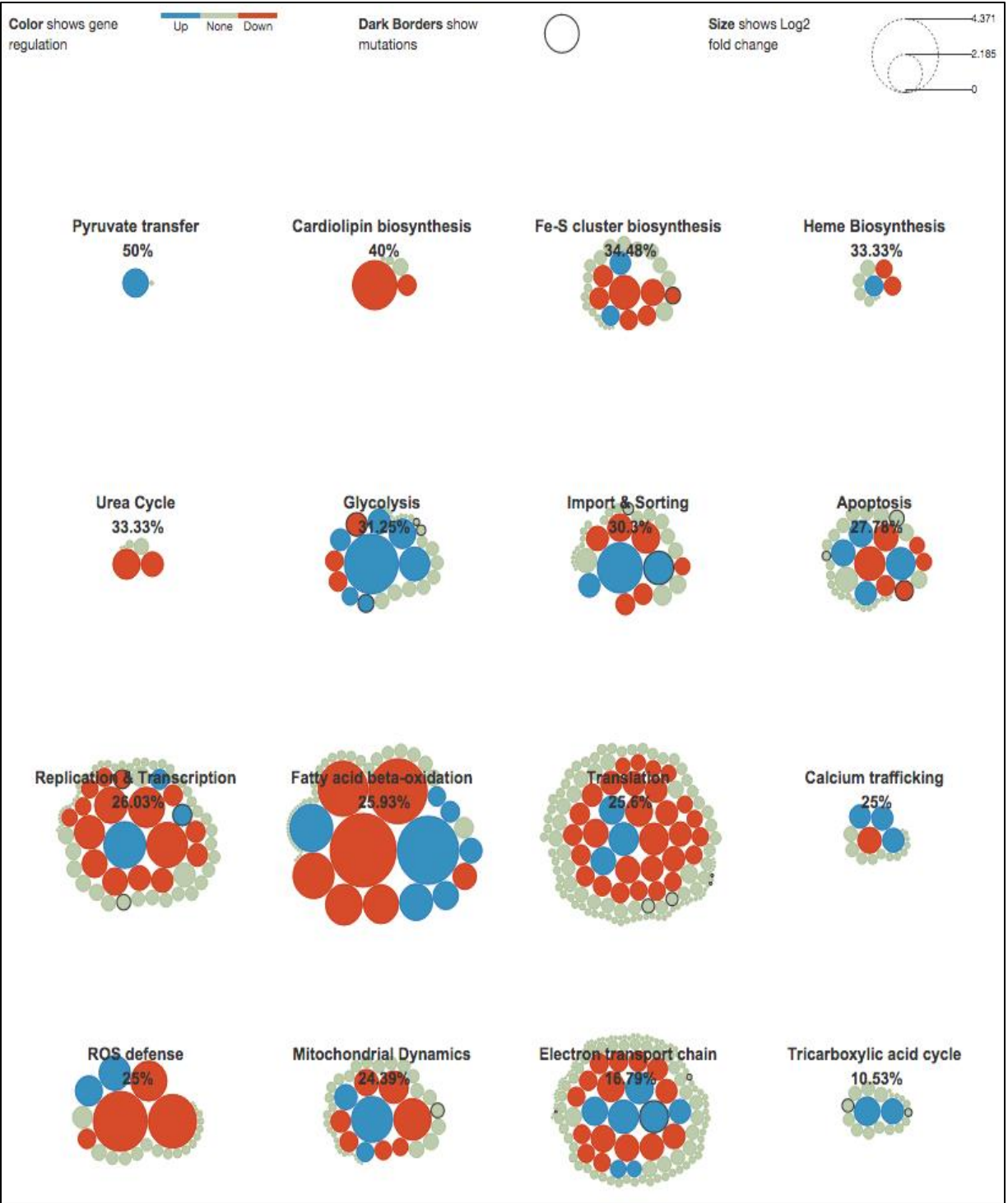


Figure 12: Percentage (%) of affected functions observed on the HCT116 5/4 MitoModel

To understand the role of variant genes, each function and the roles of the variant genes in them were further studied.

Electron transport chain and energy production

Seven genes were up-regulated (Table 4), fifteen genes were down-regulated (Table 5) and three genes were mutated (Table 6) in the electron transport function.

GENE NAME	LOG2FOLD	P-VALUE	ROLE
NDUFA2	0.850331	0.00025	Nuclear encoded essential components of complex I NADH dehydrogenase, involved in the reduction of ubiquinone by NADH
NDUFS4	0.961887	0.00005	
NDUFS8	0.424532	0.0305	
UQCRC2	0.376153	0.0433	Nuclear encoded essential components of complex III, transfers electrons from ubiquinol to cytochrome c
UQCRQ	1.00534	0.00005	
COX7C	0.668317	0.00005	Nuclear encoded cytochrome c oxidase subunits, essential components of complex IV, catalyses the reduction of oxygen to water by cytochrome c
COX20	1.09111	0.02635	Assembly factor of complex IV

Table 4: Up-regulated genes in the electron transport chain function of HCT116 5/4 cell line

GENE NAME	LOG2FOLD	P-VALUE	ROLE
NDUFA5	-0.46989	0.0244	Nuclear encoded essential components of complex I NADH dehydrogenase, involved in the reduction of ubiquinone by NADH
NDUFB9	-0.461298	0.0151	
NDUFS5	-0.523087	0.00515	
NDUFAF2	-0.499981	0.03065	Assembly factor of complex I
NDUFAF4	-0.780722	0.00085	Assembly factor of complex I
C8orf38	-0.526286	0.0299	Complex I assembly factor
SDHAF1	-0.69955	0.00405	Complex II specific assembly factor
UQCR10	-0.495375	0.01375	Nuclear encoded essential components of complex III, transfers electrons from ubiquinol to cytochrome c
PTCD2	-0.463894	0.0383	Complex III assembly factor, process RNA transcripts involving cytochrome b
CHCHD8	-0.656802	0.0018	Complex IV assembly factor

C1orf31	-0.544031	0.01835	Required for the stability of complex IV subunit
SELRC1	-0.920491	0.00005	Complex IV assembly factor
COX11	-0.75564	0.0388	Complex IV assembly factor
ATP5G1	-0.776189	0.00015	Nuclear encoded ATP synthase subunits, essential components of complex V, reversible pump of protons into matrix with formation of ATP
ATPIF1	-0.598401	0.0028	Endogenous inhibitor subunit of ATP synthase, essential component of complex V

Table 5: Down-regulated genes in the electron transport chain function of HCT116 5/4 cell line

GENE NAME	CHROMOSOME	VARIANT DESCRIPTION	ROLE
MT-ND4	M	10827 T/C: SNP: Missense_Mutation	Mitochondrially encoded NADH dehydrogenase, part of enzyme complex I, involved in the reduction of ubiquinone by NADH
CYC1	8	145151091 G/A: SNP: Missense Mutation	Nuclear encoded essential components of complex III, transfers electrons from ubiquinol to cytochrome c
UQCRC1	5	132203152 T/G: SNP: Intron	Nuclear encoded essential components of complex III, transfers electrons from ubiquinol to cytochrome c

Table 6: Mutated genes in the electron transport chain function of HCT116 5/4 cell line

We observe that several essential subunits and assembly factors of multiple complexes in the electron transport chain is down-regulated in the HCT116 5/4 cell line. For example, NDUFAF2, SDHAF1, PTCD2 and COX11, which are assembly factors of complex I, II, III, and IV respectively are down-regulated. There were also mutations in essential subunits of the complexes in the electron transport chain. This suggests that generation of energy by the electron transport chain might be lower in HCT116 5/4 cell line compared to its wild type cell line.

Fatty acid beta oxidation and generation of acetyl CoA

Seven genes were up-regulated (Table 7), seven genes were down-regulated (Table 8) in the fatty acid beta oxidation function.

GENE NAME	LOG2FOLD	P-VALUE	ROLE
SLC25A20	0.498288	0.024	Carnitine acylcarnitine translocase mediates acylcarnitine entry into mitochondria
CRAT	1.9068	0.00005	Free carnitine in the mitochondria is converted into acyl carnitine by the action of carnitine acetyltransferase
ACADVL	0.839364	0.00005	Very long chain acyl-CoAs are first catalyzed by long chain acyl-CoA dehydrogenase
SLC27A6	1.24661	0.00005	Readily converts the transported very long chain fatty acids to acyl-CoAs
ACSL1	0.698046	0.0005	Acyl-CoA synthetase activity for long chain free fatty acids and are also involved in the activation of fatty acids
ACSL4	0.545756	0.0037	
ACSL6	3.73374	0.00005	

Table 7: Up-regulated genes in the fatty acid beta-oxidation function of HCT116 5/4 cell line

GENE NAME	LOG2FOLD	P-VALUE	ROLE
SLC27A5	-1.37114	0.00005	Readily converts the transported very long chain fatty acids to acyl-CoAs
ACSL5	-4.37085	0.00005	Acyl-CoA synthetase activity for long chain free fatty acids and are also involved in the activation of fatty acids
ACSM3	-2.47286	0.0097	Acyl-CoA synthetase activity for medium chain fatty acids
ACSBG1	-1.48929	0.00075	Acyl-CoA synthetase activity for bubblegum family members
FABP5	-1.77518	0.00005	Fatty acid binding proteins involved in the import and export of fatty acids
CPT1C	-3.3842	0.00005	Carnitine palmitoyl transferase converts an acyl-CoA into an acylcarnitine
ACAA2	-0.755026	0.0004	Medium chain 3-ketoacyl-CoA thiolase

Table 8: Down-regulated genes in the fatty acid beta-oxidation function of HCT116 5/4 cell line

We observe that carnitine acyl-CoA translocase, which mediates the transfer acyl carnitine into mitochondria is up-regulated. In addition ACADVL, which is involved in first step metabolism of very long chain fatty acids inside mitochondria is up-regulated. This suggests that generation of acetyl-CoA inside mitochondria might be higher in HR mouse line.

Apoptosis

Four genes were up-regulated (Table 9), six genes were down-regulated (Table 10) and three genes were mutated (Table 11) in the apoptosis function.

GENE NAME	LOG2FOLD	P-VALUE	ROLE
APAF1	0.654363	0.0017	Binds CASP9 forming an apoptosome and activates it
BCL2L1	0.762541	0.00005	Bcl-2 family member Anti-apoptotic proteins
PMAIP1	0.761637	0.00015	Noxa Bcl-2 family member propagating apoptosis
VDAC1	1.02475	0.00005	Voltage dependent anion channel forms part of permeability transition pore

Table 9: Up-regulated genes in the apoptosis function of HCT116 5/4 cell line

GENE NAME	LOG2FOLD	P-VALUE	ROLE
BIK	-1.10509	0.00005	Bcl-2 family member propagating apoptosis
BID	-0.397959	0.0441	Bcl-2 family member propagating apoptosis
TP53	-0.527106	0.0115	Directly binds both BAK and BAX and activates them
SLC25A5	-0.417006	0.02385	Adenine nucleotide translocator forms part of permeability transition pore
PPIF	-0.782612	0.00005	Cyclophilin D forms part of permeability transition pore
ANP32A	-0.509277	0.00615	Enhances APAF1 function

Table 10: Down-regulated genes in the apoptosis function of HCT116 5/4 cell line

GENE NAME	CHROMOSOME	VARIANT DESCRIPTION	ROLE
-----------	------------	---------------------	------

MAPK1	22	22117726 CT/C: DEL: 3'UTR	Inhibitors of CASP9 activity
BAX	19	49459104 A/G: SNP: Intron	Bcl-2 family member propagating apoptosis
ANP32A	15	69072241 C/A: SNP: 3'UTR	Enhances APAF1 function

Table 11: Mutated genes in the apoptosis function of the HCT116 5/4 cell line

We observe several genes involved in propagating apoptosis are down-regulated. For example, BIK and BID, which propagates apoptosis are down-regulated. In addition, TP53, which activates apoptotic proteins is down-regulated and BCL2L1, which is an anti-apoptotic protein is up-regulated. Thus we hypothesize that the apoptosis handling by mitochondria in the HCT116 5/4 cell line is lower and the cell death is rather deviated.

Heme biosynthesis

One gene was up-regulated (Table 12) and two genes were down-regulated (Table 13) in the heme biosynthesis function.

GENE NAME	LOG2FOLD	P-VALUE	ROLE
ALAS1	0.519619	0.00555	Catalyzes the reaction in which glycine and succinyl CoA from TCA cycle condenses to form aminolevulinate (ALA) and CO ₂

Table 12: Up-regulated genes in the heme biosynthesis function of HCT116 5/4 cell line

GENE NAME	LOG2FOLD	P-VALUE	ROLE
CPOX	-0.44759	0.0161	Coproporphyrinogen III is transported to mitochondria and in the presence of coproporphyrinogen III oxidase it is oxidatively decarboxylated
UROD	-0.458474	0.02375	Uroporphyrinogen III decarboxylase catalyzes stepwise decarboxylation of the Uroporphyrinogen III forming Coproporphyrinogen III

Table 13: Down-regulated genes in the heme biosynthesis function of HCT116 5/4 cell line

We observe two genes involved in catalyzing the synthesis of heme are downregulated. For example, CPOX and UROD catalyze the consecutive steps in generation of heme. This suggests that synthesis of heme in the HCT116 5/4 cell line could be lower compared to its wild type cell line.

Glycolysis

Seven genes were up-regulated (Table 14) and three genes were down-regulated (Table 15) in the glycolysis function.

GENE NAME	LOG2FOLD	P-VALUE	ROLE
SLC2A1	0.432796	0.01935	Basal glucose uptake, present in all mammalian tissues
SLC2A3	2.87322	0.00005	
PFKP	0.582218	0.0018	Fructose 6-phosphate is phosphorylated to fructose 1,6-bisphosphate, catalyzed by phosphofructokinase
ALDOA	0.694506	0.00045	Fructose 1,6-bisphosphate converted into glyceraldehyde 3-phosphate and dihydroxyacetone phosphate catalyzed by aldolase
GAPDH	0.440829	0.0264	Glyceraldehyde 3-phosphate is converted into 1,3-bisphosphoglycerate catalyzed by glyceraldehyde 3-phosphate dehydrogenase
PKM2	1.1138	0.00005	Phosphoenolpyruvate is converted into pyruvate and ATP is produced, catalyzed by pyruvate kinase
LDHA	0.906536	0.00005	Pyruvate is converted to lactate catalyzed by lactate dehydrogenase

Table 14: Up-regulated genes in the glycolytic function of HCT116 5/4 cell line

GENE NAME	LOG2FOLD	P-VALUE	ROLE
PFKM	-0.637924	0.00065	Fructose 6-phosphate is phosphorylated to fructose 1,6-bisphosphate, catalyzed by phosphofructokinase
ENO3	-0.510749	0.0458	2-phosphoglycerate is converted into phosphoenolpyruvate catalyzed by enolase

LDHB	-0.502223	0.0062	Pyruvate is converted to lactate catalyzed by lactate dehydrogenase
------	-----------	--------	---

Table 15: Down-regulated genes in the glycolytic function of HCT116 5/4 cell line

We observe genes catalysing several steps of the glycolysis function are up-regulated. For example, PFKP, ALDOA and GAPDH catalysing consecutive steps are up-regulated. In addition PKM2, which catalyzes the conversion of phosphoenolpyruvate to pyruvate resulting in the generation of glycolytic ATP is up-regulated. Further the step in which pyruvate is converted to lactate is up-regulated. This suggests that generation of glycolytic energy is higher in HCT116 5/4 cell line compared to its wild type cell line.

TCA cycle

Two genes were up-regulated (Table 16) in the TCA function.

GENE NAME	LOG2FOLD	P-VALUE	ROLE
ACO2	0.711058	0.0058	Aconitase catalyzes the interconversion of citrate to isocitrate
SDHA	0.864782	0.00005	Part of Succinate dehydrogenase complex in oxidative phosphorylation in TCA cycle it catalyzes the oxidation of succinate to fumarate

Table 16: Up-regulated genes in the TCA cycle of HCT116 5/4 cell line

Enzymes catalysing two steps in the TCA cycle were up-regulated. For instance SDHA, which contributes electrons to the electron transport chain is up-regulated. This suggests that the energy intermediates provision to the electron transport chain is higher in HCT116 5/4 cell line compared to its wild type cell line.

Pyruvate transfer

One gene was up-regulated (Table 17) in the pyruvate transfer function.

GENE NAME	LOG2FOLD	P-VALUE	ROLE
BRP44	0.851159	0.02225	Involved in the transfer of pyruvate inside mitochondria.

Table 17: Up-regulated gene in the pyruvate transfer of HCT116 5/4 cell line

We observe that the pyruvate transfer is up-regulated in the HCT116 5/4 cell line. This suggests that there might be increased transport of pyruvate into mitochondria in the HCT116 5/4 cell line.

Fe-S cluster biosynthesis

Two genes were up-regulated (Table 18) and six genes were down-regulated (Table 20) in the Fe-S cluster biosynthesis function.

GENE NAME	LOG2FOLD	P-VALUE	ROLE
LYRM4	0.620275	0.00535	Assembles with NFS1
SLC25A28	0.495234	0.0161	Mitochondrial iron transporter

Table 18: Up-regulated genes in the Fe-S cluster biosynthesis of HCT116 5/4 cell line

GENE NAME	LOG2FOLD	P-VALUE	ROLE
FDXR	-1.10918	0.00005	Provide reducing equivalents to electron transfer chain and contribute to iron-sulfur cluster biogenesis
GLRX5	-0.491317	0.01235	Fe-S cluster transfer protein directly to the apoprotein
NUBP2	-0.403011	0.04425	Required for the assembly of cytosolic iron-sulfur proteins
CIAPIN1	-0.563682	0.03685	Facilitates NUBP1 and NUBP2 assembly
FAM96A	-0.75034	0.00035	Components of the cytosolic Fe/S protein assembly (CIA) machinery
MMS19	-0.494624	0.01025	Cytosolic Fe/S protein assembly targeting factor

Table 19: Down-regulated genes in the Fe-S cluster biosynthesis of HCT116 5/4 cell line

We observe several genes in the Fe-S cluster biosynthesis function down-regulated. For example, FDXR and GLRX5 involved in providing Fe-S clusters to the apoproteins are down-regulated. Thus we hypothesize that the amount of Fe-S clusters provided to apoproteins is lower in the HCT116 5/4 cell line.

Mitochondrial dynamics

Three genes were up-regulated (Table 20), seven genes were down-regulated (Table 21) and a single gene is mutated (Table 22) in the mitochondrial dynamics function respectively.

GENE NAME	LOG2FOLD	P-VALUE	ROLE
PINK1	0.483554	0.01525	Involved in the mitochondrial fusion, PINK1 phosphorylates PARK2 and consequently PARK2 induced ubiquitination of mitofusins
BNIP3L	0.718376	0.00055	Involved in the mitophagy, cause permeabilization of the mitochondrial membrane and also regulate mitophagy
SQSTM1	1.77694	0.00005	Involved in the mitophagy, recruited to mitochondria and binds mitochondrial substrates on the autophagosomes

Table 20: Up-regulated genes in the mitochondrial dynamics of the HCT116 5/4 cell line

GENE NAME	LOG2FOLD	P-VALUE	ROLE
STOML2	-0.472715	0.01355	Involved in the mitochondrial fusion, scaffold proteins coordinate stability of the OPA1
PLD6	-0.59024	0.00965	Involved in the mitochondrial fusion, promotes mitofusin-mediated fusion
TRAP1	-0.769066	0.0001	Involved in the mitochondrial fission, known to regulate fission proteins DNM1L and MFF
FIS1	-0.422012	0.0405	Involved in the mitochondrial fission, facilitates binding and assembly of DNM1L
PKIA	-1.03206	0.00015	Involved in the mitochondrial fission, is known to inhibit GTPase activity of DNM1L
SYBU	-1.5281	0.00005	Involved in the mitochondrial movement, have a role in linking the mitochondria to KIF5B
TRAK1	-0.521443	0.0098	Involved in the mitochondrial movement, acts as an adapter linking kinesin-1 to mitochondria

Table 21: Down-regulated genes in the mitochondrial dynamics of the HCT116 5/4 cell line

GENE NAME	CHROMOSOME	VARIANT DESCRIPTION	ROLE
KIF5B	10	32300337 AT/A: DEL: 3'UTR	Involved in the mitochondrial movement, have role in the mitochondrial distribution in neurons

Table 22: Mutated genes in the mitochondrial dynamics of HCT116 5/4 cell line

We observe that the genes involved in the mitophagy are up-regulated. For example BNIP3L and SQSTM1, which are involved in the mitochondrial membrane permeabilization and binds mitochondrial substrates on the autophagosomes are up-regulated. Thus we hypothesize that the mitochondrial clearance is higher in the HCT116 cell line.

Import and sorting

Three genes were up-regulated (Table 23), seven genes were down-regulated (Table 24) and two genes were mutated (Table 25) in the import and sorting function.

GENE NAME	LOG2FOLD	P-VALUE	ROLE
TIMM17B	2.09787	0.00015	Inner membrane translocation, might influence the channel activity formed by the TIMM23
HSPA9	1.07547	0.00005	Presequence translocase associated motor, binds to the preprotein and drives it into the matrix in association with other chaperones
GRPEL2	0.654656	0.0014	Presequence translocase associated motor, acts as a nucleotide exchange factor releasing the ADP from HSPA9

Table 23: Up-regulated genes in the import and sorting of HCT116 5/4 cell line

GENE NAME	LOG2FOLD	P-VALUE	ROLE
-----------	----------	---------	------

TOMM20	-0.414885	0.0233	Outer membrane translocation, recognize presequences on the mitochondrial outer membrane
TOMM40L	-0.686537	0.0049	Outer membrane translocation, forms the outer membrane channel forming protein
TOMM5	-0.95617	0.00005	Outer membrane translocation, transports preprotein to the import pore formed by TOMM40
GRPEL1	-0.559974	0.00565	Presequence translocase associated motor, acts as a nucleotide exchange factor releasing the ADP from HSPA9
TIMM8A	-0.540888	0.03815	Inner membrane carrier pathway, forms complex with TIMM13 and also performs the transfer of inner membrane proteins
TIMM13	-0.557188	0.0065	Inner membrane carrier pathway, forms complex with TIMM8 and performs the transfer of inner membrane proteins
IMMP2L	-0.817128	0.00225	Inner membrane peptidase that cleaves hydrophobic sorting signal

Table 24: Down-regulated genes in the import and sorting of HCT116 5/4 cell line

GENE NAME	CHROMOSOME	VARIANT DESCRIPTION	ROLE
HSPA9	5	137904629 T/C: SNP: Missense_Mutation	Presequence translocase associated motor, binds to the preprotein and drives it into the matrix in association with other chaperones
PMPCA	9	139318040 G/A: SNP: 3'UTR	Presequence of pre-proteins are removed by proteolytic enzyme mitochondrial processing peptidase

Table 25: Mutated genes in the import and sorting of the HCT116 5/4 cell line

The genes, which conduct outer membrane translocation and those which transfer of inner membrane proteins were down-regulated. This suggest that the transport of proteins into mitochondria might be lower in the HCT 116 5/4 cell line. In addition, the assembly of inner membrane proteins in HCT116 5/4 cell line might be lower too.

Replication and transcription

Three genes were up-regulated (Table 26), sixteen genes were down-regulated (Table 27) and three genes were mutated (Table 28) in the replication and transcription function.

GENE NAME	LOG2FOLD	P-VALUE	ROLE
TK2	0.558719	0.00705	Involved in the phosphorylation of recycled deoxyribonucleosides in mitochondria specific for thymidine, cytidine and uridine
CMPK2	1.83451	0.00005	Phosphorylates the deoxyribonucleoside monophosphates specifically on dAMP
TRMT2B	0.522388	0.0183	Shows posttranscriptional modifications activity in the human mitochondrial tRNAs

Table 26: Up-regulated genes in the replication and transcription of the HCT116 5/4 cell line

GENE NAME	LOG2FOLD	P-VALUE	ROLE
C10orf2	-1.0818	0.00005	Mitochondrial DNA (mtDNA) helicase (TWINKLE) plays an important role in the maintenance of mtDNA
TERT	-1.74289	0.00005	Role in the protection of mitochondrial integrity with a suggested role in mtDNA replication and/or repair
TFAM	-0.667959	0.0012	A key activator of mitochondrial transcription and also functions in replication and repair
RMRP	-1.2317	0.00875	RNA component of mitochondrial RNA processing endoribonuclease cleaves mitochondrial RNA at the priming site of mitochondrial DNA replication
APEX1	-0.692803	0.00015	Involved in the mitochondrial DNA base excision repair
POLG2	-0.807134	0.0002	Mitochondrial DNA polymerase, and also shows 3' to 5' exonuclease activity and ensure faithful replication
AK3	-0.425085	0.0288	Phosphorylates the deoxyribonucleoside monophosphates specifically on dAMP
SLC25A19	-1.45292	0.00005	Transports thiamine pyrophosphates into mitochondria
SLC29A1	-0.466474	0.0178	Equilibrative nucleoside transporter 1 imports recycled deoxyribonucleosides from cytoplasm into mitochondria
TRMT11	-0.546232	0.01295	

TRMT1	-0.460001	0.0206	Shows posttranscriptional modifications activity in the human mitochondrial tRNAs
PUS1	-0.824706	0.0001	
RPUSD4	-0.614644	0.0021	
QTRT1	-0.432503	0.04655	
QTRTD1	-0.472775	0.0176	
TRIT1	-0.563625	0.00705	

Table 27: Down-regulated genes in the replication and transcription of the HCT116 5/4 cell line

GENE NAME	CHROMOSOME	VARIANT DESCRIPTION	ROLE
TK2	16	66544965 C/T: SNP: 3'UTR	Involved in the phosphorylation of recycled deoxyribonucleosides in mitochondria specific for thymidine, cytidine and uridine
AK4	1	65696724 TA/T: DEL: 3'UTR	Phosphorylates the deoxyribonucleoside monophosphates specifically on dAMP
QTRTD1	3	113784299 A/C: SNP: Intron	Shows posttranscriptional modifications activity in the human mitochondrial tRNAs

Table 28: Mutated genes in the replication and transcription of the HCT116 5/4 cell line

We observe several genes involved in the replication and transcription is down-regulated in the HCT116 5/4 cell line e.g., POLG2, TFAM, TERT and C10orf2. Thus we hypothesize that the DNA biosynthesis might be reduced in the HCT116 5/4 cell line compared to its wild type cell line.

Translation

Three genes were up-regulated (Table 29), twenty nine genes were down-regulated (Table 30) and four genes were mutated (Table 31) in the translation function.

GENE NAME	LOG2FOLD	P-VALUE	ROLE
FARS2	0.819286	0.0013	Involved in the specific attachment of phenylalanine amino acid to its cognate tRNA
GFM2	1.05133	0.0034	Involved in the elongation and termination phases of the translation process may also be involved in the ribosome recycling
MRPS30	0.834859	0.00005	Mitoribosome which forms a part of mitochondrial translation machinery

Table 29: Up-regulated genes in the translation function of HCT116 5/4 cell line

GENE NAME	LOG2FOLD	P-VALUE	ROLE
MARS2	-0.823736	0.00015	Involved in the specific attachment of methionine amino acid to its cognate tRNA
AARS2	-0.509629	0.01985	Involved in the specific attachment of alanine amino acid to its cognate tRNA
NARS2	-0.679407	0.0018	Involved in the specific attachment of asparagine amino acid to its cognate tRNA
DARS2	-0.406307	0.0474	Involved in the specific attachment of aspartic acid amino acid to its cognate tRNA
PARS2	-0.512162	0.0259	Involved in the specific attachment of proline amino acid to its cognate tRNA
MRRF	-0.694552	0.0206	Acts as a mitochondrial ribosome recycling factor during translation process
PTCD3	-0.379742	0.0442	Associates with mitochondrial small ribosomal subunit and regulates translation
MRPL3	-0.456574	0.0165	Mitoribosome which forms a part of mitochondrial translation machinery
MRPL4	-0.466443	0.0197	
MRPL10	-0.45632	0.0178	
MRPL11	-0.542947	0.00575	
MRPL12	-1.01731	0.00005	
MRPL19	-0.39658	0.0423	
MRPL30	-0.517519	0.00755	
MRPL36	-0.603458	0.00465	
MRPL38	-0.783028	0.00005	
MRPL50	-0.691954	0.00125	
MRPS14	-0.578458	0.00845	

MRPS15	-0.416237	0.03435	Mitoribosome which forms a part of mitochondrial translation machinery
MRPS17	-0.47862	0.03125	
MRPS18B	-0.381176	0.04885	
MRPS21	-0.477955	0.0225	
MRPS26	-0.688225	0.00075	
MRPS27	-0.401445	0.03325	
MRPS33	-0.540767	0.00995	
MRPS7	-0.916785	0.00255	
TACO1	-0.65952	0.00185	Translational activator of complex IV subunit
CLPP	-0.688411	0.0009	Involved in the post translational quality control, has re-solubilization activity of protein aggregates
DDX28	-0.678136	0.02055	May be involved in the biogenesis of mitochondrial ribosomes

Table 30: Down-regulated genes in the translation function of HCT116 5/4 cell line

GENE NAME	CHROMOSOME	VARIANT DESCRIPTION	ROLE
LARS2	3	45527240 G/A: SNP: Missense Mutation	Involved in the specific attachment of leucine amino acid to its cognate tRNA
MRPL45	17	36478776 G/A: SNP: 3'UTR	Mitoribosome which forms a part of mitochondrial translation machinery
MRPL54	19	3765222 C/T: SNP: Silent	
LRPPRC	2	44145196 A/G: SNP: Missense Mutation	Might play a role in the translation and stability of COX subunits

Table 31: Mutated genes in the translation function of HCT116 5/4 cell line

Several amino acyl tRNA synthetases and mitoribosomes were down-regulated in the HCT116 5/4 cell line. Thus we hypothesize that the amount of proteins produced inside mitochondria is lower in HCT116 5/4 cell line.

Calcium transport

Three genes were up-regulated (Table 32) and one gene was down-regulated (Table 33) in the calcium transport function.

GENE NAME	LOG2FOLD	P-VALUE	ROLE
CCDC109B	0.672219	0.0025	Forms an important component of mitochondrial calcium uniporter with MCU
ITPR1	0.641122	0.00285	Component of the Inositol-1,4,5-trisphosphate receptors channels used for the fluxes of Ca ²⁺ from ER to mitochondria
PML	0.658306	0.00355	Regulates Inositol-1,4,5-trisphosphate receptor mediated Ca ²⁺ release from the ER

Table 32: Up-regulated genes in the calcium transport of the HCT116 5/4 cell line

GENE NAME	LOG2FOLD	P-VALUE	ROLE
SIGMAR1	-0.757161	0.00005	Stabilises the Inositol-1,4,5-trisphosphate receptors and ensures proper Ca ²⁺ fluxes

Table 33: Down-regulated genes in the calcium transport of the HCT116 5/4 cell line

We observe that genes which are involved in the transfer of calcium into mitochondria and those which regulate the transfer of calcium from ER into mitochondria were up-regulated. This suggests that there is an increase in the transfer of calcium into mitochondria in the HCT116 5/4 cell line.

Cardiolipin biosynthesis

Two genes were up-regulated (Table 34) in the cardiolipin biosynthesis function.

GENE NAME	LOG2FOLD	P-VALUE	ROLE
CDS1	-2.01287	0.00005	Converts phosphatidic acid to cytidine diphosphate diacylglycerol
PGS1	-0.529839	0.01175	Phosphatidylglycerol synthase converts cytidine diphosphate diacylglycerol to phosphatidylglycerol phosphate

Table 34: Down-regulated genes in the cardiolipin biosynthesis function of the HCT116 5/4 cell line

We observe that two steps in the cardiolipin biosynthesis function is up-regulated in the HCT116 5/4 cell line. This suggests that there is increase in the availability of cardiolipin in the HCT116 5/4 cell line.

ROS defence

Two genes were up-regulated (Table 35) and four genes were down-regulated (Table 36) in the ROS defence function.

GENE NAME	LOG2FOLD	P-VALUE	ROLE
GCLM	1.15434	0.00005	Catalyzes the first step reaction which combines cysteine and glutamate to form glutamylcysteine
SHC1	0.931169	0.00005	Could be involved in the generation of the hydrogen peroxide independent of superoxides in mitochondria

Table 35: Up-regulated genes in the ROS defence of the HCT116 5/4 cell line

GENE NAME	LOG2FOLD	P-VALUE	ROLE
GSR	-0.504019	0.00795	Reduces oxidized glutathione which can be re utilized by GPX1
GLRX2	-1.43993	0.00005	Involved in the control of mitochondrial protein glutathionylation
GSTA1	-2.89425	0.00835	Mitochondrial glutathione-S-transferases through glutathione conjugation or peroxide reduction detoxify harmful by-products
GSTA2	-2.34913	0.00155	

Table 36: Down-regulated genes in the ROS defence of the HCT116 5/4 cell line

We observe that GSR, which reduces oxidized glutathione and glutathione-S-transferases, which detoxify harmful by-products are down-regulated. Thus we hypothesize that there is a build up of ROS in the mitochondria in the HCT116 5/4 cell line.

3.1.3.1 Summary for HCT116 5/4 MitoModel

In total, there were 16 function that were observed to be affected in the HCT116 5/4 cell line. Further we observe that the MitoModel had more down- (102) compared to up-regulated genes (49). Most number of down-regulated genes were present in the translation function with 29 genes affected. We also observed several (22) genes with mutations HCT116 5/4 MitoModel (Figure 13).

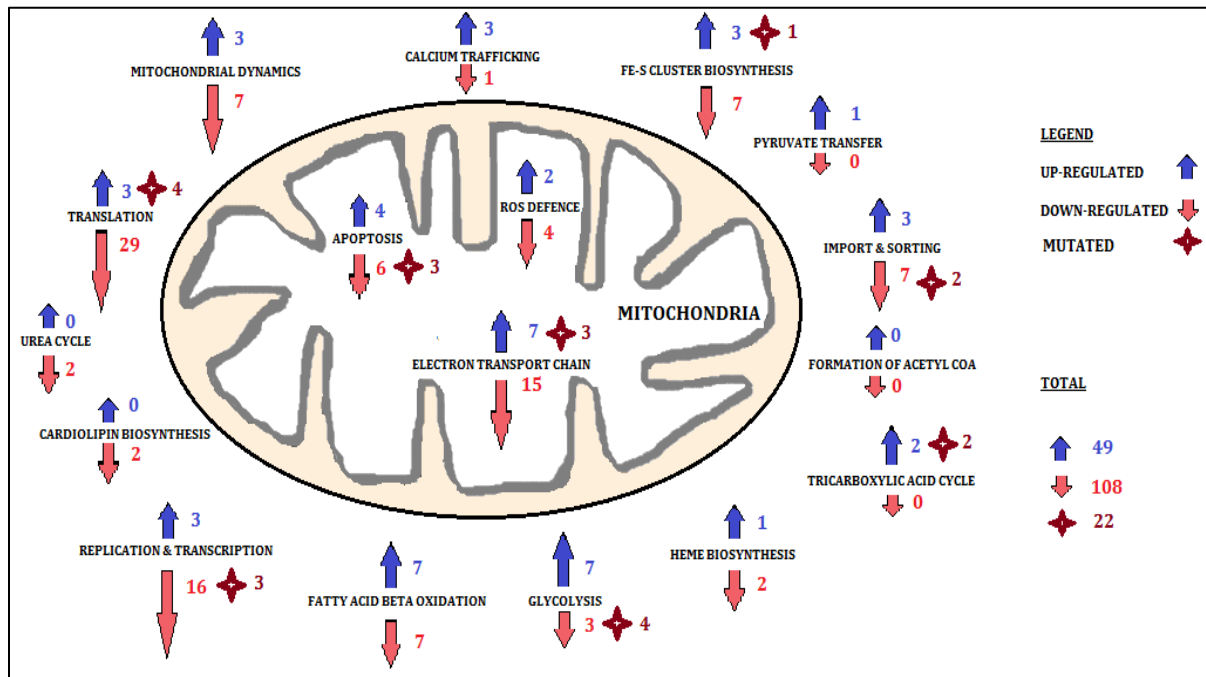


Figure 13: Number of affected genes observed on all the functions of HCT116 5/4 MitoModel

3.1.4 MitoModel of the RPE1 5/3 12/3 cell line:

After mapping the input mutation and expression files, the visual representation of the RPE1 5/3 12/3 MitoModel (Figure 14), displays the genes which are up-regulated, down-regulated and mutated.

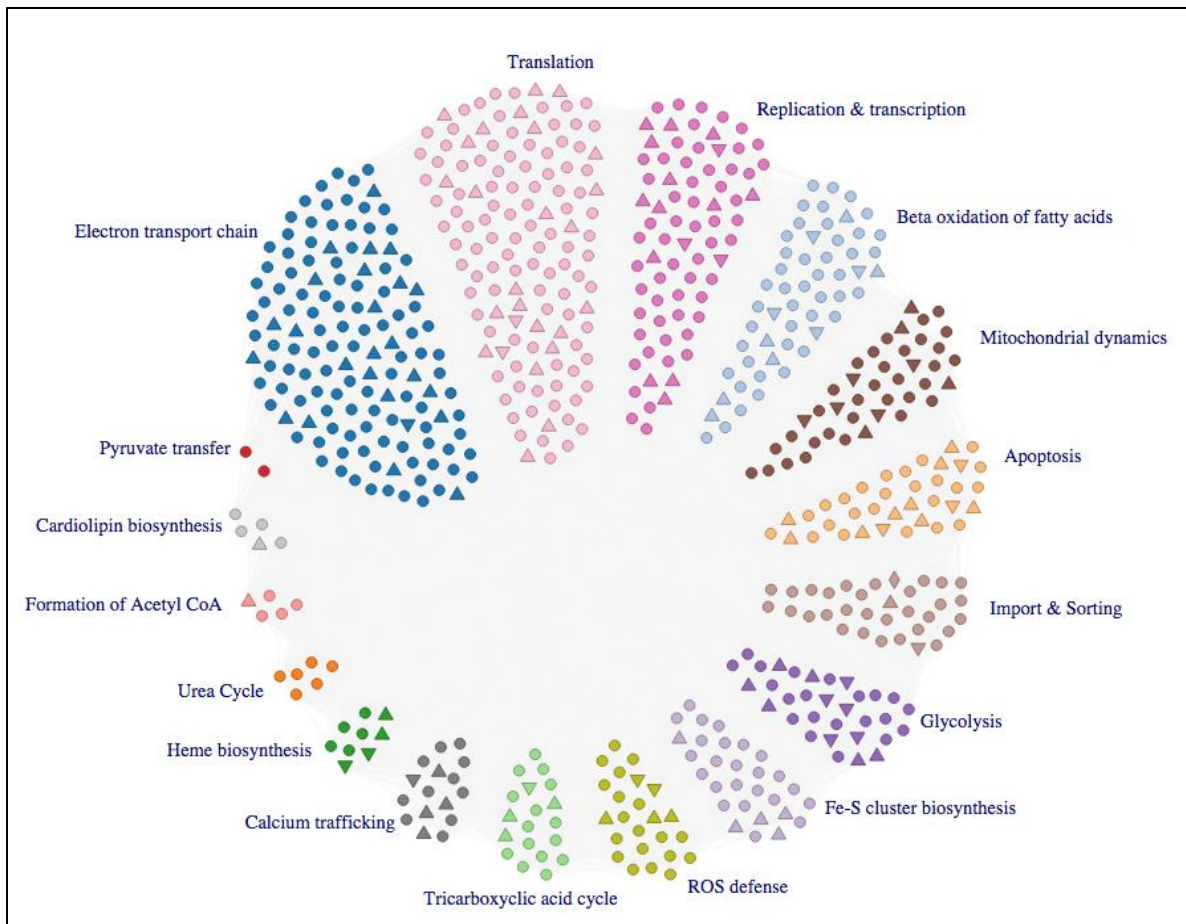


Figure 14: Visual display of the RPE1 5/3 12/3 MitoModel

Principal functions were observed to be misregulated (Figure 15) based on the percentage, and they are: Heme biosynthesis with 44% genes affected; glycolysis with 34% genes impaired; Apoptosis with 33% genes inflicted; Calcium transport with 31% genes defective, and so on.

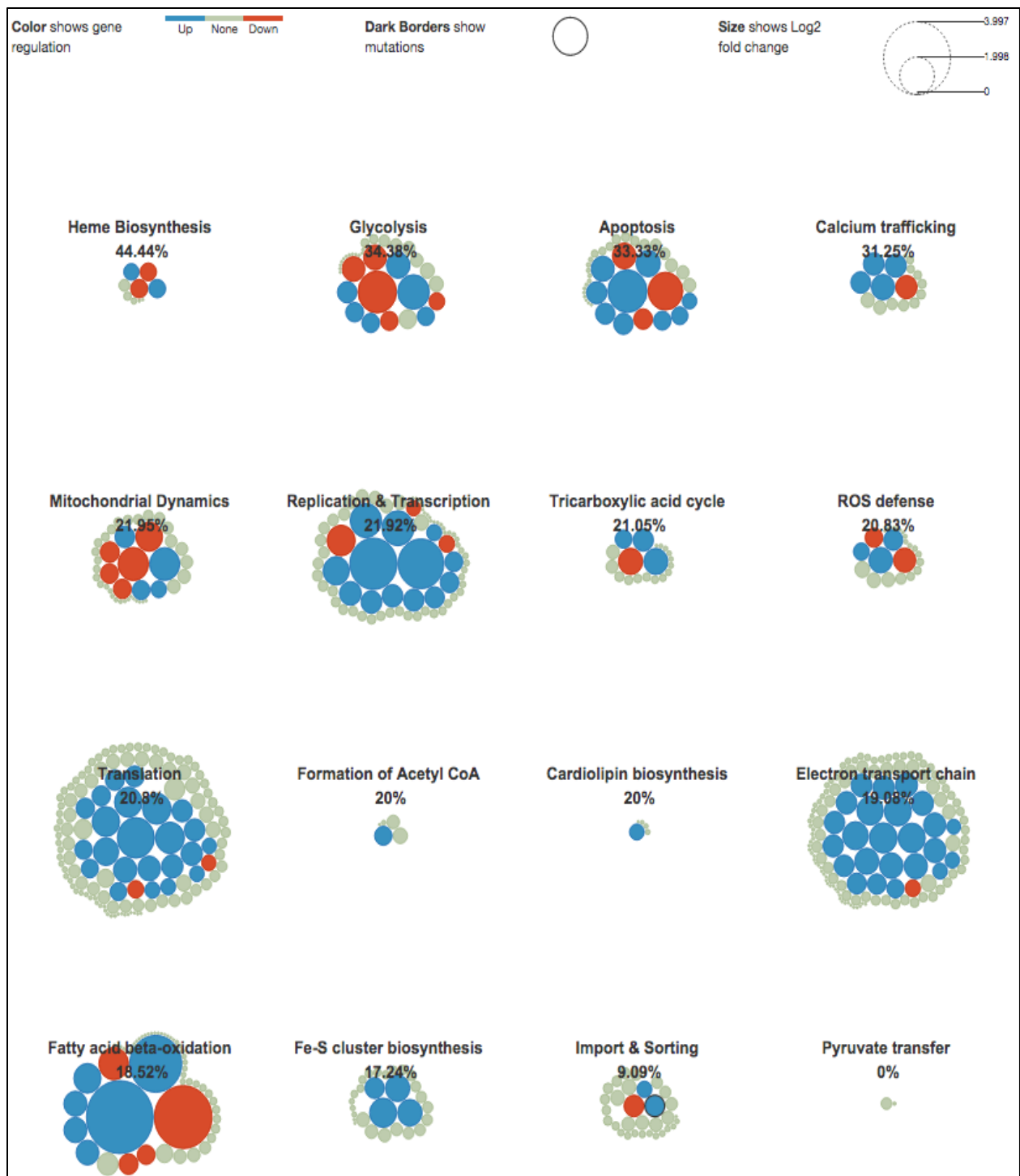


Figure 15: Percentage (%) of affected functions observed on the RPE1 5/3 12/3 MitoModel

To further explore the roles of the variant genes, each function was studied for the variant genes and its roles.

Electron transport chain and energy production

Twenty four genes were up-regulated (Table 37) and a single gene was down-regulated (Table 38) in the electron transport chain function.

GENE NAME	LOG2FOLD	P-VALUE	ROLE
NDUFA2	0.847609	0.00005	Nuclear encoded essential components of complex I NADH dehydrogenase, involved in the reduction of ubiquinone by NADH
NDUFA9	0.697875	0.00005	
NDUFA12	0.571784	0.0009	
NDUFB4	0.330836	0.0442	
NDUFS4	0.796412	0.00005	
NDUFS6	0.887836	0.00005	
NDUFS8	0.507377	0.00305	
NDUFV1	0.573347	0.001	
FOXRED1	0.824873	0.00005	
NDUFAF2	0.639314	0.00085	
TMEM126B	0.616229	0.00065	
UQCRQ	0.686108	0.00005	Nuclear encoded essential component of complex III, transfers electrons from ubiquinol to cytochrome c
COX5A	0.3649	0.02995	Nuclear encoded cytochrome c oxidase subunits, essential components of complex IV, catalyses the reduction of oxygen to water by cytochrome c
COX6A1	0.636835	0.0001	
COX7C	0.722798	0.00005	
COX8A	0.583068	0.00045	
C7orf44	0.448529	0.0107	Complex IV assembly factor
CHCHD8	0.595943	0.00085	
COX14	0.553737	0.00275	
COX17	0.522548	0.008	

SURF1	0.361213	0.0482	
ATP5B	0.645664	0.00045	Nuclear encoded ATP synthase subunits, essential components of complex V, reversible pump of protons into matrix with formation of ATP
ATP5G2	0.855464	0.00005	
ATP5L	0.647057	0.0066	

Table 37: Up-regulated genes in the electron transport chain of RPE1 5/3 12/3 cell line

GENE NAME	LOG2FOLD	P-VALUE	ROLE
NUBPL	-0.389781	0.0426	Complex I assembly factor

Table 38: Down-regulated gene in the electron transport chain function of RPE1 5/3 12/3 cell line

We observe that several genes involved in the complex I, III, IV and V are up-regulated in the RPE1 5/3 12/3 cell line. Further assembly factors of complex I and IV are up-regulated. This suggests that there might be an increased stress for energy production by electron transport chain in the RPE1 5/3 12/3 cell line.

Fatty acid beta oxidation and generation of acetyl CoA

Six genes were up-regulated (Table 39) and four genes were down-regulated (Table 40) in the fatty acid beta oxidation function.

GENE NAME	LOG2FOLD	P-VALUE	ROLE
SLC27A3	0.675558	0.0193	Readily converts the transported very long chain fatty acids to acyl-CoAs
ACSL5	3.99654	0.00005	Acyl-CoA synthetase activity for long chain free fatty acids and are also involved in the activation of fatty acids
ACSS3	2.46516	0.00005	Acyl-CoA synthetase activity for short chain fatty acids
FABP5	0.682189	0.0001	Fatty acid binding proteins involved in the import and export of fatty acids
ACAD8	0.665542	0.0004	Involved in the catabolism of fatty acids

ACAD10	0.8601	0.00005	Involved in the catabolism of fatty acids with significant activity towards branched chains
--------	--------	---------	---

Table 39: Up-regulated genes in the fatty acid beta oxidation function of RPE1 5/3 12/3 cell line

GENE NAME	LOG2FOLD	P-VALUE	ROLE
ACSL1	-0.518211	0.0031	Acyl-CoA synthetase activity for long chain free fatty acids and are also involved in the activation of fatty acids
CPT1C	-2.98183	0.00005	Carnitine palmitoyl transferase converts an acyl-CoA into an acylcarnitine
SLC25A20	-0.474659	0.0271	Carnitine acylcarnitine translocase mediates acylcarnitine entry into mitochondria
ACAA2	-0.980128	0.00005	Medium chain 3-ketoacyl-CoA thiolase

Table 40: Down-regulated genes in the fatty acid beta oxidation function of RPE1 5/3 12/3 cell line

We observe that several crucial genes are down-regulated in the RPE1 5/3 12/3 cell line. For example, Carnitine palmitoyl transferase (CPT1C), which converts acyl-CoA to acylcarnitine, SLC25A20, which mediates acylcarnitine entry into mitochondria. Further ACAA2, involved in the last step of beta-oxidation inside mitochondria is down-regulated. This suggests that the acetyl-CoA generation inside mitochondria by the beta-oxidation of fatty acids might be lower in RPE1 5/3 12/3 cell line compared to its wild type cell line.

Apoptosis

Nine genes were up-regulated (Table 41) and three genes were down-regulated (Table 42) in the apoptosis function.

GENE NAME	LOG2FOLD	P-VALUE	ROLE
APAF1	0.359293	0.04345	Binds CASP9 forming an apoptosome and activates it
DIABLO	0.532655	0.00165	Acts as caspase activator by inhibiting the inhibitors of apoptotic proteins

BAD	0.461006	0.04085	Bcl-2 family member propagating apoptosis
BCL2L11	1.50067	0.00005	Bim Bcl-2 family member propagating apoptosis
PMAIP1	0.729481	0.0002	Noxa Bcl-2 family member propagating apoptosis
BBC3	0.571182	0.0134	Puma Bcl-2 family member propagating apoptosis
VDAC1	0.678414	0.0001	Voltage dependent anion channel forms part of permeability transition pore
SLC25A5	0.423884	0.01255	Adenine nucleotide translocator forms part of permeability transition pore
EIF3M	0.531998	0.0027	PCI domain containing protein 1 can negatively regulate CASP9 activity

Table 41: Up-regulated genes in the apoptosis function of RPE1 5/3 12/3 cell line

GENE NAME	LOG2FOLD	P-VALUE	ROLE
BAK1	-0.706554	0.0004	Bcl-2 family member propagating apoptosis
SLC25A4	-0.509158	0.00335	Adenine nucleotide translocator forms part of permeability transition pore
DNM1	-1.24561	0.0267	Recruited to mitochondria can induce cristae remodelling to release cytochrome c and subsequent apoptosis

Table 42: Down-regulated genes in the apoptosis function of RPE1 5/3 12/3 cell line

We observe several genes coding for pro-apoptotic proteins are up-regulated. In addition, gene coding for voltage dependent anion channel, which control the release of cytochrome c from mitochondria is up-regulated. This suggests that there is an increase in the mitochondrial handling of apoptosis in the RPE1 5/3 12/3 cell line compared to its wild type cell line.

Heme biosynthesis

Two genes were up-regulated (Table 43) and two genes were down-regulated (Table 44) in the heme biosynthesis function.

GENE NAME	LOG2FOLD	P-VALUE	ROLE
ALAS1	0.382534	0.03435	Catalyzes the reaction in which glycine and succinyl CoA from TCA cycle condenses to form

			aminolevulinate (ALA) and CO ₂
HMBS	0.440116	0.01605	Hydroxymethylbilane synthase catalyzes head to tail condensation of four PBG and subsequent deamination to form a linear tetrapyrrole, Hydroxymethylbilane

Table 43: Up-regulated genes in the heme biosynthesis function of RPE1 5/3 12/3 cell line

GENE NAME	LOG2FOLD	P-VALUE	ROLE
FECH	-0.423414	0.0145	Ferrochelatase catalyzes the step involving the addition of Ferrous iron into the protoporphyrin IX to form the protoheme IX
CPOX	-0.446662	0.0117	Coproporphyrinogen III is transported to mitochondria and in the presence of coproporphyrinogen III oxidase it is oxidatively decarboxylated

Table 44: Down-regulated genes in the heme biosynthesis function of RPE1 5/3 12/3 cell line

We observe that crucial genes coding for the proteins required for the heme biosynthesis is down-regulated in the RPE1 5/3 12/3 cell line. For example, CPOX and FECH in the mitochondria are down-regulated, which play an import role in the heme biosynthesis. This suggests that there is a decreased synthesis of heme in the RPE1 5/3 12/3 cell line compared to its wild type cell line.

Glycolysis

Six genes were up-regulated (Table 45) and two genes were down-regulated (Table 46) in the glycolysis function.

GENE NAME	LOG2FOLD	P-VALUE	ROLE
SLC2A3	1.08432	0.00005	Basal glucose uptake, present in all mammalian tissues
PFKM	0.538878	0.0011	Fructose 6-phosphate is phosphorylated to fructose 1,6-bisphosphate, catalyzed by phosphofructokinase
GAPDH	0.700267	0.00455	Glyceraldehyde 3-phosphate is converted into 1,3-bisphosphoglycerate catalyzed by glyceraldehyde

			3-phosphate dehydrogenase
ENO1	0.467245	0.0223	2-phosphoglycerate is converted into phosphoenolpyruvate catalyzed by enolase
ENO2	0.446011	0.00905	
LDHB	0.476498	0.00725	Pyruvate is converted to lactate catalyzed by lactate dehydrogenase

Table 45: Up-regulated genes in the glycolysis function of RPE1 5/3 12/3 cell line

GENE NAME	LOG2FOLD	P-VALUE	ROLE
SLC2A1	-0.673644	0.0002	Basal glucose uptake, present in all mammalian tissues
GPI	-0.667722	0.00005	Isomerization of glucose 6-phosphate to fructose 6-phosphate by the phosphoglucose isomerase
PFKL	-0.400993	0.0185	Fructose 6-phosphate is phosphorylated to fructose 1,6-bisphosphate, catalyzed by phosphofructokinase
PFKP	-0.463312	0.0062	
ALDOC	-1.46654	0.00455	Fructose 1,6-bisphosphate converted into glyceraldehyde 3-phosphate and dihydroxyacetone phosphate catalyzed by aldolase

Table 46: Down-regulated genes in the glycolysis function of RPE1 5/3 12/3 cell line

We observe two genes involved in the generation of pyruvate to be up-regulated. For example, ENO1 and ENO2, catalyzes the formation of phosphoenolpyruvate leading to the generation of pyruvate in the next step. Further, LDHB, which converts pyruvate to lactate is up-regulated. This suggests that the pyruvate generation by glycolysis in the RPE1 5/3 12/3 cell line is higher compared to its wild type cell line.

Formation of Acetyl-CoA

There was a single gene up-regulated (Table 47) in the formation of acetyl-CoA function.

GENE NAME	LOG2FOLD	P-VALUE	ROLE
DLAT	0.460836	0.0075	Component of pyruvate dehydrogenase complex,

			catalyzes the overall conversion of pyruvate to acetyl CoA
--	--	--	--

Table 47: Up-regulated genes in the formation in the acetyl-CoA function of RPE1 5/3 12/3 cell line

We observe that the DLAT, a subunit of the pyruvate dehydrogenase complex is up-regulated in the RPE1 5/3 12/3 cell line. This suggests that the overall conversion of pyruvate to acetyl-CoA is higher in the RPE1 5/3 12/3 cell line compared to its wild type cell line.

TCA cycle

Three genes were up-regulated (Table 48) and one gene was down-regulated (Table 49) in the TCA cycle function.

GENE NAME	LOG2FOLD	P-VALUE	ROLE
CS	0.441377	0.0096	Citrate synthase catalyzes the synthesis of citrate from oxaloacetate and acetyl CoA
SDHA	0.567448	0.0004	Part of Succinate dehydrogenase complex in oxidative phosphorylation in TCA cycle it catalyzes the oxidation of succinate to fumarate
SDHD	0.71975	0.00005	

Table 48: Up-regulated genes in the TCA cycle function of RPE1 5/3 12/3 cell line

GENE NAME	LOG2FOLD	P-VALUE	ROLE
IDH2	-0.728959	0.00005	Isocitrate dehydrogenase catalyze the oxidative decarboxylation of isocitrate to 2-oxoglutarate

Table 49: Down-regulated gene in the TCA cycle function of RPE1 5/3 12/3 cell line

Crucial components of the succinate dehydrogenase complex are up-regulated. For example, SDHA and SDHD are upregulated in the RPE1 5/3 12/3 cell line. This suggests that the oxidation of succinate to fumarate and electron feeding to the electron transport chain is higher in the RPE1 5/3 12/3 cell line compared to its wild type cell line.

Fe-S cluster biosynthesis

4 genes were up-regulated (Table 50) in the Fe-S cluster biosynthesis function.

GENE NAME	LOG2FOLD	P-VALUE	ROLE
ISCU	0.735633	0.00005	Iron sulfur cluster assembly enzyme, Fe-S cluster intermediate is formed on it
SLC25A37	0.846412	0.00005	Functions as an essential iron importer
FDX1	0.740183	0.00005	Small iron-sulfur protein, transfers electrons from NADPH to mitochondrial cytochrome P450
NUBP1	0.529257	0.00305	Essential for both cytosolic iron-sulfur protein assembly and iron homeostasis

Table 50: Up-regulated genes in the Fe-S cluster biosynthesis of RPE1 5/3 12/3 cell line

We observe that several genes involved in the Fe-S cluster biosynthesis is up-regulated. For example; SLC25A37, required for the import of iron; and ISCU, required for the formation of Fe-S cluster intermediates inside mitochondria are up-regulated. This suggests that the biosynthesis of Fe-S cluster intermediates is higher in the RPE1 5/3 12/3 cell line compared to its wild type cell line.

Mitochondrial dynamics

Four genes were up-regulated (Table 51) and five genes were down-regulated (Table 52) in the mitochondrial dynamics function.

GENE NAME	LOG2FOLD	P-VALUE	ROLE
PHB2	0.546811	0.00085	Involved in the mitochondrial fusion, scaffold proteins coordinate stability of the OPA1
TRAP1	0.46533	0.0075	Involved in the mitochondrial fission, known to regulate fission proteins DNM1L and MF1
DNM1L	0.390909	0.02075	Involved in the mitochondrial fission, mediates the division of mitochondria
SQSTM1	0.999647	0.00005	Involved in the mitophagy, recruited to mitochondria and binds mitochondrial substrates on the autophagosomes

Table 51: Up-regulated genes in the mitochondrial dynamics function of RPE1 5/3 12/3 cell line

GENE NAME	LOG2FOLD	P-VALUE	ROLE
OPA3	-0.48298	0.03035	Involved in the mitochondrial fusion, interacts with MFN1 and involved in mitochondrial fragmentation
PLD6	-1.02164	0.0005	Involved in the mitochondrial fusion, promotes mitofusin-mediated fusion
MTFP1	-0.520328	0.01475	Involved in the mitochondrial fission, role in mitochondrial fragmentation and is dependent on DNMI1L expression
GDAP1	-0.837419	0.0002	Involved in the mitochondrial fission, known to have a role in the mitochondrial fragmentation
TRAK2	-0.47557	0.0043	Involved in the mitochondrial movement, acts as an adapter linking kinesin-1 to mitochondria

Table 52: Down-regulated genes in the mitochondrial dynamics function of RPE1 5/3 12/3 cell line

We observe that several crucial genes involved in the mitochondrial fusion, fission and movement are down-regulated. At the same time SQSTM1, which binds mitochondrial substrates to autophagosomes during mitophagy is up-regulated. This suggests that there is an increased clearing of mitochondria and deviation in mitochondrial dynamics of RPE1 5/3 12/3 cell line compared to its wild type cell line.

Import and sorting

Two genes were up-regulated (Table 53), one gene is down-regulated (Table 54) and one gene is mutated (Table 55) in the import and sorting function.

GENE NAME	LOG2FOLD	P-VALUE	ROLE
HSPA9	0.544413	0.0009	Presequence translocase associated motor, binds to the preprotein and drives it into the matrix in association with other chaperones and also involved in the mediation of the interaction between VDAC1 and Inositol-1,4,5-trisphosphate

			receptors.
GRPEL2	0.373354	0.04305	Presequence translocase associated motor, acts as a nucleotide exchange factor releasing the ADP from HSPA9.

Table 53: Up-regulated genes in the import and sorting function of RPE1 5/3 12/3 cell line

GENE NAME	LOG2FOLD	P-VALUE	ROLE
TOMM40L	-0.551265	0.00795	Outer membrane translocation, forms the outer membrane channel forming protein.

Table 54: Down-regulated genes in the import and sorting function of RPE1 5/3 12/3 cell line

GENE NAME	CHROMOSOME	VARIANT DESCRIPTION	ROLE
HSPA9	5	137892170 G/A: SNP: Silent, 137902339 T/C: SNP: Silent	Presequence translocase associated motor, binds to the preprotein and drives it into the matrix in association with other chaperones and also involved in the mediation of the interaction between VDAC1 and Inositol-1,4,5-trisphosphate receptors.

Table 55: Mutated genes in the import and sorting function of RPE1 5/3 12/3 cell line

We observe that the outer membrane channel forming protein facilitating the protein translocation into mitochondria is down-regulated. In addition, proteins involved in driving preproteins into matrix are up-regulated. This suggests that there might be an increased stress for proteins to enter into the mitochondria in the RPE1 5/3 12/3 cell line compared to its wild type cell line.

Replication and transcription

Thirteen genes were up-regulated (Table 56), three genes were down-regulated (Table 57) in the replication and transcription function.

GENE NAME	LOG2FOLD	P-VALUE	ROLE
TOP1MT	0.583414	0.0041	Suggested to have a role in the removal of

			positive supercoils created by helicase activity
TERT	2.06388	0.00005	Role in the protection of mitochondrial integrity with a suggested role in mtDNA replication and/or repair
RMRP	1.94861	0.00005	RNA component of mitochondrial RNA processing endoribonuclease cleaves mitochondrial RNA at the priming site of mitochondrial DNA replication
UNG	0.37312	0.0336	Prevent mutagenesis by eliminating uracil from DNA molecules
NTHL1	0.509429	0.0086	Involved in the repair of mismatches in DNA
POLG2	0.479997	0.0385	Acts as catalytic subunit of mitochondrial DNA polymerase
TRMT112	0.814351	0.00005	Shows posttranscriptional modifications activity in the human mitochondrial tRNAs
PUS1	0.565226	0.00435	
RPUSD4	1.09897	0.00005	
OSGEPL1	0.538049	0.0167	
PUS3	1.06192	0.00005	
NSUN2	0.629669	0.0001	
SLC25A3	0.587619	0.0011	Involved in the transport of phosphate into the mitochondrial matrix

Table 56: Up-regulated genes in the replication and transcription function of RPE1 5/3 12/3 cell line

GENE NAME	LOG2FOLD	P-VALUE	ROLE
AK4	-0.904575	0.00005	Phosphorylates the deoxyribonucleoside monophosphates specifically on dAMP
NME4	-0.344994	0.0405	Shows mitochondrial nucleoside diphosphate kinase activity
TRIT1	-0.391003	0.0405	Shows posttranscriptional modifications activity in the human mitochondrial tRNAs

Table 57: Down-regulated genes in the replication and transcription function of RPE1 5/3 12/3 cell line

Several genes are up-regulated in the replication and transcription function. For example; POLG2 and TERT which are required for the replication and repair are up-

regulated. This suggest that there is an increase in the requirement of the mitochondrial DNA in the RPE1 5/3 12/3 cell line compared to its wild type cell line.

Translation

Twenty three genes were up-regulated (Table 58) and 2 genes were down-regulated (Table 59) in the translation function.

GENE NAME	LOG2FOLD	P-VALUE	ROLE
YARS2	0.351731	0.04695	Involved in the specific attachment of tyrosine amino acid to its cognate tRNA
HARS2	0.612305	0.0005	Involved in the specific attachment of histidine amino acid to its cognate tRNA
TSFM	0.432196	0.0234	Involved in the elongation and termination phases of the translation process
MRPL10	0.574735	0.00085	Mitoribosomes which forms a part of mitochondrial translation machinery
MRPL11	0.668759	0.0001	
MRPL21	0.881521	0.00005	
MRPL22	0.781109	0.00005	
MRPL23	0.51228	0.00385	
MRPL36	0.872328	0.00005	
MRPL40	0.358002	0.0484	
MRPL42	0.464519	0.00745	
MRPL45	0.375467	0.03045	
MRPL48	0.527918	0.0049	
MRPL51	0.567403	0.00115	
MRPS18B	0.499942	0.00415	
MRPS27	0.937786	0.00005	
MRPS30	0.68526	0.0002	
MRPS31	0.448401	0.02095	
MRPS34	0.371246	0.03245	
MRPS35	0.612735	0.0003	

MRPS36	0.917542	0.00005	
RNASEL	1.38777	0.00005	Modulate the stability of mitochondrial mRNAs by interacting with MTIF2
OXA1L	0.496889	0.0029	May have a role in the insertion of proteins into inner membrane and also a complex V assembly factor

Table 58: Up-regulated genes in the translation function of RPE1 5/3 12/3 cell line

GENE NAME	LOG2FOLD	P-VALUE	ROLE
RARS2	-0.35519	0.04425	Involved in the specific attachment of arginine amino acid to its cognate tRNA
MRPS21	-0.410857	0.0272	Mitoribosomes which forms a part of mitochondrial translation machinery

Table 59: Down-regulated genes in the translation function of RPE1 5/3 12/3 cell line

Several mitoribosomes are up-regulated in the RPE1 5/3 12/3 cell line. Further amino acyl tRNA synthetases such as YARS2 and HARS2 are up-regulated. This suggests that there might be a higher production of mitochondrial polypeptides in the RPE1 5/3 12/3 cell line compared to its wild type cell line.

Calcium transport

Four genes were up-regulated (Table 60) and one gene was down-regulated (Table 61) in the calcium transport function.

GENE NAME	LOG2FOLD	P-VALUE	ROLE
SLC24A6	0.582622	0.0032	Involved in the calcium homeostasis by counteracting the calcium accumulation in the mitochondria
ITPR2	0.601475	0.0004	Component of the Inositol-1,4,5-trisphosphate receptors channels used for the fluxes of Ca ²⁺ from ER to mitochondria
TCHP	0.691381	0.0001	Involved in the regulation of ER mitochondria juxtaposition
PML	0.551688	0.0033	Regulates Inositol-1,4,5-trisphosphate receptor mediated Ca ²⁺ release from the ER

Table 60: Up-regulated genes in the calcium transport function of RPE1 5/3 12/3 cell line

GENE NAME	LOG2FOLD	P-VALUE	ROLE
MCU	-0.609827	0.0003	Involved in the accumulation of calcium ions in the matrix through ion impermeable inner mitochondrial membrane

Table 61: Down-regulated genes in the calcium transport function of RPE1 5/3 12/3 cell line

We observe several genes regulating the calcium release from ER into mitochondria is up-regulated. This suggests that there is an increase in the calcium release from ER to the mitochondria in RPE1 5/3 12/3 cell line.

Cardiolipin biosynthesis

One gene was up-regulated (Table 62) in the cardiolipin biosynthesis function.

GENE NAME	LOG2FOLD	P-VALUE	ROLE
PGS1	0.365077	0.04765	Phosphatidylglycerol synthase converts cytidine diphosphate diacylglycerol to phosphatidylglycerol phosphate

Table 62: Up-regulated genes in the Cardiolipin biosynthesis function of RPE1 5/3 12/3 cell line

A single step in cardiolipin biosynthesis function is up-regulated, as a consequence there could more production of cardiolipin in the RPE1 5/3 12/3 cell line.

ROS defence

Three genes were up-regulated (Table 63) and two genes were down-regulated (Table 64) in the ROS defence function.

GENE NAME	LOG2FOLD	P-VALUE	ROLE
GCLM	0.700054	0.00005	Catalyzes the first step reaction which combines cysteine and glutamate to form glutamylcysteine
SOD2	0.518861	0.00415	Dismutates the superoxide generated in the mitochondrial matrix to hydrogen peroxide
GSTP1	0.406851	0.019	Mitochondrial glutathione-S-transferases

			through glutathione conjugation or peroxide reduction detoxify harmful byproducts
--	--	--	---

Table 63: Up-regulated genes in the ROS defence function of RPE1 5/3 12/3 cell line

GENE NAME	LOG2FOLD	P-VALUE	ROLE
SLC25A1	-0.467231	0.0063	May be involved in the transport of glutathione into the mitochondria
GSTA4	-0.646611	0.00195	Mitochondrial glutathione-S-transferases through glutathione conjugation or peroxide reduction detoxify harmful byproducts

Table 64: Down-regulated genes in the ROS defence function of RPE1 5/3 12/3 cell line

We observe that genes involved in the reducing the ROS elements in the RPE1 5/3 12/3 cell line. For example SOD2, which reduces the superoxides generated in the mitochondrial matrix. Thus we hypothesize that superoxides in the mitochondria might be at a minimal level in RPE1 5/3 12/3 cell line.

3.1.4.1 Summary for RPE1 5/3 12/3 MitoModel

In total, there were 15 functions that were observed to be affected in the RPE1 5/3 12/3 MitoModel. Further, we observe that the MitoModel had more up- (107 genes) compared to down-regulated (30 genes) genes. Most number of the up-regulated genes were present in the electron transport chain function and translation function with 24 and 24 genes affected (Figure 16) respectively.

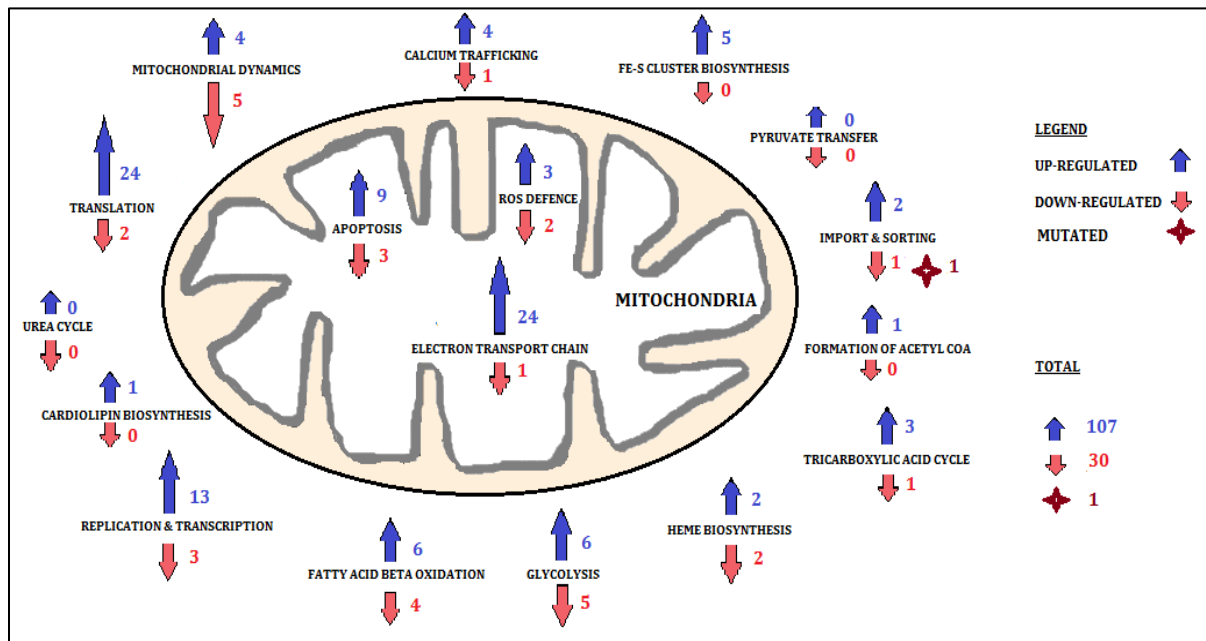


Figure 16: Number of affected genes observed on all the functions of RPE1H2B 5/3 12/3 MitoModel

3.1.5 MitoModel of the RPE1H2B 21/3 cell line:

Visual display of RPE1H2B 21/3 MitoModel after mapping the expression and mutation input files, describes the nodes which were up- and down-regulated (Figure 17).

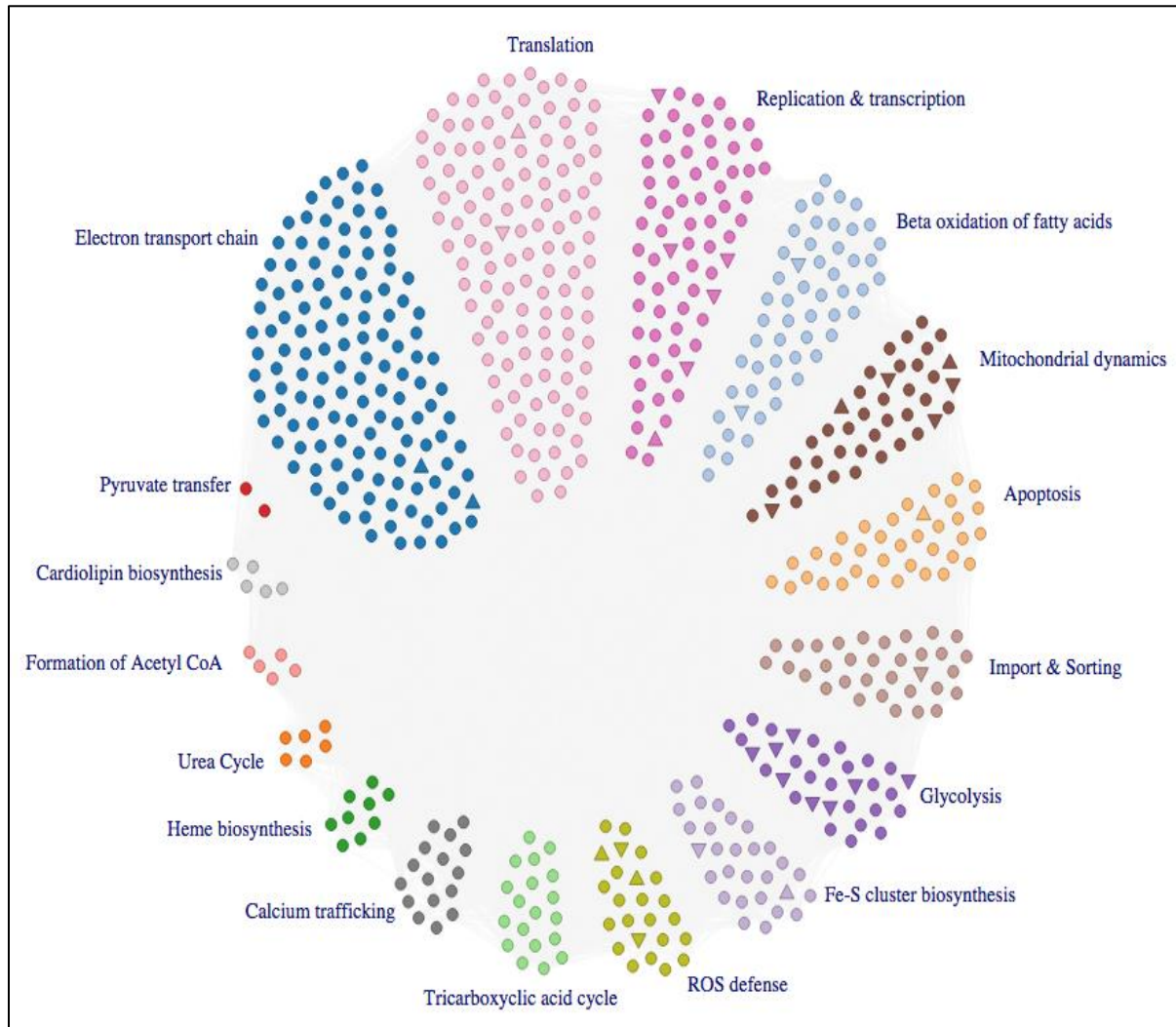


Figure 17: A visual representation of the RPE1H2B 21/3 MitoModel

Crucial functions that were observed to be affected based on the percentage are: Glycolysis with 25%; ROS defence with 17%; Mitochondrial dynamics with 15%; Replication and transcription with 8%; and so on (Figure 18).

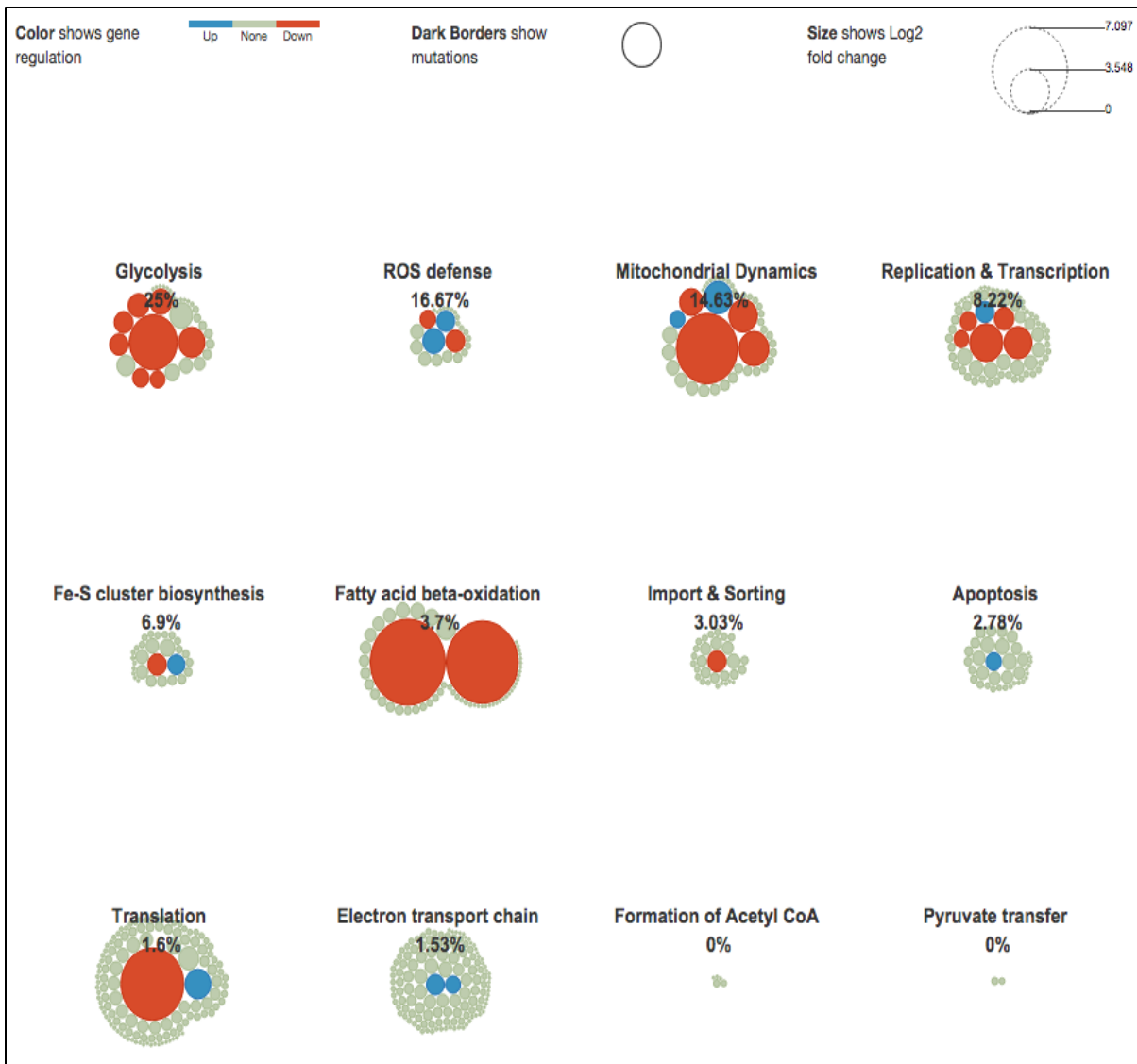


Figure 18: Percentage (%) of affected functions observed on the RPE1H2B 21/3 MitoModel

To further understand the affected functions, variant genes are grouped into tables with brief information on their roles in the function.

Electron transport chain and energy production

Two genes were up-regulated (Table 65) and no genes were down-regulated in the electron transport chain function.

GENE NAME	ROLE	LOG2FOLD	P-VALUE
NDUFV3	Nuclear encoded essential components of complex I NADH dehydrogenase, involved in the reduction of ubiquinone by NADH	0.55768	0.0172
ATP50	Nuclear encoded ATP synthase subunits, essential components of complex V, reversible pump of protons into matrix with formation of ATP	0.433419	0.0347

Table 65: Up-regulated genes in the electron transport chain of RPE1H2B 21/3 cell line

There were only two genes which were up-regulated in the electron transport chain function of the RPE1H2B 21/3 cell line. They are NDUFV3, which is an essential component of complex I NADH dehydrogenase complex. This indicate that there might be an increased reduction of ubiquinone and simultaneously increased electron leakage and ROS production in the mitochondria.

Further up-regulation of the ATP50, which is an essential component of mitochondrial respiratory chain ATP synthase complex, might contribute to the imbalance in the normal subunit composition of ATP synthase complex in the mitochondria of RPE1H2B 21/3 cell line.

Finally with only one gene in the complex I and the complex V up-regulated, it might suggest that the energy production function in the RPE1H2B 21/3 cell line might be comparable with its wild type cell line.

Fatty acid beta oxidation and generation of acetyl CoA

Two genes were down-regulated (Table 66) and none of the genes were up-regulated in the fatty acid beta oxidation function.

GENE NAME	ROLE	LOG2FOLD	P-VALUE
ACSS3	Acyl-CoA synthetase activity for short chain fatty acids	-7.09682	0.0596
ACSM5	Acyl-CoA synthetase activity for medium chain fatty acids	-6.39182	0.15815

Table 66: Down-regulated genes in the fatty acid beta oxidation of RPE1H2B 21/3 cell line
ACSS3 and ACSM5, which shows Acyl-CoA synthetase activity for short and medium chain fatty acids respectively in the cytoplasm are down-regulated in the RPE1H2B 21/3 cell line. This suggests that there might be a build-up of short and medium chain fatty acids in the cytoplasm. Further there are no misregulations of genes in any steps of the fatty acid beta-oxidation inside mitochondria. Thus the wild-type levels of acetyl-CoA might be generated in the RPE1H2B 21/3 cell line.

Apoptosis

A single gene was observed to be up-regulated (Table 67) and none of the genes were down-regulated in the apoptosis function.

GENE NAME	ROLE	LOG2FOLD	P-VALUE
CASP3	Executioner caspases leading to apoptosis	0.448259	0.03275

Table 67: Up-regulated genes in the apoptosis function of RPE1 H2B 21/3 cell line

There were no misregulations of the apoptotic proteins handled by the mitochondria apart from the up-regulation of CASP3, which is an executioner caspase leading to the apoptosis. Thus we do not expect an impaired apoptotic handling by the mitochondria in the RPE1H2B 21/3 cell line.

Glycolysis

There were 8 genes observed to be down-regulated (Table 68) and none were up-regulated in the glycolysis function.

GENE NAME	ROLE	LOG2FOLD	P-VALUE
SLC2A5	Fructose transporter, present in the small intestine	-2.70097	0.0016
HK2	Glucose is phosphorylated to glucose 6-phosphate	-0.589886	0.0057

	catalysed by the hexokinase		
PFKP	Fructose 6-phosphate is phosphorylated to fructose 1,6-bisphosphate, catalyzed by phosphofructokinase	-0.684619	0.00045
ALDOA	Fructose 1,6-bisphosphate converted into glyceraldehyde 3-phosphate and dihydroxyacetone phosphate catalyzed by aldolase	-0.493325	0.03895
TPI1	Dihydroxyacetone phosphate is converted into glyceraldehyde 3-phosphate catalyzed by triose phosphate isomerase	-0.759242	0.001
PGK1	1,3-bisphosphoglycerate is converted to 3-phosphoglycerate and ATP is released, catalyzed by Phosphoglycerate kinase	-0.99524	0.00005
PGAM1	3-phosphoglycerate is converted into 2-phosphoglycerate catalyzed by phosphoglycerate mutase	-0.600223	0.00835
ENO2	2-phosphoglycerate is converted into phosphoenolpyruvate catalyzed by enolase	-0.427012	0.03585

Table 68: Down-regulated genes in the glycolytic function of the RPE1 H2B 21/3 cell line

Enzymes involved in catalysing several steps of the glycolytic pathway are down-regulated in the RPE1H2B 21/3 cell line. In conclusion, we hypothesize that lower levels of pyruvate will be produced, which might have an effect on the overall energy production in the cells.

Fe-S cluster biosynthesis

There was a single gene observed to be up- (Table 69) and also a single gene which was down-regulated (Table 70) in the Fe-S cluster biosynthesis function.

GENE NAME	ROLE	LOG2FOLD	P-VALUE
FDXR	Provide reducing equivalents to electron transfer chain and contribute to iron-sulphur cluster biogenesis	0.527734	0.02135

Table 69: Up-regulated gene in the Fe-S cluster biosynthesis function of the RPE1H2B 21/3 cell line

GENE NAME	ROLE	LOG2FOLD	P-VALUE
-----------	------	----------	---------

HSCB	Mitochondrial iron-sulphur cluster co-chaperone	-0.591209	0.02905
------	---	-----------	---------

Table 70: Down-regulated gene in the Fe-S cluster biosynthesis function of the RPE1H2B 21/3 cell line

FDXR, which mediates the transport of electrons to the mitochondrial proteins is up-regulated. This suggests that there is an increased need for reducing equivalents by the mitochondrial proteins in the RPE1H2B 21/3 cell line.

Further down-regulation of HSCB, which is required for the biogenesis of Fe-S cluster implies that the Fe-S cluster biogenesis might be affected and the generation is reduced in the RPE1H2B 21/3 cell line.

Mitochondrial dynamics

There were 2 and 4 genes observed to be up- (Table 71) and down-regulated (Table 72) respectively in the mitochondrial dynamics function.

GENE NAME	ROLE	LOG2FOLD	P-VALUE
PINK1	Involved in the mitochondrial fusion, PINK1 phosphorylates PARK2 and consequently PARK2 induced ubiquitination of mitofusins	0.420517	0.0425
SYBU	Involved in the mitochondrial movement, have a role in linking the mitochondria to KIF5B	1.0989	0.0003

Table 71: Up-regulated genes in the mitochondrial dynamics of the RPE1H2B 21/3 cell line

GENE NAME	ROLE	LOG2FOLD	P-VALUE
MTFP1	Involved in the mitochondrial fission, role in mitochondrial fragmentation and is dependent on DNM1L expression	-0.832433	0.00155
GDAP1	Involved in the mitochondrial fission, known to have a role in the mitochondrial fragmentation	-1.12083	0.0002
BNIP3	Involved in the mitophagy, cause permeabilization of the mitochondrial membrane and also acts as a proapoptotic factor	-1.21804	0.00005
MAP1LC3A	Involved in the mitophagy, interacts with BNIP3 and BNIP3L to remove mitochondria via autophagy	-4.427	0.20795

Table 72: Down-regulated genes in the mitochondrial dynamics of the RPE1H2B 21/3 cell line

Several genes coding for proteins, which are involved in the mitochondrial dynamics are up-regulated. For example, up-regulation of PINK1 which is involved in the mitochondria fusion. We also observe that there were several genes, which were down-regulated. For example, BNIP3, which causes permeabilization of the mitochondrial membrane during mitophagy and MAP1LC3A, which is known to interact with BNIP3 and BNIP3L to remove mitochondria via autophagy. This suggests that there could be changed mitochondrial dynamics in the RPE1H2B 21/3 cell line.

Import and sorting

There was a single gene which was down-regulated (Table 73) and none of the genes were up-regulated in the import and sorting function.

GENE NAME	ROLE	LOG2FOLD	P-VALUE
IMMP2L	Inner membrane peptidase that cleaves hydrophobic sorting signal	-0.578531	0.0417

Table 73: Down-regulated gene in the import and sorting function of the RPE1H2B 21/3 cell line

The down-regulation of IMMP2L in the RPE1H2B 21/3 cell line might suggest that there would be an accumulation of proteins with hydrophobic sorting signals inside mitochondria. As a consequence the incoming proteins with hydrophobic sorting signals might not be functional.

Replication and transcription

There was a single gene up-regulated (Table 74) and 5 genes down-regulated (Table 75) in the replication and transcription function.

GENE NAME	ROLE	LOG2FOLD	P-VALUE
RRM2B	Required for the de novo deoxyribonucleotide synthesis in non-proliferating cells supplying dNTPs to mtDNA synthesis	0.570357	0.00775

Table 74: UP-regulated gene in the replication and transcription function of the RPE1H2B 21/3 cell line

GENE NAME	ROLE	LOG2FOLD	P-VALUE
TFB2M	Essential transcription factor involved in the transcription of mitochondrial genes	-0.495879	0.0371
RMRP	RNA component of mitochondrial RNA processing endoribonuclease cleaves mitochondrial RNA at the priming site of mitochondrial DNA replication	-1.41059	0.00365
AK4	Phosphorylates the deoxyribonucleoside monophosphates specifically on dAMP	-1.08976	0.00005
NME4	Shows mitochondrial nucleoside diphosphate kinase activity	-0.428476	0.04045
SLC25A3	Mitochondrial pyrimidine nucleotide carrier	-0.641129	0.00315

Table 75: Down-regulated genes in the replication and transcription function of the RPE1H2B 21/3 cell line

Several genes involved in handling mitochondrial replication and transcription are down-regulated. For example, TFB2M, which is an essential transcription factor involved in the transcription of mitochondrial genes and RMRP, which is RNA component of mitochondrial RNA processing endoribonuclease. A down-regulated mitochondrial replication and transcription suggests that the number of mitochondria should not deviate from wild type in the aneuploid cells. It also suggests that mitochondrial function is more or less normal and that no need for higher levels of energy are required in this trisomic cell line.

Translation

Only a single gene was up-regulated (Table 76) and a single gene was down-regulated (Table 77) in the translation function.

GENE NAME	ROLE	LOG2FOLD	P-VALUE
RNASEL	Modulate the stability of mitochondrial mRNAs by interacting with MTIF2	0.962145	0.00155

Table 76: UP-regulated gene in the translation function of the RPE1H2B 21/3 cell line

GENE NAME	ROLE	LOG2FOLD	P-VALUE
MRPS21	Mitoribosome which forms a part of mitochondrial translation machinery	-4.71909	0.00005

Table 77: Down-regulated gene in the translation function of the RPE1H2B 21/3 cell line

The up-regulation of RNASEL in the RPE1H2B 21/3 cell line might suggest that there could be an increase in the stability of mitochondrial mRNAs. There are only two genes affected in the translation function and hence suggest that translation function in RPE1H2B 21/3 cell line is comparable with its wild type cell line.

ROS defence

There are 2 genes which were up-regulated (Table 78) and 2 genes which were also down-regulated (Table 79) in the ROS defence function.

GENE NAME	ROLE	LOG2FOLD	P-VALUE
SOD1	May be involved in the removal of superoxides in the inter membrane space of mitochondria	0.742468	0.00015
GPX1	Reduces hydrogen peroxide to water by using reducing equivalents from glutathione	0.563187	0.0063

Table 78: UP-regulated gene in the ROS defence function of the RPE1H2B 21/3 cell line

GENE NAME	ROLE	LOG2FOLD	P-VALUE
SOD2	Dismutates the superoxide generated in the mitochondrial matrix to hydrogen peroxide	-0.613678	0.0078

BCKDHA	Involved in the catabolism of amino acids in mitochondria and may also be involved in the production of superoxides and hydrogen peroxide	-0.455574	0.0453
--------	---	-----------	--------

Table 79: Down-regulated gene in the ROS defence function of the RPE1H2B 21/3 cell line

Two genes involved in balancing ROS in the mitochondria are up-regulated. These include SOD1, which removes superoxides in the intermembrane space of mitochondria and GPX1, which further reduces the hydrogen peroxide to water. In contrary SOD2, which removes superoxides in the matrix space of the mitochondria is down-regulated. This implies that there might be an increase in the build-up of ROS in the matrix space of the mitochondria in the RPE1H2B 21/3 cell line.

3.1.5.1 Summary for RPE1H2B 21/3 MitoModel

In total, there were 10 functions that were observed to be affected in the RPE1H2B 21/3 MitoModel. Further, we observe that the MitoModel had more down- (24 genes) compared to up-regulated (10 genes) genes. Most number of the down-regulated genes were present in the glycolysis function with 8 genes affected (Figure 19).

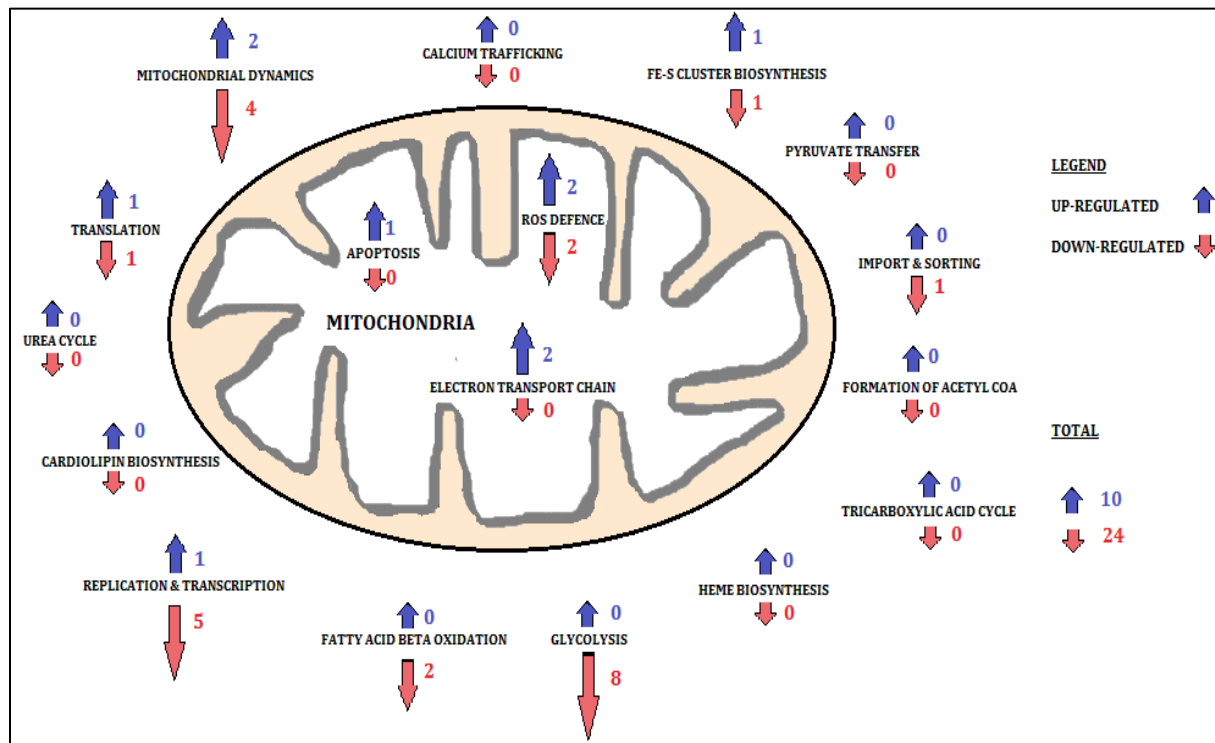


Figure 19: Number of affected genes observed on all the functions of RPE1H2B 21/3 MitoModel

3.1.6 Comparison between HCT116 5/4, RPE1 5/3 12/3 and RPE1H2B 21/3

MitoModels:

Differentially expressed genes from five functions: Electron transport chain, glycolysis; translation; fatty acid beta oxidation; and replication and transcription were recorded and used to compare the MitoModels for each cell line (Figure 20).

From Figure 20 it is clear that the differential expression of genes is more towards up-regulation compared to down-regulation in translation electron transport chain and replication and transcription functions of RPE1 5/3 12/3 cell line when compared with the HCT116 5/4 cell line. Whereas in RPE1H2B 21/3 cell line glycolysis with more differentially expressed genes tend towards downregulation.

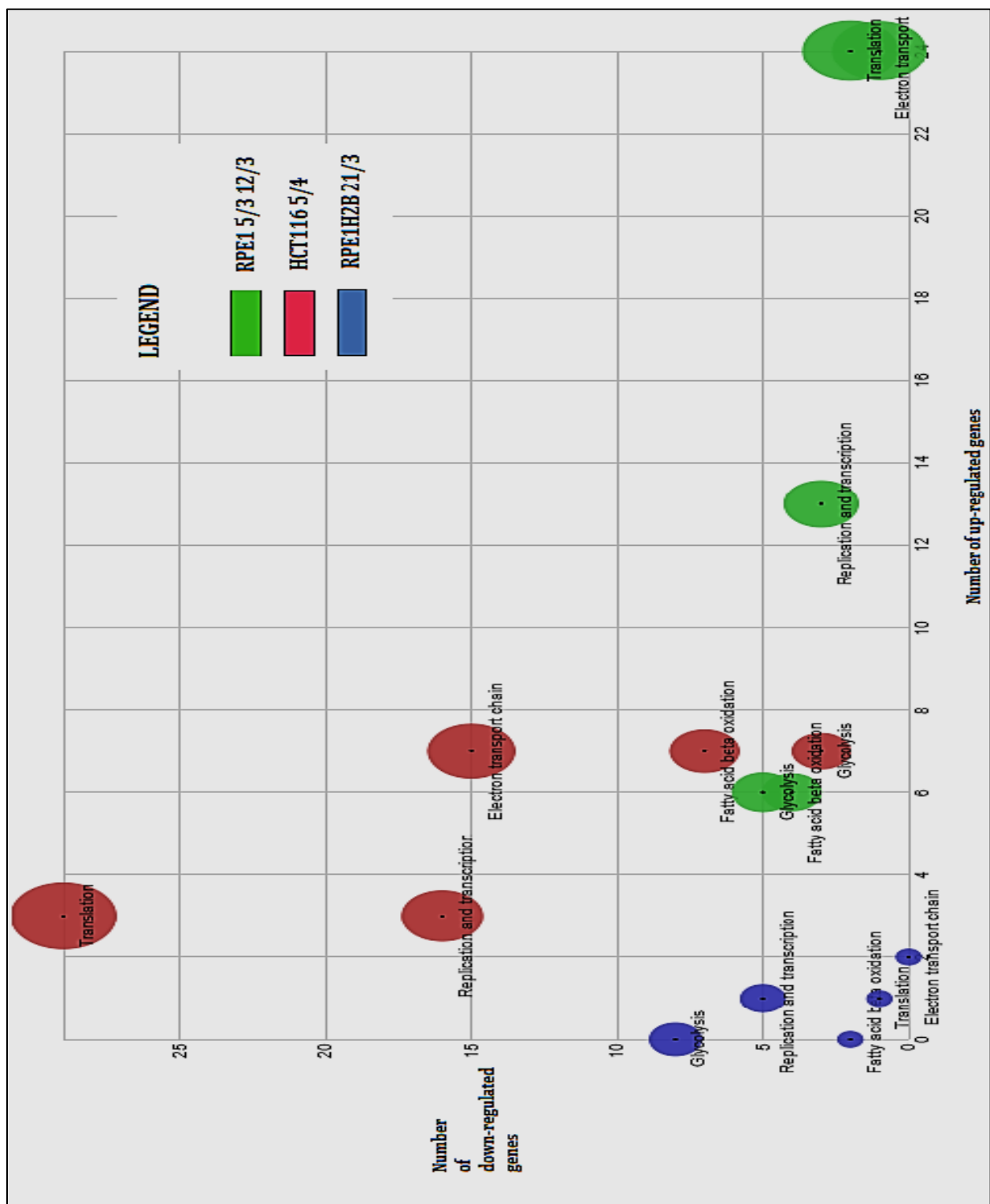


Figure 20: Comparison of HCT116 5/4, RPE1 5/3 12/3 and RPE1H2B 21/3 MitoModels

CHAPTER 3.2

Analysis of expression difference between LR and HR stress reactivity mice: impact of mitochondrial function

Many studies suggest a relationship between hypothalamus-pituitary-adrenocortical (HPA) axis dysregulation and major depression (MD) [Heinzmann et al., 2014]. About 60 to 80% of depressed patients are observed to have neuroendocrine alterations in HPA axis activity [Heinzmann et al., 2014]. Reports also suggest the improvement of clinical symptoms with normalisation of HPA axis function [Heinzmann et al., 2014]. Therefore dysregulated HPA axis as one of the key endophenotype of MD and may provide an opportunity to elucidate underlying mechanism of the disease [Heinzmann et al., 2014].

Mouse model selected for extremes in HPA axis reactivity were established by Touma and colleagues [Touma et al., 2008] and kindly provided for us for mitochondrial analysis. This 'stress reactivity' (SR) mouse model system consists of a high (HR), intermediate (IR) and low (LR) reactivity mouse line. Distinct differences in their corticosterone (CORT) secretion response to stressors are observed in these mouse line [Touma et al., 2008].

To understand the different phenotypes in the three mouse lines, differential expression data was generated by our collaborators generated using SAGE [Velculescu et al., 1995]. RNA was derived from Hippocampus tissue from brain from the LR and HR mice and libraries were pooled from six animals. Our aim was to understand the mitochondrial contribution to different stress reactivity types.

3.2.1 DATA ANALYSIS:

The data we received consisted of the mouse gene symbols and expression values of LR pool and HR pool with log2fold change and respective p-values.

In order to analyse mouse differential expression data, we generated a mouse MitoModel by using the orthologs of the genes present in the human MitoModel.

3.2.2 LR VS. HR MITOMODEL:

Mouse MitoModel is an amalgamation, consisting of 659 genes which are functionally associated with the mitochondria. The model is further classified into 17 mitochondria specific processes grouped into clusters (Figure 21).

After mapping expression data on to the mouse MitoModel, some of the crucial functions that were observed to be impaired, based on the percentage are: tricarboxylic acid cycle, which heavily affected with 84.21% of the genes either up- or down-regulated (Figure 22); cardiolipin biosynthesis, with 66.67% genes implicated; the electron transport chain, with 58.78% genes differentially regulated; Mitochondrial dynamics, with 57.5%; Glycolysis, with 56.25% affected genes.

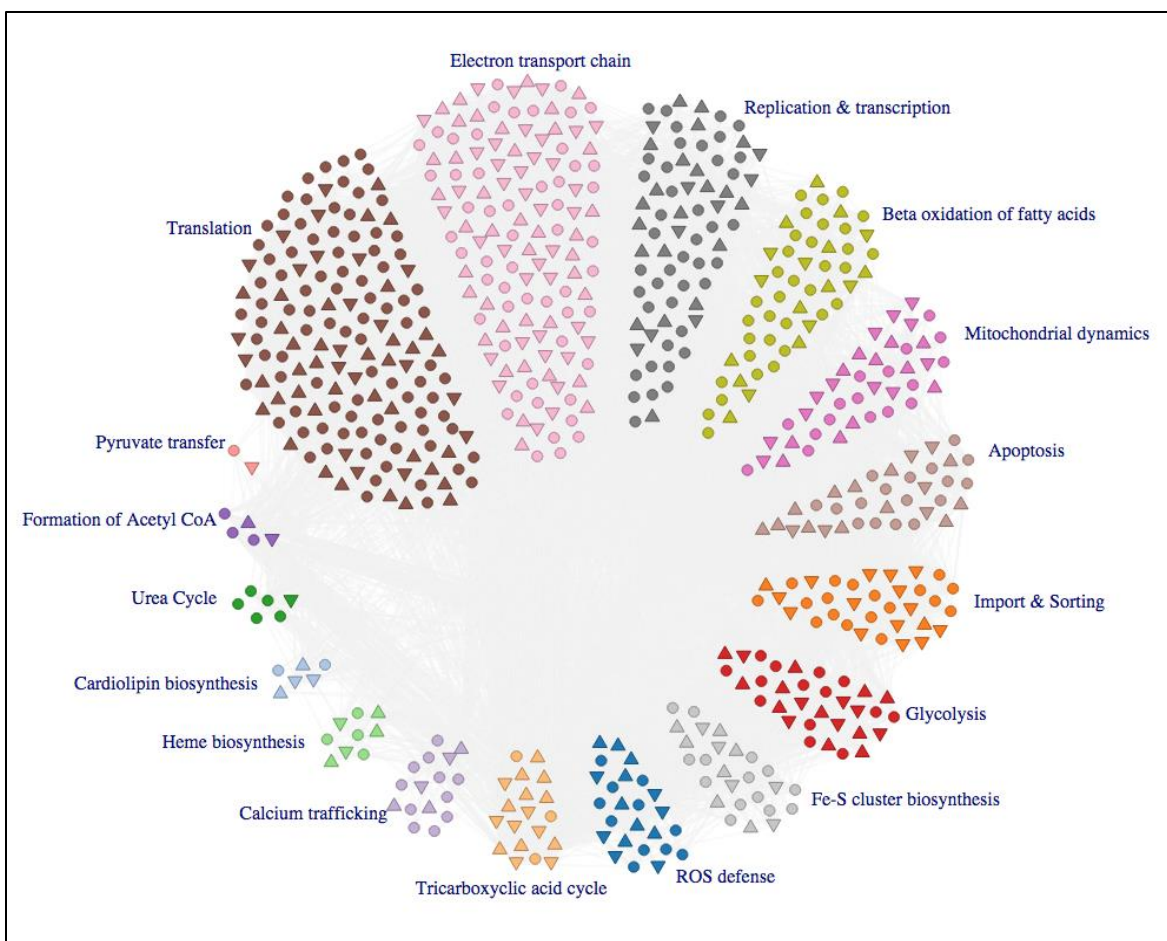


Figure 21: Visual representation of LR vs. HR mouse MitoModel with functions as clusters annotated with their names

In addition to being the most dis-regulated mitochondrial function, the TCA cycle also harbours genes with highest log₂fold change: *Sdhc* and *Fh1* (Figure 23). In contrast, beta-oxidation of fatty acids exhibits the lowest log₂fold change with *Acsbg2* followed by *Aars2* in the translation function.

There were 313 genes that were misregulated (either up- or down-regulated) out of 659 genes in the MitoModel. To draw a brief understanding of the biological functions, only top 5 up- and down-regulated genes from each function were further studied.

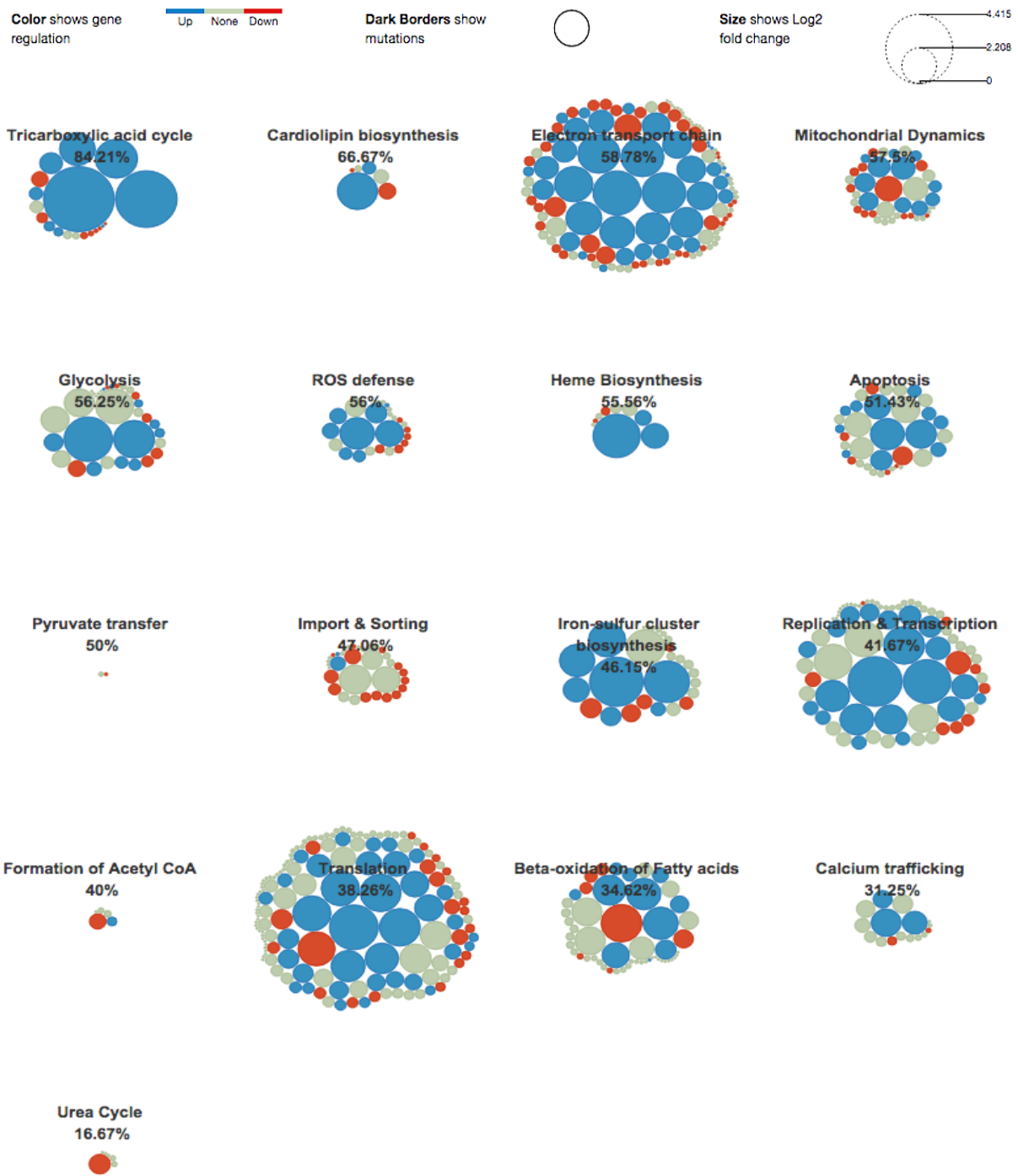


Figure 22: Percentage (%) of affected functions observed on the mouse MitoModel; the size of the node corresponds to the log2fold change value (higher log2fold change corresponds to bigger circle and vice versa) and colour corresponds to gene regulation (Blue: Up, Green: None and Red: Down)

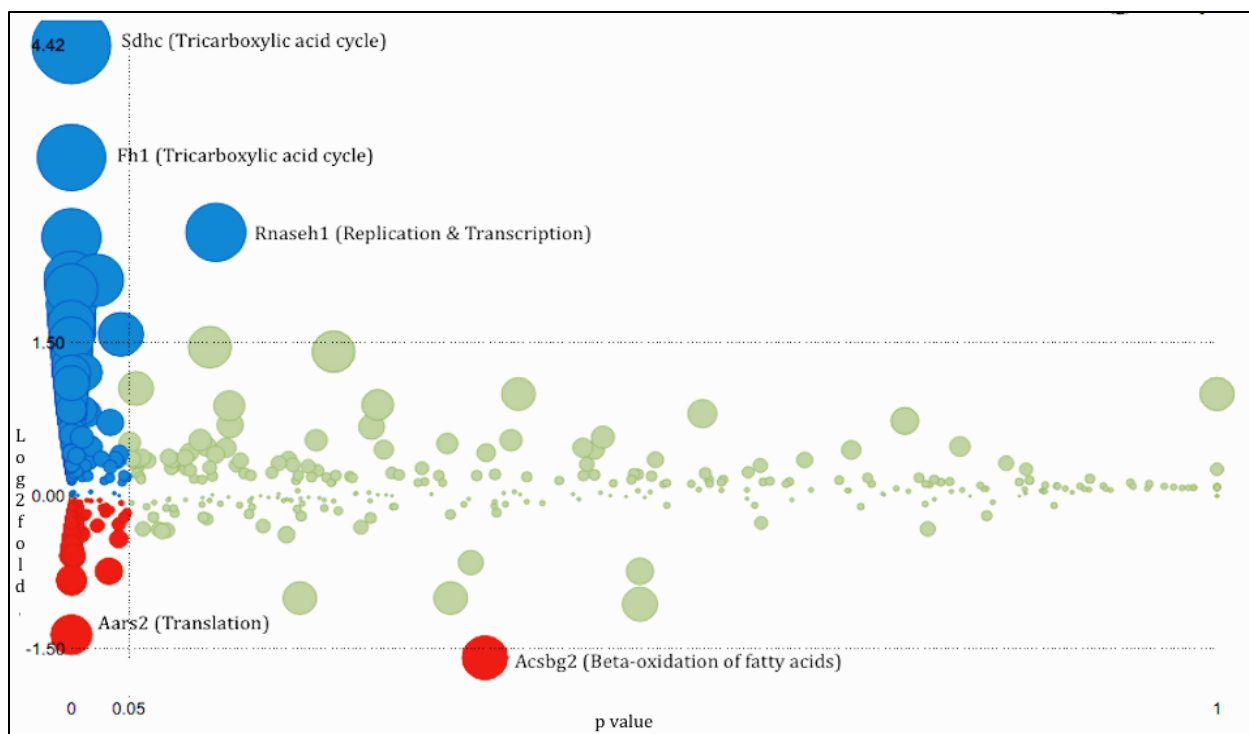


Figure 23: Graphical display of model parameters, two horizontal lines describing log2fold change cutoff values (up: 1.50 and down -1.50) and a vertical line describing p-value cutoff (0.05).

Tricarboxylic acid (TCA) cycle

Top five up-regulated and down-regulated genes in the TCA cycle with their roles are defined below in the tables 80 and 81 respectively.

GENE NAME	LOG2FOLD	P-VALUE	ROLE
Sdhc	4.41504	1,49E-16	Part of Succinate dehydrogenase complex in oxidative phosphorylation in TCA cycle it catalyzes the oxidation of succinate to fumarate
Fh1	3.31872	5,66E-66	Fumarase catalyzes the formation of L-malate from fumarate
Suclg1	1.6939	1,62E-16	Succinyl CoA synthetase catalyzes the conversion of succinyl CoA to succinate
Aco2	1.28326	6,79E-16	Aconitase catalyzes the interconversion of citrate to isocitrate
Suclg2	0.656476	8,58E+04	Succinyl CoA synthetase catalyzes the conversion of succinyl

			CoA to succinate
--	--	--	------------------

Table 80: The top 5 up-regulated genes of the TCA cycle, in the LR vs. HR comparison

GENE NAME	LOG2FOLD	P-VALUE	ROLE
Dld	-0.412284	8,47E-17	Catalyzes the overall conversion of 2-oxoglutarate to succinyl-CoA and CO ₂
Cs	-0.225687	4,69E-30	Citrate synthase catalyzes the synthesis of citrate from oxaloacetate and acetyl CoA
Ogdh	-0.11583	1,15E-20	Catalyzes the overall conversion of 2-oxoglutarate to succinyl-CoA and CO ₂
Sdhb	-0.0759846	0.000276975	Part of Succinate dehydrogenase complex in oxidative phosphorylation in TCA cycle it catalyzes the oxidation of succinate to fumarate
Idh3a	-0.0372824	0.000009775	Isocitrate dehydrogenase catalyze the oxidative decarboxylation of isocitrate to 2-oxoglutarate

Table 81: The top 5 down-regulated genes of the TCA cycle, in the LR vs. HR comparison

Enzymes catalysing several steps of the TCA cycle in series are up-regulated: *Suclg1* and *Suclg2*, which catalyse the conversion of succinyl CoA to succinate; *Sdhc*, which catalyses the oxidation of succinate to fumarate; and finally *Fh1*, which catalyse the conversion of fumarate to malate. Consequently this suggests that three consecutive steps in HR mouse line, are up-regulated compared to LR mouse line.

Enzymes catalysing two steps of the TCA cycle are at the same time down-regulated: *Idh3a*, which catalyses the conversion of Isocitrate into alpha-ketoglutarate; and, *Dld* and *Ogdh*, which catalyses the overall conversion of alpha-ketoglutarate to succinyl-CoA and Co₂. As a consequence two continuous steps in TCA cycle are down-regulated in HR mouse line.

In conclusion the TCA cycle is massively up-regulated in the HR mouse line, which in turn could directly create an environment for an elevated aerobic energy production via the electron transport chain.

Cardiolipin biosynthesis

Up-regulated and down-regulated genes in the cardiolipin biosynthesis function are defined below in the tables 82 and 83 respectively.

GENE NAME	LOG2FOLD	P-VALUE	ROLE
Pgs1	1.54432	2,67E-03	Phosphatidylglycerol synthase converts cytidine diphosphate diacylglycerol to phosphatidylglycerol phosphate
Cds2	0.305926	2,52E+00	Converts phosphatidic acid to cytidine diphosphate diacylglycerol

Table 82: The top up-regulated genes of the cardiolipin biosynthesis, in the LR vs. HR comparison

GENE NAME	LOG2FOLD	P-VALUE	ROLE
Cds1	-0.439357	5,83E-06	Converts phosphatidic acid to cytidine diphosphate diacylglycerol
Crls1	-0.0385575	0.0248569	Catalyzes the condensation of cytidine diphosphate diacylglycerol and phosphatidylglycerol forming a nascent cardiolipin

Table 83: The top down-regulated genes of the cardiolipin biosynthesis, in the LR vs. HR comparison

Several genes are misregulated in cardiolipin biosynthesis function. Pgs1, involved in the conversion of cytidine diphosphate diacylglycerol to phosphatidylglycerol phosphate, and Cds2, involved in the conversion of phosphatidic acid to cytidine diphosphate diacylglycerol are up-regulated; Cds1, on the other hand, which is involved in the conversion of phosphatidic acid to cytidine diphosphate

diacylglycerol, and Crls1, known to catalyse the formation of nascent cardiolipin are down-regulated in the HR mouse line.

Consequently with several genes misregulated in cardiolipin biosynthesis function, we suggest that cardiolipin phospholipid availability in the HR mouse line is insufficient compared to LR mouse line.

Electron transport chain (ETC)

Top five up-regulated and down-regulated genes in the ETC function with their roles are defined below in the tables 84 and 85 respectively.

GENE NAME	LOG2FOLD	P-VALUE	ROLE
Ndufb11	2.07342	6.91E-94	Nuclear encoded essential components of complex I NADH dehydrogenase, involved in the reduction of ubiquinone by NADH
Atp5o	1.77797	1.13E-126	Nuclear encoded ATP synthase subunits, essential components of complex V, reversible pump of protons into matrix with formation of ATP
Ndufa4	1.72249	1.05E-85	Nuclear encoded essential components of complex I NADH dehydrogenase, involved in the reduction of ubiquinone by NADH
Atp5h	1.67456	6.44E-111	Nuclear encoded ATP synthase subunits, essential components of complex V, reversible pump of protons into matrix with formation of ATP
Atp5e	1.43982	1.8E-12	Nuclear encoded ATP synthase subunits, essential components of complex V, reversible pump of protons into matrix with formation of ATP

Table 84: The top 5 up-regulated genes of the ETC, in the LR vs. HR comparison

GENE NAME	LOG2FOLD	P-VALUE	ROLE
Sdhaf1	-0.813245	1,85E-13	Complex II specific assembly factor
Cox7a1	-0.578704	0.00183884	Nuclear encoded cytochrome c oxidase subunits, essential components of complex IV, catalyses the reduction of oxygen to water by cytochrome c

Tmem126b	-0.499571	0.000175685	Complex I assembly factor
Cox6c	-0.48796	0	Cytochrome c oxidase subunit VIc essential component of complex IV
Ndufa5	-0.369577	9,43E-64	Nuclear encoded essential components of complex I NADH dehydrogenase, involved in the reduction of ubiquinone by NADH

Table 85: The top 5 down-regulated genes of the ETC, in the LR vs. HR comparison

We observe several genes coding for the complexes in the electron transport chain up-regulated. For example, Ndufb11 and Ndufa4, which are essential components of complex I and Atp5h, Atp5o and Atp5e, which are essential components of complex V were up-regulated.

In addition several essential assembly factors of complexes were down-regulated. For example, Sdhaf1 and Tmem126b, which are the components required for the complex II and complex I assembly respectively were down-regulated.

As a consequence, these misregulations could lead to a receding energy production capacity of the electron transport chain. In conclusion, the assembly of complexes and energy generation activity of electron transport chain in the HR mouse line could be lower compared to LR mouse line.

Mitochondrial dynamics

Top five up-regulated and down-regulated genes in the mitochondrial dynamics function with their roles are defined below in the tables 86 and 87 respectively.

GENE NAME	LOG2FOLD	P-VALUE	ROLE
Sh3glb1	0.706269	0.00292318	Involved in the mitochondrial fission, proposed to be involved in the lipid remodeling of the outer membrane during fission
Kif1b	0.505454	0	

Kif5b	0.617298	1,96E-33	Involved in the mitochondrial movement, have role in the mitochondrial distribution in neurons
Bnip3	0.553819	0.0000017509	Involved in the mitophagy, cause permeabilization of the mitochondrial membrane and also acts as a proapoptotic factor
Mfn2	0.403356	3,53E-08	Involved in the mitochondrial fusion, mitofusins dimerize resulting in the tethering of the outer membranes of the fusing mitochondria

Table 86: The top 5 up-regulated genes of the mitochondrial dynamics, in the LR vs. HR comparison

GENE NAME	LOG2FOLD	P-VALUE	ROLE
Park2	-0.83335	0.000130524	Involved in the mitochondrial fusion, Park2 induces ubiquitination of mitofusins
Opa3	-0.238638	0.00275452	Involved in the mitochondrial fusion, interacts with Mfn1 and involved in mitochondrial fragmentation
Smcr7	-0.1752	0.0131032	Involved in the mitochondrial fission, suggested to have roles in recruiting Dnm11
Stoml2	-0.166312	5,72E-02	Involved in the mitochondrial fusion, scaffold proteins Phb2 and Stoml2 coordinate stability of the Opa1
Sqstm1	-0.166026	5,15E-37	Involved in the mitophagy, recruited to mitochondria and binds mitochondrial substrates on the autophagosomes

Table 87: The top 5 down-regulated genes of the mitochondrial dynamics, in the LR vs. HR comparison

We observe crucial genes involved in the mitochondrial movement and distribution in neurons, such as Kif1b and Kif5b are up-regulated. Mfn2, known to be involved in the mitochondrial fusion are up-regulated. On the other hand, downregulated gene include Sqstm1, which binds mitochondrial substrates on to the autophagosomes during mitophagy.

In conclusion, these misregulations suggests that there could be increased availability of mitochondria for neuronal activity in addition to reduced clearing of mitochondria in HR compared to LR mouse line.

Glycolysis

Top five up-regulated and down-regulated genes in the glycolytic function with their roles are defined below in the tables 88 and 89 respectively.

GENE NAME	LOG2FOLD	P-VALUE	ROLE
Slc2a4	2.11	0.0221416	Glucose transport in the muscle and fat cells
Pgam1	1.59	0	3-phosphoglycerate is converted into 2-phosphoglycerate catalyzed by phosphoglycerate mutase
Hk1	0.502583	7,95E-19	Glucose is phosphorylated to glucose 6-phosphate catalysed by the hexokinase
Pkm2	0.361301	3,06E-13	Phosphoenolpyruvate is converted into pyruvate and ATP is produced, catalyzed by pyruvate kinase
Pfkm	0.296095	0.0109634	Fructose 6-phosphate is phosphorylated to fructose 1,6-bisphosphate, catalyzed by phosphofructokinase

Table 88: The top 5 up-regulated genes of the glycolysis, in the LR vs. HR comparison

GENE NAME	LOG2FOLD	P-VALUE	ROLE
Pgam2	-0.43837	0.00125861	3-phosphoglycerate is converted into 2-phosphoglycerate catalyzed by phosphoglycerate mutase
Tpi1	-0.258795	0	Dihydroxyacetone phosphate is converted into glyceraldehyde 3-phosphate catalyzed by triose phosphate isomerase
Ldha	-0.251461	4,35E-30	Pyruvate is converted to lactate catalyzed by lactate dehydrogenase
Gpi1	-0.186933	0	Isomerization of glucose 6-phosphate to fructose 6-phosphate by the phosphoglucose isomerase
Pgk1	-0.133702	1,50E-28	1,3-bisphosphoglycerate is converted to 3-phosphoglycerate and ATP is released, catalyzed by Phosphoglycerate kinase

Table 89: The top 5 down-regulated genes of the glycolysis, in the LR vs. HR comparison

Several enzymes were identified to be misregulated in glycolytic function in HR compared to LR mouse line. Up-regulation of Pgam1 but down-regulation of Pgam2, both of which are known to catalyse the reversible reaction of 3-phosphoglycerate to 2-phosphoglycerate could suggest the specificity of the phenotype. Further genes included Slc2a4, a facilitated glucose transporter; Hk1, which phosphorylates glucose to glucose-6-phosphate; and Pkm2, which is known to catalyse the transphosphorylation of phosphoenolpyruvate into pyruvate and ATP are up-regulated.

In addition to up-regulated genes several down-regulated genes were also observed, including Ldha, which catalyses the interconversion of pyruvate to lactate and Gpi1, which interconverts glucose-6-phosphate and fructose-6-phosphate.

In conclusion, the up-regulation of Pkm2 suggests that there might be a shift in the energy production to glycolysis with a possible impaired electron transport chain in HR mouse line.

ROS defense

Top five up-regulated and down-regulated genes in the ROS defence function with their roles are defined below in the tables 90 and 91 respectively.

GENE NAME	LOG2FOLD	P-VALUE	ROLE
Slc25a10	1.21	0.0102904	May be involved in the transport of glutathione into the mitochondria
Gclm	0.878009	5,04E-03	Catalyzes the first step reaction which combines cysteine and glutamate to form glutamylcysteine
Gsta4	0.596482	2,32E-18	Mitochondrial glutathione-S-transferases through glutathione conjugation or peroxide reduction detoxify harmful byproducts
Sod1	0.426256	4,42E-24	May be involved in the removal of superoxides in the inter membrane space of mitochondria

Sod2	0.419814	3,74E-03	Dismutates the superoxide generated in the mitochondrial matrix to hydrogen peroxide
------	----------	----------	--

Table 90: The top 5 up-regulated genes of the ROS defense, in the LR vs. HR comparison

GENE NAME	LOG2FOLD	P-VALUE	ROLE
Mpv17l	-0.170958	3,14E-16	May have a role in the metabolism of reactive oxygen species
Bckdha	-0.162173	0.0290465	Involved in the catabolism of amino acids in mitochondria and may also be involved in the production of superoxides and hydrogen peroxide
Gstp1	-0.110822	1,49E-05	Mitochondrial glutathione-S-transferases through glutathione conjugation or peroxide reduction detoxify harmful byproducts
Txn2	-0.104875	0.0000420124	Mitochondrial thioredoxin reduces peroxiredoxin to their superoxide scavenging state
Gstp2	-0.0918683	0.000860817	Mitochondrial glutathione-S-transferases through glutathione conjugation or peroxide reduction detoxify harmful byproducts

Table 91: The top 5 down-regulated genes of the ROS defense, in the LR vs. HR comparison

Several genes involved in counter balancing the build up of ROS were misregulated in HR mouse line. For example Sod1 and Sod2, involved in the removal of superoxides in the inter membrane space and matrix of mitochondria respectively were observed to be up-regulated. At the same time Gstp1 and Gstp2, which are mitochondrial glutathione-S-transferases, involved in the detoxification of harmful byproducts were down-regulated.

Consequently with misregulations in countering ROS balance inside mitochondria, there might be an elevated ROS levels inside mitochondria in the HR compared to LR mouse line.

Heme biosynthesis

Crucial up-regulated and down-regulated genes in the heme biosynthesis function with their roles are defined below in the tables 92 and 93 respectively.

GENE NAME	LOG2FOLD	P-VALUE	ROLE
Ppox	2.02	0.00000160321	Protoporphyrinogen oxidase converts Protoporphyrinogen IX to Protoporphyrin IX
Alad	0.834941	2,64E-02	ALA dehydratase catalyzes the reaction where two molecules of ALA condenses to form monopyrrole porphobilinogen (PBG)
Fech	0.411865	0.0000419872	Ferrochelatase catalyzes the step involving the addition of Ferrous iron into the protoporphyrin IX to form the protoheme IX

Table 92: The top up-regulated genes of the heme biosynthesis, in the LR vs. HR comparison

GENE NAME	LOG2FOLD	P-VALUE	ROLE
Urod	-0.1657	0.030189	Uroporphyrinogen III decarboxylase catalyzes stepwise decarboxylation of the Uroporphyrinogen III forming Coproporphyrinogen III
Cpox	-0.0437044	0.0245879	Coproporphyrinogen III is transported to mitochondria and in the presence of coproporphyrinogen III oxidase it is oxidatively decarboxylated

Table 93: The top down-regulated genes of the heme biosynthesis, in the LR vs. HR comparison

Out of eight steps in the biosynthetic pathway leading to the formation of heme, genes coding for enzymes participating in five steps were misregulated. Up-regulated genes included Ppox and Fech, which catalyse the last two steps in the formation of protoheme IX. Down-regulated genes included the Urod, which catalyses the formation of coproporphyrinogen III and Cpox, which catalyses the formation of protoporphyrinogen IX.

In conclusion, there seems to exist an erroneous heme biosynthetic pathway in the HR mouse line.

Apoptosis

Top five up-regulated and down-regulated genes in the ROS defence function with their roles are defined below in the tables 94 and 95 respectively.

GENE NAME	LOG2FOLD	P-VALUE	ROLE
Apaf1	1.18	4,48E-02	Binds CASP9 forming an apoptosome and activates it
Bcl2l1	1.02	0.0000120163	Bcl-2 family member Anti-apoptotic proteins
Casp7	0.812914	0.0133119	Executioner caspases leading to apoptosis
Eif3m	0.60438	0.00210274	PCI domain containing protein 1 can negatively regulate CaspP9 activity
Mapk3	0.368087	0.00313329	Inhibitors of CASP9 activity

Table 94: The Top 5 up-regulated genes of the apoptosis, in the LR vs. HR comparison

GENE NAME	LOG2FOLD	P-VALUE	ROLE
Bbc3	-0.534657	0.000649336	Puma Bcl-2 family member propagating apoptosis
Bax	-0.274262	0.00104904	Bcl-2 family member propagating apoptosis
Cyca	-0.163199	5,66E-22	Binds to apoptosis inducing factor 1 (Apaf1) forming a structure called apoptosome
Vdac2	-0.141557	9,01E-09	Voltage dependent anion channel forms part of permeability transition pore and is also involved in the take up of calcium ions from the Endoplasmic reticulum
2810002N01Rik	-0.0676993	0.0435408	Localizes to the mitochondria and stimulates the release of cytochrome c

Table 95: The top 5 down-regulated genes of the apoptosis, in the LR vs. HR comparison

The HR mouse line contains misregulations in important apoptotic genes: for example Apaf1, is observed to be up-regulated and Cycs, is down-regulated. Eif3m and Mapk3, are also up-regulated, which negatively regulate and inhibit Casp9 activity respectively.

MOMP, controlled by the Bcl-2 family members are divided into pro and anti-apoptotic members. Bcl2l1, an anti-apoptotic member was up-regulated, while Bbc3 and Bax were down-regulated, which are proapoptotic members.

Consequently, with misregulations in crucial genes conducting mitochondria dependent death pathway, apoptosis by mitochondria seems impaired in the HR mouse line.

Pyruvate transfer

One of out of two genes coding for the proteins to import pyruvate inside mitochondria is down-regulated (Table 96).

GENE NAME	LOG2FOLD	P-VALUE	ROLE
Brp44l	-0.0208261	0.000281613	Involved in the transfer of pyruvate inside mitochondria

Table 96: The top down-regulated gene of the pyruvate transfer, in the LR vs. HR comparison

With the observed down-regulation in the gene responsible for the transfer of pyruvate inside mitochondria, there might be lower levels of pyruvate available in the HR mouse line.

Import & Sorting

Genes up-regulated and down-regulated in the Import and sorting function with their roles are defined below in the tables 97 and 98 respectively.

GENE NAME	LOG2FOLD	P-VALUE	ROLE
Timm22	0.364572	0.0263139	Inner membrane carrier pathway, forms the core channel and inserts proteins into inner membrane
Timm13	0.0269357	0.0373801	Inner membrane carrier pathway, forms complex with Timm8 and performs the transfer of inner membrane proteins

Table 97: The top up-regulated genes of the import and sorting, in the LR vs. HR comparison

GENE NAME	LOG2FOLD	P-VALUE	ROLE
Gfer	-0.405053	0.0000127714	Intermembrane transport and assembly, it is known to oxidize Chchd4 and then the oxidized Chchd4 acts as a receptor for the pre proteins and it also facilitates assembly of cytosolic Fe-S proteins
Tomm40	-0.333747	3,04E-14	Outer membrane translocation, forms the outer membrane channel forming protein
Tomm40l	-0.27109	0.0000198714	Outer membrane translocation, forms the outer membrane channel forming protein
Mipep	-0.212018	0.000142321	Secondary cleavage of the pre proteins processed by the mitochondrial processing peptidase
Samm50	-0.192098	0.0116551	Outer membrane sorting and assembly machinery, central component of SAMM complex and inserts beta barrel proteins into the outer membrane

Table 98: The top 5 down-regulated genes of the import and sorting, in the LR vs. HR comparison

The HR mouse line had several mis-regulated genes in the import and sorting pathway. These included Timm22 and Timm13, which play important roles in the insertion of proteins into inner membrane are up-regulated, whereas Tomm40 and Tomm40l, which form the outer membrane channel forming proteins are down-regulated.

As a consequence, there might be a reduction in the protein import function on the outer membrane with a possible consequence on the insertion of inner membrane proteins. In conclusion, misregulations on the import and sorting function may impair the transport of crucial proteins inside mitochondria in HR mouse line.

Fe-S cluster biosynthesis

Top five up-regulated and down-regulated genes in the Fe-S cluster biosynthesis function with their roles are defined below in the tables 99 and 100 respectively.

GENE NAME	LOG2FOLD	P-VALUE	ROLE
Nfu1	2.53	0.0000482391	Protein assembles and transfers 4Fe-4S clusters to target apoproteins
Fdxr	1.88	1,80E-02	Provide reducing equivalents to electron transfer chain and contribute to iron-sulfur cluster biogenesis
Isca1	1.36	2,91E-07	Involved in the biogenesis and assembly of iron-sulfur clusters
Mms19	1.25	0.0000020733	Cytosolic Fe-S protein assembly targeting factor
Iscu	0.804449	0.00072882	Iron sulfur cluster assembly enzyme, Fe-S cluster intermediate is formed on it

Table 99: Top 5 up-regulated genes of the Fe-S cluster biosynthesis, in the LR vs. HR comparison

GENE NAME	LOG2FOLD	P-VALUE	ROLE
Fdx1	-0.580097	5,66E-05	Small iron-sulfur protein, transfers electrons from NADPH to mitochondrial cytochrome P450
Fdx1l	-0.494986	9,80E-19	Transfers electrons from NADPH to mitochondrial cytochrome P450
Slc25a37	-0.368901	0.000448722	Functions as an essential iron importer
Nubp2	-0.30274	3,08E-04	Required for the assembly of cytosolic iron-sulfur proteins
Fam96b	-0.155651	0.000664285	Components of the cytosolic Fe/S protein assembly (CIA) machinery

Table 100: The top 5 down-regulated genes of the Fe-S cluster biosynthesis, in the LR vs. HR comparison

Several crucial genes involved in the Fe-S cluster biosynthesis were misregulated in the HR mouse line. For example, *Iscu*, which facilitates Fe-S cluster intermediate formation and *Nfu1*, which assembles and transfers 4Fe-4S clusters to target apoproteins, including succinate dehydrogenase were up-regulated, but *Slc25a37*, which functions as an mitochondrial iron importer, *Fdx1* and *Fdx1l*, which are involved in transferring electrons from NADPH to mitochondrial cytochrome P450 were down-regulated.

Consequently, we expect a consequence also for the electron transport chain, which contains many Fe-S proteins. In conclusion, HR mouse line exhibits an impaired Fe-S cluster biosynthesis function compared to the LR mouse line.

Replication & transcription

Top five up-regulated and down-regulated genes in the replication and transcription function with their roles are defined below in the tables 101 and 102 respectively.

GENE NAME	LOG2FOLD	P-VALUE	ROLE
Rnaseh1	2.58	0.12614	May have role in the removal of RNA primers at the origin of replication on heavy and light strands
Pus1	2.05	0.000378398	Shows posttranscriptional modifications activity in the human mitochondrial tRNAs
Osgpl1	1.60	0.00144795	
Mterfd2	1.18	0.000438003	Mitochondrial transcription termination factor
Nfe2l2	1.17	0.000154098	Regulates the expression of TFB1M and TFB2M which are two mitochondrial transcription factors

Table 101: The top 5 up-regulated genes of the replication and transcription, in the LR vs. HR comparison

GENE NAME	LOG2FOLD	P-VALUE	ROLE
Mutyh	-0.736966	0.0327108	Involved in the mitochondrial DNA base excision repair
Dguok	-0.376268	0.00072044	Involved in the phosphorylation of recycled deoxyribonucleosides in mitochondria specific for guanosine, adenosine and inosine
Cmpk2	-0.295153	6,16E-04	Phosphorylates the deoxyribonucleoside mono phosphates specifically on dCMP
Rpusd2	-0.289393	0.0225809	Shows posttranscriptional modifications activity in the human mitochondrial tRNAs
Trnt1	-0.281249	0.00521788	Mitochondrial CCA adding enzyme, adds CCA sequence to the 3' end of tRNA

Table 102: The top 5 down-regulated genes of the replication and transcription, in the LR vs. HR comparison

Genes required for the replication and transcription of the mtDNA were observed to be misregulated in HR mouse line. Rnaseh1, which is implicated in the removal of RNA primers at the origin of replication on heavy and light strands; and Mterfd2, which is a mitochondrial transcription termination factor are up-regulated. Mutyh, which is involved in the mitochondrial DNA base excision repair; and Dguok, which is required for the phosphorylation of recycled deoxyribonucleosides in mitochondria are down-regulated.

As a consequence of these differential expressions, it could be that replication and transcription are higher with the impaired error correction mechanism in the HR mouse line.

Formation of Acetyl CoA

Up-regulated and down-regulated genes in the formation of acetyl-CoA function with their roles are defined in the tables 103 and 104 respectively.

GENE NAME	LOG2FOLD	P-VALUE	ROLE
Pdha1	0.197907	0.000122616	Pyruvate dehydrogenase complex catalyzes the overall conversion of pyruvate to acetyl CoA

Table 103: The up-regulated gene of the 'formation of acetyl CoA', in the LR vs. HR comparison

GENE NAME	LOG2FOLD	P-VALUE	ROLE
Pdhh	-0.421138	0.041229	Pyruvate dehydrogenase complex catalyzes the overall conversion of pyruvate to acetyl CoA

Table 104: The down-regulated gene of the 'formation of acetyl CoA', in the LR vs. HR comparison

We observe two genes showing contradictory expression patterns in the pyruvate dehydrogenase complex, which converts pyruvate to acetyl-CoA. This suggests that acetyl-CoA formation in the mitochondria of HR mouse line is misregulated.

Translation

Top five up-regulated and down-regulated genes in the translation function with their roles are defined below in the tables 105 and 106 respectively.

GENE NAME	LOG2FOLD	P-VALUE	ROLE
Kars	2.14	1,49E-14	Involved in the specific attachment of lysine aminoacid to its cognate tRNA
Tars2	1.58	0.0431267	Involved in the specific attachment of threonine aminoacid to its cognate tRNA
Mtif2	1.58	0.0000845711	Translation initiation factor could assist

			the tRNA to bind to rRNAs
Mrpl39	1.42	3,71E-03	Mitoribosome which forms a part of mitochondrial translation machinery
Mrpl42	1.42	1,22E-02	

Table 105: The top 5 up-regulated genes of the translation, in the LR vs. HR comparison

GENE NAME	LOG2FOLD	P-VALUE	ROLE
Aars2	-1.35	1,79E-07	Involved in the specific attachment of alanine aminoacid to its cognate tRNA
Mrpl36	-0.58738	8,10E-03	Mitoribosome which forms a part of mitochondrial translation machinery
Mrpl14	-0.387381	0.000138142	
Mrpl38	-0.375404	8,84E-04	
Phb	-0.400145	1,38E-23	Involved in the post translational quality control, stabilizes mitochondrially synthesized proteins

Table 106: Top 5 down-regulated genes of the translation, in the LR vs. HR comparison

Aminoacyl-tRNA synthetase family members were misregulated in the HR line. Kars and Tars2, implicated in the specific attachment of lysine and threonine amino acids to its cognate tRNAs were up-regulated. Aars2, involved in the attachment of alanine to its cognate tRNA was down-regulated. Mitochondrial ribosomes forming part of mitochondrial translation machinery were misregulated. Further it was also observed that Phb, which is involved in the post translational quality control and stabilization of mitochondrially synthesized proteins is down-regulated in the HR mouse line.

These misregulations in the translation machinery could lead to a disturbance in the protein translation inside mitochondria. In conclusion, HR mouse line harbours a defective mitochondrial translation machinery.

Beta-oxidation of fatty acids

Top five up-regulated and down-regulated genes in the fatty acid beta-oxidation function with their roles are defined below in the tables 107 and 108 respectively.

GENE NAME	LOG2FOLD	P-VALUE	ROLE
Slc27a1	1.24	1,20E-18	Readily converts the transported very long chain fatty acids to acyl-CoAs
Hadhb	1.20	0.0000248563	Mitochondrial trifunctional protein catalyzes the Very long and long chain fatty acids
Acadsb	1.10	1,98E-05	Involved in the metabolism of short branched chain fatty acids
Cpt1c	0.849409	7,98E-06	Carnitine palmitoyl transferase converts an acyl-CoA into an acylcarnitine
Acadl	0.575312	0.00921484	Long chain hydroxyacyl-CoA dehydrogenase

Table 107: The top 5 up-regulated genes of the beta-oxidation of fatty acids, in the LR vs. HR comparison

GENE NAME	LOG2FOLD	P-VALUE	ROLE
Acsbg2	-1.58	0.360927	Acyl-CoA synthetase activity for bubblegum family members
Acsm3	-0.531705	0.00114038	Acyl-CoA synthetase activity for medium chain fatty acids
Fabp3	-0.287257	4,27E-03	Fatty acid binding proteins are also involved in the import and export of fatty acids
Slc27a4	-0.281893	0.00000653627	Readily converts the transported very long chain fatty acids to acyl-CoAs
Fabp5	-0.274065	2,63E-38	Fatty acid binding proteins are also involved in the import and export of fatty acids

Table 108: The top 5 down-regulated genes of the beta-oxidation of fatty acids, in the LR vs. HR comparison

Several genes involved in the metabolism of fatty acids in the mitochondria were differentially regulated. *Hadhb*, which catalyses the metabolism of very-long and long chain fatty acids and *Acadl*, involved in the metabolism of long chain fatty acids were up-regulated. In addition, *Acadsb*, involved in the metabolism of short or branched chain fatty acids was up-regulated. *Acsbg2* and *Acsm3*, which have acyl-CoA synthetase activity for bubblegum family members and medium chain fatty acids respectively were down-regulated. As a consequence, there might be a significant drift towards the consumption of very-long and long chain fatty acids and short or branched fatty acids as compared to medium chain fatty acids in the HR mouse line.

Calcium transport

Up-regulated and down-regulated genes in the calcium transport function with their roles are defined in the tables 109 and 110 respectively.

GENE NAME	LOG2FOLD	P-VALUE	ROLE
Efha1	0.976153	0.0000725016	Regulates the mitochondrial calcium uniporter by inhibiting and permitting the calcium, depending upon the cytosolic calcium concentrations
1500032L24Rik	0.743222	6,26E-04	Forms a important component of mitochondrial calcium uniporter
Cbara1	0.5115	0.00195838	Regulates the mitochondrial calcium uniporter by inhibiting and permitting the calcium, depending upon the cytosolic calcium concentrations

Table 109: The top up-regulated genes of the Calcium transport, in the LR vs. HR comparison

GENE NAME	LOG2FOLD	P-VALUE	ROLE
Efha2	-0.181187	1,58E-02	Regulates the mitochondrial calcium uniporter by inhibiting and permitting the calcium depending upon the cytosolic calcium concentrations

Pacs2	-0.0676387	0.00525857	Involved in the control of ER mitochondria apposition
-------	------------	------------	---

Table 110: The top down-regulated gene of the Calcium transport, in the LR vs. HR comparison

We observe that the genes responsible for the maintaining the balance of calcium in the mitochondria were up-regulated. For example Efha1 and Cbara1 were up-regulated. In addition, a crucial component of the mitochondrial calcium uniporter is up-regulated. This suggests that the accumulation of calcium in the mitochondria is higher in HR mouse line.

Urea Cycle

A single gene was down-regulated in the urea cycle (Table 111) function.

GENE NAME	LOG2FOLD	P-VALUE	ROLE
Arg2	-0.597902	0.00155513	Arginase catalyzes the step where Arginine is hydrolyzed to form urea and ornithine

Table 111: The top down-regulated gene of the Urea cycle, in the LR vs. HR comparison

The down-regulation of Arg2 suggests that the urea synthesis in the mitochondria might be lower in the HR mouse line compare to the LR mouse line.

CHAPTER 3.3

Representative MitoModel in 16 samples of primary colorectal cancer and liver metastases

Colorectal cancer (CRC) is one of the most diagnosed cancer in humans, with an estimated death of about 600,000 to have occurred worldwide in 2008 [Jemal et al., 2011]. CRC is primarily asymptomatic until it progresses to advanced stages and hence numerous patients are diagnosed, when the cancer has grown large enough to cause symptoms [Read & Kodner, 1999]. Liver forms a major common site of CRC metastases [Sheth & Clary, 2005].

Sporadic genetic and /or epigenetic changes are observed in many cases of CRC. Nevertheless, 10% to 20% cases might be familial [Gonzalez & Cruz, 2015]. Several studies also highlight the diverse prognostic signatures for CRC with different tumour behaviors [Kim et al., 2014].

Our interest was to understand the contribution of mitochondrial function on cancer development and progression. To this end, we used 16 RNA-seq samples of matched primary CRC and synchronous liver metastases histologically identified as adenocarcinoma in addition to normal colonic epithelium [Kim et al., 2014].

We expected a general high variation between patients. As we already observed a high divergence between aneuploid cell lines (Chapter 3.1.), the clonal nature of cancer and metastasis will typically yield a diverse set of mutations present in different patients. Therefore, we decided to identify representative groups of patients, which could give us a general idea of the mitochondrial contribution to this disease.

3.3.1 TASK DESCRIPTION:

The task was thus to cluster the 16 MitoModels of the primary CRC and the liver metastases to generate representative patient groups and identify genes that are consistently affected.

We first retrieved the mutations and differential expression data specific to the primary CRC and the liver metastases as compared to the patients' normal colonic epithelium. The resulting data is then mapped on to the MitoModel, resulting in the constitution of 16 distinct MitoModels for primary CRC and liver metastases.

3.3.2 DATA ANALYSIS:

Mutation sites and expression differences between the normal colonic epithelium versus primary CRC and normal colonic epithelium versus liver metastases were achieved by following the workflow defined in section (2.13).

The obtained mutation sites and differentially expressed genes of the 16 samples were mapped on to obtain 16 distinct MitoModels of primary CRC and liver metastases.

3.3.3 CLUSTER ANALYSIS:

Cluster analysis was implemented to group the 16 different MitoModels of the primary CRC's. Groups of these models was based on the expression values of 563 mitochondria associated genes participating in the MitoModel from 16 primary CRC samples. Hierarchical clustering using euclidean distance as similarity metric was used [Maimon & Rokach, 2005].

Clustering resulted in four groups depicted as cluster 1, 2, 3 and 4 (Figure 24).

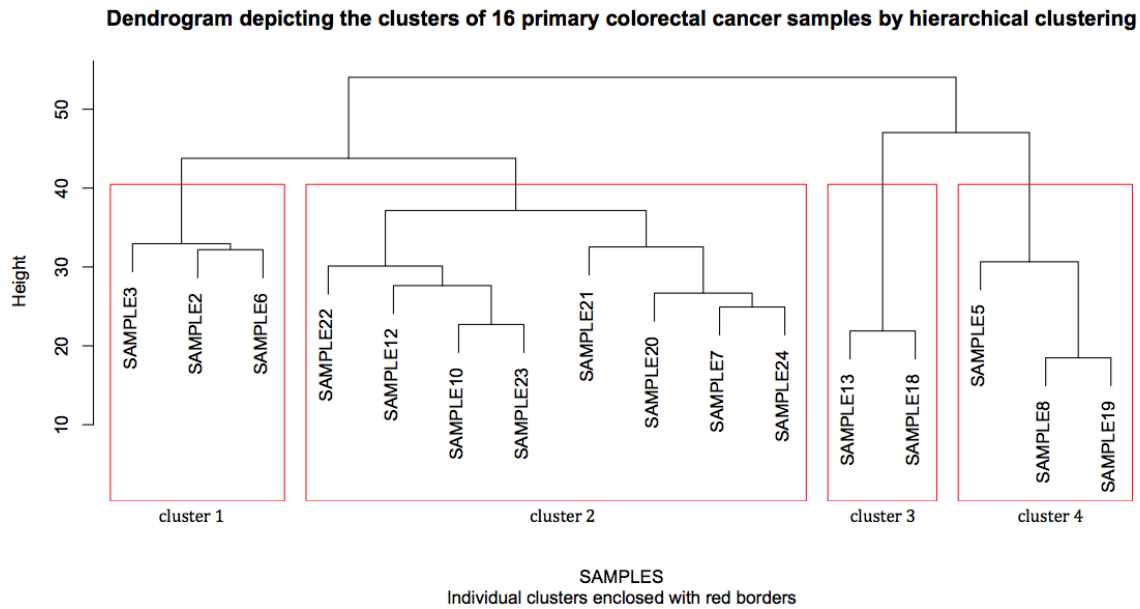


Figure 24: Dendrogram showing 4 distinct clusters derived from 16 primary CRC samples.

3.3.4 REPRESENTATIVE MITOMODELS:

To achieve the representative MitoModel for a single cluster, individual MitoModels from each cluster were combined.

Representative expression data were generated by using the mean value of the log₂fold change and p-values of individual cluster members for the different conditions.

For generating the representative mutations, mutation sites observable in at least two members of the cluster were collected.

The representative expression and mutation data for each cluster was mapped to the MitoModel to obtain the representative MitoModels.

For liver metastases samples, we took the four clusters based on the CRC expression and mutation data and followed the same procedure.

3.3.5 CHARACTERIZING REPRESENTATIVE GENES:

Representative genes that are consistently affected in each and every cluster, and in both the primary CRC and the liver metastases were analysed further.

This was achieved by creating tables with the affected genes divided in the 4 clusters and subdivided into primary CRC and liver metastases (see for instance Table 112 for the electron transport chain). Several symbols define the expression profile in the table. For example, “↑” blue up arrow shows up-regulation, “↓” green down arrow represents down-regulation and “X” red X is used for no change. For mutations, “+” black + represent that the gene is mutated and “X” light blue X indicates that the gene does not have any mutations (see for instance Table 113).

Electron transport chain

Representative differentially expressed genes and mutated genes in the electron transport chain function are defined below in the tables 112 and 113 respectively.

Genes	cluster 1		cluster 2		cluster 3		cluster 4	
	Primary CRC	Liver Metastases						
COX6B2	↓	↓	↓	↓	↓	↓	X	↓
COX4I2	X	X	X	X	X	X	X	↓

Table 112: Differentially expressed, representative genes observed in both primary CRC and liver metastases of all the clusters in the electron transport chain function.

GENES	cluster 1		cluster 2		cluster 3		cluster 4	
	Primary	Liver	Primary	Liver	Primary	Liver	Primary	Liver

	CRC	Metastases	CRC	Metastases	CRC	Metastases	CRC	Metastases
MT-ND5	+	+	X	X	X	X	X	X
MT-CO1	X	X	+	+	X	X	X	X
MT-CYB	X	X	+	X	X	X	X	X
COX411	X	X	X	+	X	X	X	X
MT-CO2	X	X	X	X	X	X	X	+

Table 113: Representative genes with mutation sites observed in both the primary CRC and the liver metastases of all the clusters in the electron transport chain function.

COX6B2 expression was lower in the primary CRC and liver metastases samples of all most all the clusters. COX6B2 is an essential component of cytochrome c oxidase, complex IV in the electron transport chain [Hüttemann et al., 2003].

COX6B2 was also observed to be down-regulated in the rho(0) cell line [Hashiguchi & Zhang-akiyama, 2009] devoid of mitochondrial DNA that exhibit Warburg effect [Ayyasamy et al., 2011].

This study also revealed mutations in core subunits of the mitochondrial electron transport chain. For example, mutated MT-ND5 was observed in both the primary CRC and the liver metastases of cluster 1 and mutated MT-CO1 was observed in both the primary CRC and liver metastases of cluster 2. Similarly, mutations in the coding regions of MT-ND5 and MT-CO1 was observed in the human colorectal cancer cell lines as well as human colon cancer [Chatterjee et al., 2006].

In conclusion, the misregulation of COX6B2 identified in multiple clusters both in the primary CRC and the liver metastases and mutations in core subunits of the electron transport chain, suggests a reduction in energy production via the electron transport chain in most of the patient groups.

Beta oxidation of fatty acids

Representative differentially expressed genes and mutated genes in the Beta oxidation of fatty acids function are defined below in the tables 114 and 115 respectively.

GENES	cluster 1		cluster 2		cluster 3		cluster 4	
	Primary CRC	Liver Metastases						
FABP6	↑	↑	↑	↑	↑	↑	X	↑
FABP4	↓	↓	↓	↓	↓	↓	X	↓
FABP2	↓	↓	↓	↓	X	↓	X	↓
ACSL6	↑	↑	↑	↑	X	↑	X	X
SLC27A5	↑	↑	X	↑	X	↑	X	↑
SLC27A6	↓	↓	↓	↓	X	X	X	↓
ACADS	↓	X	↓	X	↓	↓	X	↓
ACSL1	X	↑	X	↑	X	↑	X	↑
ACSS3	X	↑	X	↑	X	↑	X	↑
ACSM5	X	↑	X	↑	X	↑	X	↑
ACSM2A	X	↑	X	↑	X	↑	X	↑
ACSM2B	X	↑	X	↑	X	↑	X	↑
ACADL	X	↑	X	↑	X	↑	X	↑
CD36	↓	X	↓	X	↓	X	X	↓
ACSM1	↓	X	↓	X	X	↓	X	↓
FABP1	↓	X	↓	↓	X	X	X	X
ACAA2	X	X	↓	X	X	X	X	↓
ACADM	X	X	X	X	↓	X	X	X

ACSM3	X	X	X	X	X	X	X	↓
-------	---	---	---	---	---	---	---	---

Table 114: Differentially expressed, representative genes observed in both primary CRC and liver metastases of all the clusters in the beta oxidation of fatty acids function.

GENES	cluster 1		cluster 2		cluster 3		cluster 4	
	Primary CRC	Liver Metastases						
ACSL3	X	X	X	+	X	+	X	X
ACSL5	X	X	X	+	X	X	X	X
ACSL6	+	X	X	X	X	X	X	X
ACSS3	X	X	X	+	X	X	X	X
FABP6	X	X	X	+	X	X	X	+

Table 115: Representative genes with mutation sites observed in both the primary CRC and the liver metastases of all the clusters in the beta oxidation of fatty acids function.

Observations from this study throws light on the misregulations in multiple fatty acid binding proteins such as FABP2 and FABP4, which were down-regulated but FABP6, was up-regulated in primary CRC and liver metastases of all the clusters. Similarly, it was also reported that FABP6 was overexpressed in the colorectal cancer [Ohmachi et al., 2006].

The two acyl-CoA dehydrogenases showed contradictory behaviour. ACADL, which catalyses initial steps of beta oxidation and is involved in the metabolism of long chain fatty acids is up-regulated only in the liver metastases of 4 clusters whereas ACADS, which catalyse the final step of beta oxidation and is involved in the metabolism of short chain fatty acids is down-regulated in the primary CRC's of almost all the cluster.

As a consequence of misregulations in the fatty acid binding proteins in both primary CRC and liver metastases, observed in almost all the clusters, we predict a shift in lipid metabolism in both the primary CRC as well as liver metastases. AS we further observed a misregulations in Acyl-CoA dehydrogenases, such as ACADS, observed in primary CRC's and ACADL only in liver metastases, we hypothesize that fatty acid metabolims changes from primary CRC to liver metastases inside mitochondria.

Glycolysis

Representative differentially expressed genes and mutated genes in the glycolytic function are defined below in the tables 116 and 117 respectively.

GENES	cluster 1		cluster 2		cluster 3		cluster 4	
	Primary CRC	Liver Metastases						
ALDOB	X	↑	↑	↑	X	↓	X	↑
ALDOC	X	X	X	X	X	↑	X	↑
SLC2A1	X	X	X	X	X	↑	X	↑
SLC2A2	X	↑	X	↑	X	↑	X	↑
SLC2A3	X	X	X	X	X	↑	X	↑
SLC2A5	↓	X	X	X	X	X	X	X
HK2	X	X	X	↓	X	X	X	↓
HK3	X	X	X	↑	X	X	X	X
ENO3	X	X	X	↑	X	X	X	X
PGAM2	X	X	X	X	X	↓	X	X
PKLR	X	↑	X	↑	X	X	X	↑

Table 116: Differentially expressed, representative genes observed in both primary CRC and liver metastases of all the clusters in the glycolytic function.

GENES	cluster 1		cluster 2		cluster 3		cluster 4	
	Primary CRC	Liver Metastases						
HK1	X	X	+	X	X	X	X	X
PFKP	X	X	+	X	X	X	X	X
ALDOB	X	X	+	+	X	X	X	X
SLC2A2	X	+	X	+	X	X	X	X
PKLR	X	+	X	+	X	X	X	X
ENO1	X	X	X	+	X	X	X	X

Table 117: Representative genes with mutation sites observed in both the primary CRC and the liver metastases of all the clusters in the glycolysis function.

This study highlights misregulations in two critical genes in glycolysis: SLC2A2, which is a facilitated glucose transporter, was up-regulated only in the liver metastases of 4 clusters and was also mutated in the liver metastases of cluster 1 and 2; PKLR, which catalyses the transphosphorylation of phosphoenolpyruvate into pyruvate and ATP was noticed to be up-regulated in the liver metastases of all clusters and was also mutated in the liver metastases of cluster 1 and 2.

We propose that due to up-regulation of SLC2A2 and PKLR in the liver metastases of all the clusters, there might be an increase in glucose utilization and ATP production via glycolytic pathway in the liver metastases compared to primary CRC.

Urea cycle

Representative differentially expressed genes and mutated genes in the urea cycle function are defined below in the tables 118 and 119 respectively.

GENES	cluster 1		cluster 2		cluster 3		cluster 4	
	Primary CRC	Liver Metastases						
CPS1	↑	↑	X	↑	X	↑	X	↑
OTC	X	↑	X	↑	X	X	X	X
ARG1	X	↑	X	↑	X	↑	X	↑

Table 118: Differentially expressed, representative genes observed in both primary CRC and liver metastases of all the clusters in the Urea cycle function.

GENES	cluster 1		cluster 2		cluster 3		cluster 4	
	Primary CRC	Liver Metastases						
CPS1	X	+	X	+	X	X	X	+

Table 119: Representative genes with mutation sites observed in both the primary CRC and the liver metastases of all the clusters in the Urea cycle function.

Several genes of the urea cycle were misregulated, including CPS1, which catalyses the first step of urea cycle, the formation of carbamoyl phosphate with the available free ammonia and bicarbonate, is up-regulated in liver metastases of all the clusters and is also mutated in the liver metastases of almost all the clusters. ARG1, which catalyses the final step, where arginine is hydrolyzed to form urea and ornithine is up-regulated in the liver metastases of all the clusters.

Based on our observations in the liver metastases, we hypothesize a build up of NH_4^+ in the blood, which could lead to toxicity due to the absence of alternative pathways for the generation of urea.

Mitochondrial dynamics:

Representative differentially expressed genes and mutated genes in the mitochondrial dynamics function are defined below in the tables 120 and 121 respectively.

GENES	cluster 1		cluster 2		cluster 3		cluster 4	
	Primary CRC	Liver Metastases						
PLD6	↑	X	X	X	X	X	X	X
TRAP1	↑	X	X	X	X	X	X	X
GDAP1	↑	X	X	X	X	X	X	X
BNIP3	X	↑	X	↑	X	↑	X	↑
PINK1	↓	X	↓	X	X	X	X	X
PARK2	X	X	X	X	X	X	X	↓
PKIA	X	X	X	↓	X	X	X	X

Table 120: Differentially expressed, representative genes observed in both primary CRC and liver metastases of all the clusters in the mitochondrial dynamics function.

GENES	cluster 1		cluster 2		cluster 3		cluster 4	
	Primary CRC	Liver Metastases						
MFF	+	X	X	X	X	X	X	X
SQSTM1	X	X	X	+	X	X	X	X

Table 121: Representative genes with mutation sites observed in both the primary CRC and the liver metastases of all the clusters in the mitochondrial dynamics function.

The most important gene observed to be misregulated is BNIP3, which is up-regulated in the liver metastases of all the clusters. As a consequence, there might be an increase in the permeabilization of the mitochondrial membrane leading to mitophagy in the liver metastases.

Apoptosis

Representative differentially expressed genes and mutated genes in the apoptosis function are defined below in the tables 122 and 123 respectively.

GENES	cluster 1		cluster 2		cluster 3		cluster 4	
	Primary CRC	Liver Metastases						
PMAIP1	↑	X	↑	↑	X	↑	X	X
CDK1	↑	X	↑	X	X	↑	X	↑
CASP7	↓	↓	↓	↓	X	↓	X	↓
BCL2	↓	X	↓	↓	↓	X	X	↓
BCL2L11	↓	X	X	X	X	X	X	X

Table 122: Differentially expressed, representative genes observed in both primary CRC and liver metastases of all the clusters in the apoptosis function.

GENES	cluster 1		cluster 2		cluster 3		cluster 4	
	Primary CRC	Liver Metastases						

BAX	+	X	X	X	X	X	X	X
TP53	+	X	+	+	X	X	X	+

Table 123: Representative genes with mutation sites observed in both the primary CRC and the liver metastases of all the clusters in the apoptosis function.

Critical genes were observed to be misregulated in apoptotic function mediated by mitochondria such as CASP7, which is one of the executioner caspase leading to apoptosis is down-regulated in both primary CRC and liver metastases. BCL2, which is an anti-apoptotic member of Bcl-2 protein family is down-regulated in both primary CRC and liver metastases of almost all the clusters.

TP53, which directly binds to Bcl-2 family members propagating apoptosis was noticed to be mutated in both the primary CRC and the liver metastases.

Consequently, with misregulations in the crucial genes that prevailed in both primary CRC and liver metastases suggests an inability of mitochondria to induce the intrinsic apoptotic pathway.

Replication and transcription

Representative differentially expressed genes and mutated genes in the replication and transcription function are defined below in the tables 124 and 125 respectively.

GENES	cluster 1		cluster 2		cluster 3		cluster 4	
	Primary CRC	Liver Metastases						
C10orf2	↑	X	X	X	X	X	X	↑
TOP1MT	↑	X	X	X	X	X	X	↑

SLC29A1	↑	↑	↑	↑	X	↑	X	↑
TRMT6	↑	X	X	X	X	X	X	X
AK4	X	X	X	X	X	X	X	↑
PUS1	X	X	X	X	X	X	X	↑
YRDC	X	X	X	X	X	X	X	↑
PPARGC1A	↓	X	↓	X	X	X	X	↓

Table 124: Differentially expressed, representative genes observed in both primary CRC and liver metastases of all the clusters in the replication and transcription function.

GENES	cluster 1		cluster 2		cluster 3		cluster 4	
	Primary CRC	Liver Metastases						
GTPBP3	+	+	X	X	X	X	X	X
C10orf2	X	X	+	+	X	X	X	X
NSUN2	X	X	X	+	X	X	X	X

Table 125: Representative genes with mutation sites observed in both the primary CRC and the liver metastases of all the clusters in the replication and transcription function.

One gene, which was up-regulated in both the primary CRC and liver metastases of almost all the clusters was SLC29A1, which is involved in the import of recycled deoxyribonucleosides from cytoplasm into mitochondria. As a consequence, there might be an increase in the synthesis and maintenance of mtDNA. This would be in concordance with the observed probable lower efficiency of the electron transport chain. Concurrently PPARGC1A, involved in the regulation of mitochondrial transcription factors is down-regulated mostly in the primary CRC's of a few clusters suggesting that the transcription machinery might be impaired.

ROS defence:

Representative differentially expressed genes and mutated genes in the ROS defence function are defined below in the tables 126 and 127 respectively.

GENES	cluster 1		cluster 2		cluster 3		cluster 4	
	Primary CRC	Liver Metastases						
GSTA1	↓	↑	↓	↑	X	X	X	↑

Table 126: Differentially expressed, representative genes observed in both primary CRC and liver metastases of all the clusters in the ROS defence function.

GENES	cluster 1		cluster 2		cluster 3		cluster 4	
	Primary CRC	Liver Metastases						
GSR	X	X	+	X	X	X	X	X
GSTA2	X	X	X	+	X	X	X	X
SOD2	X	X	+	X	X	X	X	+

Table 127: Representative genes with mutation sites observed in both the primary CRC and the liver metastases of all the clusters in the ROS defence function.

GSTA1 showed differential expression in primary CRC and liver metastases. In primary CRC it was observed to be down-regulated, whereas in the liver metastases it was up-regulated. This suggests a potential build up of reactive molecules with the progression of the cancer in the metastatic state.

CHAPTER 4

DISCUSSION

Mitochondria are indispensable organelles present in the eukaryotic cell. They are primarily involved in the energy production in the form of ATP through oxidative phosphorylation. In addition, they are involved in diverse functions such as beta oxidation of fatty acids, apoptosis, biosynthesis of heme, FE-S cluster biosynthesis and calcium signalling. Mitochondrial disorders arise from defects in mtDNA, encoding essential components of OXPHOS. The nuclear genome also contributes the majority of the OXPHOS proteins and hence variations in the proteins encoded by nuclear genome can also cause mitochondrial disorders.

The MitoModel server

In this study we have developed a web-based platform named “MitoModel” that has brought together 659 mitochondria associated genes encoded by both mitochondria and nuclear genomes. We classified them into 17 functional groups. All the genes in the MitoModel are annotated for their role via comprehensive literature survey and carefully put into their functional groups. MitoModel is designed as a web server, which allows users to map mutation and differential expression data. The advantage that MitoModel extends is the fact that it is highly interactive and enables users to interpret their data in the functional context of mitochondria.

Compiling the genes to be part of a mitochondrial function included identifying the investigated or well reviewed functions related to mitochondria and taking note of all the genes and their roles. While the advantage of our approach was that we could capture the mitochondria associated genes and their roles at a detailed level in each

function, the disadvantage was that it took a lot of time and effort to compile 659 genes. Though time consuming our approach appropriately pinpoints the roles of genes, which was a primary requirement for us to achieve in conducting functional studies of mitochondria.

Comparing our approach to other resources hosting mitochondria proteomics data, it is evident that the inventory of the genes compiled by us had only literature evidence compared to MitoCarta. This resource provides evidence through literature, targetP signals for mitochondrial localization prediction, homologs of yeast mitochondrial proteins, Rickettsia homologs, domains exclusive for mitochondria, induction, coexpression and mass spectrometry, providing GO term annotation for the genes [Pagliarini et al., 2008], whereas MitoMiner includes data from 52 large-scale proteomic datasets of mitochondrial localisation from both mass spectrometry and green fluorescent protein- (GFP-) tagging studies, providing GO term annotations and functions curated by UniProt [Smith & Robinson, 2016].

The inventory of 659 genes was initially generated for *Homo sapiens* and further extended to mouse, deriving 659 mouse orthologous genes from the human gene set, using the HCOP's human orthology prediction [Eyre et al., 2007]. The STRING database [Szklarczyk et al. 2015] was used to derive the interactions for our gene sets and for human and mouse genes we got 10985 and 12571 interactions, respectively. Similar efforts were made to achieve mitochondrial interactome from budding yeast, resulting in nearly 10000 interactions for 800 genes extracted from 24 published datasets [Perocchi et al., 2006].

A database was created for the gene catalog and the interactions of the MitoModel web server. This enables the user to interact with user-provided variants data. The disadvantage of MitoModel is that users cannot access the gene list and its functions

without providing input data from their side. The output text file generated by MitoModel returns only the variant genes. This is not the case with MitoCarta and MitoMiner, which allows users to query for individual or group of genes. The advantages of MitoModel are that it is the only tool known to us until now, which maps user-defined variation data of different diseases onto the mitochondria associated genes. It is furthermore highly interactive, providing users with simple visual cues, appropriate gene information and the mapped variants data information. Similar web resource created by another study called MitoInteractome allowed users to query for interacting partners, SNPs within proteins, the number of SNPs, disease related proteins [Reja et al., 2009] but never allowed the analysis of user data.

Though MitoModel is a robust, interactive network, it still lacks several aspects such as providing the whole gene set and functions to the user, which limits the user knowledge only to the variant genes. Second, the roles of the genes are manually curated and are presently static, which means only database administrators can curate it. At present MitoModel does not link to any other web resources, which make its outcome specific only to variants data of the user-provided disease.

Use cases tested for MitoModel

We tested MitoModel on three different data sets: First, we used data from aneuploid cell lines. In HCT116 5/4 aneuploid cell line, we identified PKM2 up-regulated, which catalyzes the conversion of phosphoenolpyruvate to pyruvate, resulting in the generation of glycolytic ATP. It was reported that chromosomally-unstable cancer lines displayed increased glycolytic and TCA-cycle flux [Sheltzer, 2013], indicating that the generation of glycolytic energy might be higher in HCT116 5/4 cells compared to its wild type cell line. We also identified several genes down-regulated, harboring mutation sites in electron transport chain, replication and

transcription, and translation functions. Thus we hypothesize that mitochondrial biogenesis and energy production inside mitochondria are severely affected in HCT116 5/4 cell line compared to its wild type cell line.

In RPE1 5/3 12/3 aneuploid cells, we identified several genes in electron transport chain, replication and transcription, and translation up-regulated. In ROS defense, we observe that several genes involved in the reducing the ROS elements to be up-regulated. Thus we hypothesize that increased stress created during energy production caused a buildup of ROS in RPE1 5/3 12/3 aneuploidy cell line compared to its wild type cell line.

In RPE1H2B 21/3 aneuploidy cell line, we identified two up-regulated genes in electron transport chain and two up-regulated genes in ROS defence such as SOD1, which removes superoxides in the intermembrane space of mitochondria and GPX1, which further reduces the hydrogen peroxide to water. It was reported that the superoxide production and oxidative stress were observed to be 3 times higher in Down Syndrome fibroblasts [Coskun & Busciglio, 2012], thus we hypothesize that a mis-regulated mitochondrial OXPHOS leads to the buildup of mitochondrial ROS in the RPE1H2B 21/3 aneuploidy cell line compared to its wild type cell line.

Comparing the MitoModels of three aneuploid cell lines throws light on the fact that they were highly different from each other. Though we could observe that the functions replication and transcription, translation and electron transport chain were the most affected in the HCT116 5/4 and RPE1 5/3 12/3, they were showing contradictory behaviors. RPE1H2B 21/3 cells compared to other aneuploidy cell lines, accumulating only few variations in the mitochondria associated genes. Thus using MitoModels we could show that each aneuploidy cell line behaves individually when compared to each other.

Second, we tested MitoModel on the expression data of expression of high (HR) and low (LR) stress resistance mouse line. Here we identified *Atp5h*, *Atp5o* and *Atp5e* from the electron transport chain, which are three essential subunits of ATP synthase complex V to be up-regulated, suggesting that there might be an increased conversion of ADP to ATP in the HR mouse line. In glycolysis, *Slc2a4*, a facilitated glucose transporter was up-regulated. In addition *Pkm2*, which is known to catalyse the transphosphorylation of phosphoenolpyruvate into pyruvate and ATP was upregulated. The hippocampal proteomic analysis identified several proteins differentially expressed in HR and LR mice, including proteins involved in energy metabolism [Knapman et al., 2012]. We hypothesize that there might be a increased need of energy in HR mouse line, whereby glycolysis is also contributing to this.

Finally, we tested MitoModel on RNA-seq data of normal colon , primary Colorectal cancer (CRC) and liver metastases from 16 patients [Kim et al., 2014]. 16 MitoModels of primary CRC and liver metastases were reduced to 4 representative MitoModels representing clustering patient groups. We analysed those 4 representative groups for mitochondrial contribution. In the electron transport chain, *COX6B2* was down-regulated in both primary CRC and liver metastases of most clusters. Interestingly, *COX6B2* was also observed to be down-regulated in the rho(0) cell line [Hashiguchi & Zhang-akiyama, 2009] devoid of mitochondrial DNA that exhibit the Warburg effect [Ayyasamy et al., 2011]. This indicates that down-regulation of *COX6B2* may be involved in both the development and progression of CRC. Mutations in *MT-ND5* and *MT-CO1* were observed in the primary CRC and liver metastases of cluster 1 and 2. Similarly, mutations in the coding regions of *MT-ND5* and *MT-CO1* were observed in the human colorectal cancer cell line as well as human colon cancer [Chatterjee et al., 2006]. This suggests that the mutations might lead to changes in the OXPHOS process. In the beta oxidation of fatty acids, *FABP6*, was up-regulated in both primary CRC and liver metastases of most clusters and it

was also reported to be overexpressed in the colorectal cancer [Ohmachi et al., 2006]. In addition, we also identified ACADL, which catalyses the metabolism of long chain fatty acids. This mRNA was up-regulated only in the liver metastases of all clusters. ACADS, which catalyses the metabolism of short chain fatty acids was down-regulated in primary CRC of all clusters. We therefore hypothesize that there might be an up-regulated first step of beta oxidation in liver metastases due to decrease in the catalysing ability of ACADS in primary CRC, which functions at the tail end of the beta oxidation. In urea cycle, ARG1 was up-regulated only in the liver metastases of all clusters. ARG1 is involved in catalysing the final step of urea cycle, hydrolyzing arginine to urea and ornithine. It has been reported that there was a buildup of urea cycle metabolites (purines, pyrimidines and amino acids) in colon carcinoma [Denkert et al., 2008]. Thus we hypothesize that there might be an increase in the intermediate products of urea cycle in liver metastases. In apoptosis, CASP7 which is one of the executioner caspases leading to apoptosis, as well as BCL2, which is an anti-apoptotic member of Bcl-2 protein family are down-regulated in both primary CRC and liver metastases of most clusters. TP53, which directly binds to Bcl-2 family members propagating apoptosis was noticed to be mutated in both the primary CRC and the liver metastases. A study suggests that BCL2 suppresses TP53 dependent apoptosis in colorectal cancer cells [Jiang and Milner, 2003], and variations in both, the BCL2 and TP53 gene in both the primary CRC and liver metastases indicates, that there might be an inability of mitochondria to induce the intrinsic apoptotic pathway.

The above research findings demonstrates that with MitoModel, user can map their variant data and efficiently describe mitochondria in a disease state. Thus MitoModel is an infrastructure, which enables user to make primary hypothesis of mitochondrial biology in the disease of interest. It should be noted that MitoModel

only enables hypothesis, which should be verified in the lab before making final conclusions.

CHAPTER 5

Conclusions and future perspectives

5.1 CONCLUSION:

An array of human diseases are implicated to contain atypical mitochondria, which not only have a pivotal role in efficient energy generation but also several other important functions in the cell. Mutations in mtDNA and nDNA, both inherited and spontaneous, and differential expression patterns of mitochondrial genes encoded in mitochondria and the nucleus lead to altered mitochondrial functions, which has a critical impact on cell physiology and survival.

The availability of large scale sequencing data of several disease samples has opened up avenues to identify variants carried or developed during disease progression. The advantage of analysing diseases with RNA-seq data, are two-fold: it provides differential expression of genes, as well as efficient capture of mutations.

This study has established a mitochondria-based model in the form of the MitoModel web-server, which is an program to efficiently comprehend the variants carried by mitochondria in a disease state. This approach allows users to make a primary hypothesis about the mitochondrial biology and physiology in disease by mapping expression and mutation variants on to the MitoModel.

This work also highlights the applicability of MitoModel to various disease types. We have used it to understand mitochondrial variants carried by different aneuploid cell lines, highlighting the different mitochondrial variations observed in the MitoModels for HCT116 5/4, RPE1 5/3 12/3 and RPE1H2B 21/3 cell lines. In a

second comparison, we have used a mouse MitoModel to analyse the differential mitochondrial expression between high and low stress reactivity mouse lines. The data mapped on the mouse MitoModel revealed that most of the mitochondrial functions were up-regulated in the HR stress reactivity mice. It also showed a deviation in the energy production, which was increased in glycolysis due to a potential damage to the efficient energy production by mitochondria.

Analysing the representative MitoModel genes accommodated by the 16 samples of CRC and liver metastases identified numerous affected genes, that contribute to the tweaking of the metabolic makeup of the mitochondria. For instance, PKLR which catalyses the reaction producing glycolytic ATP was up-regulated only in the liver samples; ACADS and ACADL contradictory misregulations inside mitochondria in primary CRC's and liver metastases samples might play an important role in creating an imbalance in the generation of acetyl CoA. Due to this metabolic imbalance, there might be an increased stress to the mitochondria leading to the mitochondrial clearance via mitophagy, which was also observed only in the liver metastases samples with an up-regulated BNIP3, causing the permeabilization of the mitochondrial membrane during mitophagy.

Thus, MitoModel an interactive network with mitochondria associated genes provides an infrastructure to the user to understand the biology of mitochondria and the changes it accommodates in the different diseases.

5.2 FUTURE PERSPECTIVES:

Improvements to the existing MitoModel will be achieved by expansion of the model to include additional genes and functions. A diverse set of mass-spec studies of whole mitochondria from several organisms are available to date [Smith AC et al., 2012]. One possibility is to built an extended MitoModel based on these experimental data.

At present NCBI gene symbols are accepted by the MitoModel for mapping the variants. Since NCBI gene symbols might have several synonyms but only a single numeric ID, using in the future the numeric IDs would prevent the mismatching of synonyms to their gene symbols in the database.

The MitoModel enables users store and interactively use their data. Hence a mitochondrial disease database could prove as an important portal to store and catalogue mitochondrial variants in different disease types. Users could control public accessibility of their data, enabling a more comprehensive analysis of mitochondrial variants.

The network framework of the MitoModel can be further explored. One easy to establish improvement would be to give the user the options to view the first interacting partners of the genes.

APPENDIX A

Bibliography

- [Andrews et al., 1999] Andrews RM, Kubacka I, Chinnery PF, Lightowlers RN, Turnbull DM, Howell N. Reanalysis and revision of the Cambridge reference sequence for human mitochondrial DNA. *Nat Genet.* 1999;23(2):147
- [Anesti & Scorrano, 2006] Anesti V, Scorrano L. The relationship between mitochondrial shape and function and the cytoskeleton. *Biochim Biophys Acta.* 2006;1757(5-6):692-9
- [Ardail et al., 1990] Ardail D, Privat JP, Egret-charlier M, Levrat C, Lerme F, Louisot P. Mitochondrial contact sites. Lipid composition and dynamics. *J Biol Chem.* 1990;265(31):18797-802
- [Ayyasamy et al., 2011] Ayyasamy V, Owens KM, Desouki MM, et al. Cellular model of Warburg effect identifies tumor promoting function of UCP2 in breast cancer and its suppression by genipin. *PLoS ONE.* 2011;6(9):e24792.
- [Baertling et al., 2015] Baertling F, A m van den brand M, Hertecant JL, et al. Mutations in COA6 cause cytochrome c oxidase deficiency and neonatal hypertrophic cardiomyopathy. *Hum Mutat.* 2015;36(1):34-8
- [Banci et al., 2011] Banci L, Bertini I, Cefaro C, Ciofi-baffoni S, Gallo A. Functional role of two interhelical disulfide bonds in human Cox17 protein from a structural perspective. *J Biol Chem.* 2011;286(39):34382-90.
- [Battersby et al., 2003] Battersby BJ, Loredano-osti JC, Shoubridge EA. Nuclear genetic control of mitochondrial DNA segregation. *Nat Genet.* 2003;33(2):183-6.
- [Berg et al., 2002] Berg JM, Tymoczko JL, Stryer L. (2002). *BIOCHEMISTRY*. 5th edition, W H Freeman, New York

- [Bestwick et al., 2010] Bestwick M, Jeong MY, Khalimonchuk O, Kim H, Winge DR. Analysis of Leigh syndrome mutations in the yeast SURF1 homolog reveals a new member of the cytochrome oxidase assembly factor family. *Mol Cell Biol.* 2010;30(18):4480-91.
- [Biancotti & Benvenisty, 2011] Biancotti JC, Benvenisty N. Aneuploid human embryonic stem cells: origins and potential for modeling chromosomal disorders. *Regen Med.* 2011;6(4):493-503.
- [Bricker et al., 2012] Bricker DK, Taylor EB, Schell JC, et al. A mitochondrial pyruvate carrier required for pyruvate uptake in yeast, *Drosophila*, and humans. *Science.* 2012;337(6090):96-100.
- [Brown et al., 2001] Brown DT, Samuels DC, Michael EM, Turnbull DM, Chinnery PF. Random genetic drift determines the level of mutant mtDNA in human primary oocytes. *Am J Hum Genet.* 2001;68(2):533-6.
- [Chatterjee et al., 2006] Chatterjee A, Mambo E, Sidransky D. Mitochondrial DNA mutations in human cancer. *Oncogene.* 2006;25(34):4663-74.
- [Chen & Chan, 2009] Chen H, Chan DC. Mitochondrial dynamics--fusion, fission, movement, and mitophagy--in neurodegenerative diseases. *Hum Mol Genet.* 2009;18(R2):R169-76.
- [Chinnery, 2014] Chinnery PF. Mitochondrial Disorders Overview. 2000 Jun 8 [Updated 2014 Aug 14]. In: Pagon RA, Adam MP, Ardinger HH, et al., editors. *GeneReviews®* [Internet]. Seattle (WA): University of Washington, Seattle; 1993-2015. Available from: <http://www.ncbi.nlm.nih.gov/books/NBK1224/>
- [Coenen et al., 2004] Coenen MJ, Van den heuvel LP, Ugalde C, et al. Cytochrome c oxidase biogenesis in a patient with a mutation in COX10 gene. *Ann Neurol.* 2004;56(4):560-4.
- [Coskun et al., 2012] Coskun PE, Busciglio J. Oxidative Stress and Mitochondrial Dysfunction in Down's Syndrome: Relevance to Aging and Dementia. *Curr Gerontol Geriatr Res.* 2012;2012:383170

- [Cullis et al., 1986] Cullis PR, Hope MJ, Tilcock CP. Lipid polymorphism and the roles of lipids in membranes. *Chem Phys Lipids*. 1986;40(2-4):127-44.
- [Dailey, 1997] Dailey HA. Enzymes of heme biosynthesis. *Journal of Biological Inorganic Chemistry*, 2 (1997), pp. 411–417.
- [Denkert et al., 2008] Denkert C, Budczies J, Weichert W, et al. Metabolite profiling of human colon carcinoma – deregulation of TCA cycle and amino acid turnover. *Molecular Cancer*. 2008;7:72.
- [Depristo et al., 2011] Depristo MA, Banks E, Poplin R, et al. A framework for variation discovery and genotyping using next-generation DNA sequencing data. *Nat Genet*. 2011;43(5):491-8.
- [Dobin et al., 2013] Dobin A, Davis CA, Schlesinger F, et al. STAR: ultrafast universal RNA-seq aligner. *Bioinformatics*. 2013;29(1):15-21
- [Dolezal et al., 2006] Dolezal P, Likic V, Tachezy J, Lithgow T. Evolution of the molecular machines for protein import into mitochondria. *Science*. 2006;313(5785):314-8.
- [Dürrbaum et al., 2014] Dürrbaum M, Kuznetsova AY, Passerini V, Stingle S, Stoehr G, Storchová Z. Unique features of the transcriptional response to model aneuploidy in human cells. *BMC Genomics*. 2014;15:139
- [Dyall et al., 2004] Dyall SD, Brown MT, Johnson PJ. Ancient invasions: from endosymbionts to organelles. *Science*. 2004;304(5668):253-7.
- [Ewing & Green, 1998] Ewing B, Green P. Base-calling of automated sequencer traces using phred. II. Error probabilities. *Genome Res*. 1998;8(3):186-94.
- [Eyre et al., 2007] Eyre TA, Wright MW, Lush MJ, Bruford EA. HCOP: a searchable database of human orthology predictions. *Brief Bioinformatics*. 2007;8(1):2-5.

- [Falkenberg et al., 2007] Falkenberg M, Larsson NG, Gustafsson CM. DNA replication and transcription in mammalian mitochondria. *Annu Rev Biochem.* 2007;76:679-99
- [Formosa et al., 2015] Formosa LE, Mimaki M, Frazier AE, et al. Characterization of mitochondrial FOXRED1 in the assembly of respiratory chain complex I. *Hum Mol Genet.* 2015;24(10):2952-65.
- [Gardner et al., 2011] Gardner A, Boles RG. Beyond the serotonin hypothesis: mitochondria, inflammation and neurodegeneration in major depression and affective spectrum disorders. *Prog Neuropsychopharmacol Biol Psychiatry.* 2011;35(3):730-43.
- [Ghezzi et al., 2009] Ghezzi D, Goffrini P, Uziel G, et al. SDHAF1, encoding a LYR complex-II specific assembly factor, is mutated in SDH-defective infantile leukoencephalopathy. *Nat Genet.* 2009;41(6):654-6
- [Ghezzi et al., 2011] Ghezzi D, Arzuffi P, Zordan M, et al. Mutations in TTC19 cause mitochondrial complex III deficiency and neurological impairment in humans and flies. *Nat Genet.* 2011;43(3):259-63
- [Giardine et al., 2005] Giardine B, Riemer C, Hardison RC, et al. Galaxy: a platform for interactive large-scale genome analysis. *Genome Res.* 2005;15(10):1451-5
- [Gisbergen et al., 2015] M.W. van Gisbergen,A.M. Voets,M.H.W. Starmans,I.F.M. de Coo,R. Yadak, R.F. Hoffmann,P.C. Boutros,H.J.M. Smeets,L. Dubois,P. Lambin. How do changes in the mtDNA and mitochondrial dysfunction influence cancer and cancer therapy? Challenges, opportunities and models. *Mutation Research/Reviews in Mutation Research.* Volume 764, 2015; 16–3
- [Gonzalez & Cruz, 2015] Gonzalez-pons M, Cruz-correa M. Colorectal Cancer Biomarkers: Where Are We Now?. *Biomed Res Int.* 2015;2015:149014.
- [Gordon et al., 2012] Gordon DJ, Resio B, Pellman D. Causes and consequences of aneuploidy in cancer. *Nat Rev Genet.* 2012;13(3):189-203.

- [Goto et al., 2011] Goto H, Dickins B, Afgan E, et al. Dynamics of mitochondrial heteroplasmy in three families investigated via a repeatable re-sequencing study. *Genome Biol.* 2011;12(6):R59.
- [Grada & Weinbrecht, 2013] Grada A, Weinbrecht K. Next-generation sequencing: methodology and application. *J Invest Dermatol.* 2013;133(8):e11.
- [Griffiths et al., 2000] Griffiths AJF, Miller JH, Suzuki DT, et al. *An Introduction to Genetic Analysis*. 7th edition. New York: W. H. Freeman; 2000. Aneuploidy. Available from: <http://www.ncbi.nlm.nih.gov/books/NBK21870/>
- [Hashiguchi & Zhang-akiyama, 2009] Hashiguchi K, Zhang-akiyama QM. Establishment of human cell lines lacking mitochondrial DNA. *Methods Mol Biol.* 2009;554:383-91
- [Hales, 2010] Hales, K. G. Mitochondrial Fusion and Division. *Nature Education* (2010);3(9):12
- [Hao et al., 2009] Hao HX, Khalimonchuk O, Schraders M, et al. SDH5, a gene required for flavination of succinate dehydrogenase, is mutated in paraganglioma. *Science.* 2009;325(5944):1139-42
- [Heide et al., 2012] Heide H, Bleier L, Steger M, et al. Complexome profiling identifies TMEM126B as a component of the mitochondrial complex I assembly complex. *Cell Metab.* 2012;16(4):538-49
- [Heinzmann et al., 2014] Heinzmann et al. Mice selected for extremes in stress reactivity reveal key endophenotypes of major depression: A translational approach. *Psychoneuroendocrinology* (2014) 49, 229-243
- [Houten & Wanders, 2010] Houten SM, Wanders RJ. A general introduction to the biochemistry of mitochondrial fatty acid β -oxidation. *J Inherit Metab Dis.* 2010;33(5):469-77.

- [Houtkooper & Vaz, 2008] Houtkooper RH, Vaz FM. Cardiolipin, the heart of mitochondrial metabolism. *Cell Mol Life Sci.* 2008;65(16):2493-506.
- [Huigsloot et al., 2011] Huigsloot M, Nijtmans LG, Szklarczyk R, et al. A mutation in C2orf64 causes impaired cytochrome c oxidase assembly and mitochondrial cardiomyopathy. *Am J Hum Genet.* 2011;88(4):488-93
- [Hüttemann et al., 2003] Hüttemann M, Jaradat S, Grossman LI. Cytochrome c oxidase of mammals contains a testes-specific isoform of subunit VIb--the counterpart to testes-specific cytochrome c?. *Mol Reprod Dev.* 2003;66(1):8-16.
- [Janssen et al., 2002] Janssen R, Smeitink J, Smeets R, Van den heuvel L. CIA30 complex I assembly factor: a candidate for human complex I deficiency?. *Hum Genet.* 2002;110(3):264-70
- [Jemal et al., 2011] Jemal A, Bray F, Center MM, Ferlay J, Ward E, Forman D. Global cancer statistics. *CA Cancer J Clin.* 2011;61(2):69-90.
- [Jiang and Milner, 2003] Jiang M, Milner J. Bcl-2 constitutively suppresses p53-dependent apoptosis in colorectal cancer cells. *Genes & Development.* 2003;17(7):832-837.
- [Kiebish et al., 2008] Kiebish MA, Han X, Cheng H, Chuang JH, Seyfried TN. Cardiolipin and electron transport chain abnormalities in mouse brain tumor mitochondria: lipidomic evidence supporting the Warburg theory of cancer. *J Lipid Res.* 2008;49(12):2545-56.
- [Kim et al., 2013] Kim D, Pertea G, Trapnell C, Pimentel H, Kelley R, Salzberg SL. TopHat2: accurate alignment of transcriptomes in the presence of insertions, deletions and gene fusions. *Genome Biol.* 2013;14(4):R36.
- [Kim et al., 2014] Kim SK, Kim SY, Kim JH, et al. A nineteen gene-based risk score classifier predicts prognosis of colorectal cancer patients. *Mol Oncol.* 2014;8(8):1653-66.

- [Knapman et al., 2012] Knapman A, Kaltwasser SF, Martins-de-souza D, et al. Increased stress reactivity is associated with reduced hippocampal activity and neuronal integrity along with changes in energy metabolism. *Eur J Neurosci.* 2012;35(3):412-22.
- [Kozjak-pavlovic et al., 2014] Kozjak-pavlovic V, Prell F, Thiede B, et al. C1orf163/RESA1 is a novel mitochondrial intermembrane space protein connected to respiratory chain assembly. *J Mol Biol.* 2014;426(4):908-20.
- [Langmead & Salzberg, 2012] Langmead B, Salzberg SL: Fast gapped-read alignment with Bowtie 2. *Nat Methods* 2012, 9:357-359
- [Leary et al., 2007] Leary SC, Cobine PA, Kaufman BA, et al. The human cytochrome c oxidase assembly factors SCO1 and SCO2 have regulatory roles in the maintenance of cellular copper homeostasis. *Cell Metab.* 2007;5(1):9-20.
- [Li & Durbin, 2009] Li H, Durbin R. Fast and accurate short read alignment with Burrows-Wheeler transform. *Bioinformatics.* 2009;25(14):1754-60.
- [Li et al., 2008] Li H, Ruan J, Durbin R. Mapping short DNA sequencing reads and calling variants using mapping quality scores. *Genome Res.* 2008;18(11):1851-8.
- [Lill, 2009] Lill R. Function and biogenesis of iron-sulphur proteins. *Nature.* 2009;460(7257):831-8
- [Lu & Claypool, 2015] Ya-Wen Lu and Steven M. Claypool. Disorders of phospholipid metabolism: an emerging class of mitochondrial disease due to defects in nuclear genes. *Front Genet.* 2015; 6: 3
- [Lunt & Vander heiden, 2011] Lunt SY, Vander heiden MG. Aerobic glycolysis: meeting the metabolic requirements of cell proliferation. *Annu Rev Cell Dev Biol.* 2011;27:441-64
- [Maimon & Rokach, 2005] Maimon OZ, Rokach L. *Data Mining and Knowledge Discovery Handbook.* Springer Science & Business Media; 2005

- [Man et al., 2003] Man PY, Griffiths PG, Brown DT, Howell N, Turnbull DM, Chinnery PF. The epidemiology of Leber hereditary optic neuropathy in the North East of England. *Am J Hum Genet.* 2003;72(2):333-9.
- [Martin, 2011] Marcel Martin. Cutadapt removes adapter sequences from high-throughput sequencing reads. *EMBnet.journal.* 2011;17(1):pp. 10-12.
- [Mckenna et al., 2010] Mckenna A, Hanna M, Banks E, et al. The Genome Analysis Toolkit: a MapReduce framework for analyzing next-generation DNA sequencing data. *Genome Res.* 2010;20(9):1297-303.
- [Mckenzie et al., 2011] Mckenzie M, Tucker EJ, Compton AG, et al. Mutations in the gene encoding C8orf38 block complex I assembly by inhibiting production of the mitochondria-encoded subunit ND1. *J Mol Biol.* 2011;414(3):413-26
- [Meisinger et al., 2008] Meisinger C, Sickmann A, Pfanner N. The mitochondrial proteome: from inventory to function. *Cell.* 2008;134(1):22-4
- [Nouws et al., 2010] Nouws J, Nijtmans L, Houten SM, et al. Acyl-CoA dehydrogenase 9 is required for the biogenesis of oxidative phosphorylation complex I. *Cell Metab.* 2010;12(3):283-94
- [Ogilvie et al., 2005] Ogilvie I, Kennaway NG, Shoubridge EA. A molecular chaperone for mitochondrial complex I assembly is mutated in a progressive encephalopathy. *J Clin Invest.* 2005;115(10):2784-92
- [Ohmachi et al., 2006] Ohmachi T, Inoue H, Mimori K, et al. Fatty acid binding protein 6 is overexpressed in colorectal cancer. *Clin Cancer Res.* 2006;12(17):5090-5.
- [Pagliarini et al., 2008] Pagliarini DJ, Calvo SE, Chang B, et al. A mitochondrial protein compendium elucidates complex I disease biology. *Cell.* 2008;134(1):112-23.

- [Palmer et al., 2011] Palmer CS, Osellame LD, Stojanovski D, Ryan MT. The regulation of mitochondrial morphology: intricate mechanisms and dynamic machinery. *Cell Signal*. 2011;23(10):1534-45
- [Perocchi et al., 2006] Perocchi F, Jensen LJ, Gagneur J, et al. Assessing Systems Properties of Yeast Mitochondria through an Interaction Map of the Organelle. Kim SK, ed. *PLoS Genetics*. 2006;2(10): e170.
- [Petruzzella et al., 1998] Petruzzella V, Tiranti V, Fernandez P, Ianna P, Carozzo R, Zeviani M. Identification and characterization of human cDNAs specific to BCS1, PET112, SCO1, COX15, and COX11, five genes involved in the formation and function of the mitochondrial respiratory chain. *Genomics*. 1998;54(3):494-504.
- [Piskol et al., 2013] Piskol R, Ramaswami G, Li JB. Reliable identification of genomic variants from RNA-seq data. *Am J Hum Genet*. 2013;93(4):641-51.
- [Pon et al., 1989] Pon LA, Vestweber D, Yang M, Schatz G. Interaction between mitochondria and the nucleus. *J Cell Sci Suppl*. 1989;11:1-11.
- [Ramos et al., 2015] Ramos AH, Lichtenstein L, Gupta M, et al. Oncotator: cancer variant annotation tool. *Hum Mutat*. 2015;36(4):E2423-9.
- [Ranieri et al., 2013] Ranieri M, Brajkovic S, Riboldi G, et al. Mitochondrial fusion proteins and human diseases. *Neurol Res Int*. 2013;2013:293893.
- [Read & Kodner, 1999] Read TE, Kodner IJ. Colorectal cancer: risk factors and recommendations for early detection. *Am Fam Physician*. 1999;59(11):3083-92.
- [Reja et al., 2009] Rohit Reja, AJ Venkatakrisnan, Jungwoo Lee, Byoung-Chul Kim, Jea-Woon Ryu, Sungsam Gong, Jong Bhak and Daeui Park. MitoInteractome: Mitochondrial protein interactome database, and its application in 'aging network' analysis. *BMC Genomics* 2009 10(Suppl 3): S20

- [Rizzuto et al., 2012] Rizzuto R, De stefani D, Raffaello A, Mammucari C. Mitochondria as sensors and regulators of calcium signalling. *Nat Rev Mol Cell Biol.* 2012;13(9):566-78.
- [Rossignol et al., 2003] Rossignol R, Faustin B, Rocher C, Malgat M, Mazat JP, Letellier T. Mitochondrial threshold effects. *Biochem J.* 2003;370(Pt 3):751-62.
- [Rouault & Tong, 2005] Rouault TA, Tong WH. Iron-sulphur cluster biogenesis and mitochondrial iron homeostasis. *Nat Rev Mol Cell Biol.* 2005;6(4):345-51
- [Saada et al., 2009] Saada A, Vogel RO, Hoefs SJ, et al. Mutations in NDUFAF3 (C3ORF60), encoding an NDUFAF4 (C6ORF66)-interacting complex I assembly protein, cause fatal neonatal mitochondrial disease. *Am J Hum Genet.* 2009;84(6):718-27
- [Sabharwal & Schumacker, 2014] Sabharwal SS, Schumacker PT. Mitochondrial ROS in cancer: initiators, amplifiers or an Achilles' heel?. *Nat Rev Cancer.* 2014;14(11):709-21
- [Sacconi et al., 2005] Sacconi S, Trevisson E, Pistollato F, et al. hCOX18 and hCOX19: two human genes involved in cytochrome c oxidase assembly. *Biochem Biophys Res Commun.* 2005;337(3):832-9.
- [Sanger et al., 1977] Sanger F, Nicklen S, Coulson AR. DNA sequencing with chain-terminating inhibitors. *Proc Natl Acad Sci USA.* 1977;74(12):5463-7
- [Schaffer & Suleiman, 2010] Schaffer SW, Suleiman MS. Mitochondria, The Dynamic Organelle. Springer Science & Business Media; 2010.
- [Schmidt et al., 2010] Schmidt O, Pfanner N, Meisinger C. Mitochondrial protein import: from proteomics to functional mechanisms. *Nat Rev Mol Cell Biol.* 2010;11(9):655-67

- [Sheftel et al., 2009] Sheftel AD, Stehling O, Pierik AJ, et al. Human ind1, an iron-sulfur cluster assembly factor for respiratory complex I. *Mol Cell Biol.* 2009;29(22):6059-73.
- [Sheltzer, 2013] Sheltzer JM. A transcriptional and metabolic signature of primary aneuploidy is present in chromosomally-unstable cancer cells and informs clinical prognosis. *Cancer research.* 2013;73(21):6401-6412.
- [Sherry et al., 2001] Sherry ST, Ward MH, Kholodov M, Baker J, Phan L, Smigielski EM, Sirotkin K. dbSNP: the NCBI database of genetic variation. *Nucleic Acids Res.* 2001 Jan 1;29(1):308-11
- [Sheth & Clary, 2005] Sheth KR, Clary BM. Management of hepatic metastases from colorectal cancer. *Clin Colon Rectal Surg.* 2005;18(3):215-23.
- [Shimizu et al., 2010] Shimizu, S., Iida, S., Ishiguro, M., Uetake, H., Ishikawa, T., Takagi, Y. ... Sugihara, K. (2010). Methylated BNIP3 gene in colorectal cancer prognosis . *Oncology Letters*, 1, 865-872.
- [Smith et al., 2012] Smith PM, Fox JL, Winge DR. Biogenesis of the cytochrome bc(1) complex and role of assembly factors. *Biochim Biophys Acta.* 2012;1817(2):276-86
- [Smith AC et al., 2012] Smith AC, Blackshaw JA, Robinson AJ. MitoMiner: a data warehouse for mitochondrial proteomics data. *Nucleic Acids Res.* 2012;40(Database issue):D1160-7.
- [Smith & Robinson, 2016] Smith AC, Robinson AJ. MitoMiner v3.1, an update on the mitochondrial proteomics database. *Nucleic Acids Research.* 2016;44(Database issue):D1258-D1261.
- [Smits et al., 2010] Smits P, Smeitink J, Van den heuvel L. Mitochondrial translation and beyond: processes implicated in combined oxidative phosphorylation deficiencies. *J Biomed Biotechnol.* 2010;2010:737385.

- [Stingele et al., 2012] Stingele S, Stoehr G, Peplowska K, Cox J, Mann M, Storchova Z. Global analysis of genome, transcriptome and proteome reveals the response to aneuploidy in human cells. *Mol Syst Biol.* 2012;8:608.
- [Sugiana et al., 2008] Sugiana C, Pagliarini DJ, McKenzie M, et al. Mutation of C20orf7 disrupts complex I assembly and causes lethal neonatal mitochondrial disease. *Am J Hum Genet.* 2008;83(4):468-78
- [Szklarczyk et al., 2012] Szklarczyk R, Wanschers BF, Cuypers TD, et al. Iterative orthology prediction uncovers new mitochondrial proteins and identifies C12orf62 as the human ortholog of COX14, a protein involved in the assembly of cytochrome c oxidase. *Genome Biol.* 2012;13(2):R12
- [Szklarczyk et al., 2013] Szklarczyk R, Wanschers BF, Nijtmans LG, et al. A mutation in the FAM36A gene, the human ortholog of COX20, impairs cytochrome c oxidase assembly and is associated with ataxia and muscle hypotonia. *Hum Mol Genet.* 2013;22(4):656-67
- [Szklarczyk et al., 2015] Szklarczyk et al. STRING v10: protein-protein interaction networks, integrated over the tree of life. *Nucleic Acids Res.* 2015 Jan 28; 43(Database issue): D447-D452
- [Tait & Green, 2010] Tait SW, Green DR. Mitochondria and cell death: outer membrane permeabilization and beyond. *Nat Rev Mol Cell Biol.* 2010;11(9):621-32
- [Taylor & Turnbull, 2005] Taylor RW, Turnbull DM. Mitochondrial DNA mutations in human disease. *Nat Rev Genet.* 2005;6(5):389-402.
- [Thomas & Gustafsson, 2013] Thomas RL, Gustafsson AB. Mitochondrial autophagy--an essential quality control mechanism for myocardial homeostasis. *Circ J.* 2013;77(10):2449-54.
- [Torraco et al., 2012] Torraco A, Verrigni D, Rizza T, et al. TMEM70: a mutational hot spot in nuclear ATP synthase deficiency with a pivotal role in complex V biogenesis. *Neurogenetics.* 2012;13(4):375-86

- [Touma et al., 2008] Touma et al. Mice selected for high versus low stress reactivity: A new animal model for affective disorders. *Psychoneuroendocrinology* (2008) 33, 839–862
- [Trapnell et al., 2009] Trapnell C, Pachter L, Salzberg SL. TopHat: discovering splice junctions with RNA-Seq. *Bioinformatics*. 2009;25(9):1105-11
- [Trapnell et al., 2010] Trapnell C, Williams BA, Pertea G, et al. Transcript assembly and quantification by RNA-Seq reveals unannotated transcripts and isoform switching during cell differentiation. *Nat Biotechnol*. 2010;28(5):511-5.
- [Trapnell et al., 2012] Trapnell C, Roberts A, Goff L, et al. Differential gene and transcript expression analysis of RNA-seq experiments with TopHat and Cufflinks. *Nat Protoc*. 2012;7(3):562-78.
- [Tucker et al., 2013] Tucker EJ, Wanschers BF, Szklarczyk R, et al. Mutations in the UQCC1-interacting protein, UQCC2, cause human complex III deficiency associated with perturbed cytochrome b protein expression. *PLoS Genet*. 2013;9(12):e1004034
- [Van der auwera et al., 2013] Van der auwera GA, Carneiro MO, Hartl C, et al. From FastQ data to high confidence variant calls: the Genome Analysis Toolkit best practices pipeline. *Curr Protoc Bioinformatics*. 2013;11(1110):11.10.1-11.10.33.
- [Velculescu et al., 1995] Velculescu VE, Zhang L, Vogelstein B, Kinzler KW. Serial analysis of gene expression. *Science*. 1995;270(5235):484-7.
- [Vogel et al., 2007] Vogel RO, Janssen RJ, Van den brand MA, et al. Cytosolic signaling protein Ecsit also localizes to mitochondria where it interacts with chaperone NDUFAB1 and functions in complex I assembly. *Genes Dev*. 2007;21(5):615-24
- [Wallace, 2012] Wallace DC. Mitochondria and cancer. *Nat Rev Cancer*. 2012;12(10):685-98.

- [Wanders et al., 2010] Wanders RJ, Ruiten JP, Ijlst L, Waterham HR, Houten SM. The enzymology of mitochondrial fatty acid beta-oxidation and its application to follow-up analysis of positive neonatal screening results. *J Inher Metab Dis.* 2010;33(5):479-94.
- [Wang et al., 2001] Wang ZG, White PS, Ackerman SH. Atp11p and Atp12p are assembly factors for the F(1)-ATPase in human mitochondria. *J Biol Chem.* 2001;276(33):30773-8.
- [Wang et al., 2009] Wang Z, Gerstein M, Snyder M. RNA-Seq: a revolutionary tool for transcriptomics. *Nat Rev Genet.* 2009;10(1):57-63.
- [Xu et al., 2008] Xu F, Ackerley C, Maj MC, et al. Disruption of a mitochondrial RNA-binding protein gene results in decreased cytochrome b expression and a marked reduction in ubiquinol-cytochrome c reductase activity in mouse heart mitochondria. *Biochem J.* 2008;416(1):15-26
- [Zheng, 2012] Zheng J. Energy metabolism of cancer: Glycolysis versus oxidative phosphorylation (Review). *Oncol Lett.* 2012;4(6):1151-1157.
- [Zhu et al., 1998] Zhu Z, Yao J, Johns T, et al. SURF1, encoding a factor involved in the biogenesis of cytochrome c oxidase, is mutated in Leigh syndrome. *Nat Genet.* 1998;20(4):337-43
- [Zsurka and Csordás, 2009] Zsurka, Gábor and Csordás, Attila. MitoWheel, visualizing the human mitochondrial genome . Available from Nature Precedings 2009 <<http://dx.doi.org/10.1038/npre.2009.3167.1>>
- [Zurita rendón et al., 2014] Zurita rendón O, Silva neiva L, Sasarman F, Shoubbridge EA. The arginine methyltransferase NDUFAF7 is essential for complex I assembly and early vertebrate embryogenesis. *Hum Mol Genet.* 2014;23(19):5159-70

APPENDIX B

Acknowledgements

I would like to thank my advisor Dr. Bianca Habermann, for giving me an opportunity, and for being a tremendous mentor for me. I would like to thank you for your help and support.

I would also like to thank my committee members, Professor. Dr. Barbara Conratt, Professor. Dr. John Parsch, Professor. Dr. Wolfgang Enard, Professor. Dr. Jurgen Soll, Prof. Dr. Thomas Cremer and Prof. Dr. Ute Vothknecht for serving as my committee members even at hardship.

A special thanks to our collaborators from Max Planck institute of biochemistry and Max Planck Institute of Psychiatry for kindly providing data. I also take this opportunity to thank my colleague José Villaveces for kindly extending his support to the MitoModel. I would also like to thank my colleagues who have been a great support through the years of my reaserch.

A special thanks to my family. I am grateful to my mother, father, mother-in law, wife and brothers for all of the sacrifices that you've made.

Finally I thank my God, In you I trust. Thank you.

APPENDIX C: Mitochondria associated genes, functions and their references

No.	Gene	Function	Reference
<i>ELECTRON TRANSPORT CHAIN</i>			
1	MT-ND1	Mitochondrially encoded NADH dehydrogenase, part of enzyme complex I, involved in the reduction of ubiquinone by NADH	[Schaffer & Suleiman, 2010]
2	MT-ND2		
3	MT-ND3		
4	MT-ND4		
5	MT-ND4L		
6	MT-ND5		
7	MT-ND6		
8	NDUFA1	Nuclear encoded essential components of complex I NADH dehydrogenase, involved in the reduction of ubiquinone by NADH	
9	NDUFA2		
10	NDUFA3		

11	NDUFA4	Nuclear encoded essential components of complex I NADH dehydrogenase, involved in the reduction of ubiquinone by NADH	[Schaffer & Suleiman, 2010]
12	NDUFA5		
13	NDUFA6		
14	NDUFA7		
15	NDUFA8		
16	NDUFA9		
17	NDUFA10		
18	NDUFA11		
19	NDUFA12		
20	NDUFA13		
21	NDUFAB1		
22	NDUFB1		
23	NDUFB2		

24	NDUFB3	Nuclear encoded essential components of complex I NADH dehydrogenase, involved in the reduction of ubiquinone by NADH	[Schaffer & Suleiman, 2010]
25	NDUFB4		
26	NDUFB5		
27	NDUFB6		
28	NDUFB7		
29	NDUFB8		
30	NDUFB9		
31	NDUFB10		
32	NDUFB11		
33	NDUFC1		
34	NDUFC2		
35	NDUFS1		
36	NDUFS2		

37	NDUFS3	Nuclear encoded essential components of complex I NADH dehydrogenase, involved in the reduction of ubiquinone by NADH	[Schaffer & Suleiman, 2010]
38	NDUFS4		
39	NDUFS5		
40	NDUFS6		
41	NDUFS7		
42	NDUFS8		
43	NDUFV1		
44	NDUFV2		
45	NDUFV3		
46	MT-CYB	Mitochondria encoded cytochrome b, an essential component of complex III, transfers electrons from ubiquinol to cytochrome c	
47	CYC1	Nuclear encoded essential components of complex III, transfers electrons from ubiquinol to cytochrome c	
48	UQCR10		
49	UQCR11		

50	UQCRB	Nuclear encoded essential components of complex III, transfers electrons from ubiquinol to cytochrome c	[Schaffer & Suleiman, 2010]
51	UQCRC1		
52	UQCRC2		
53	UQCRFS1		
54	UQCRH		
55	UQCRQ		
56	MT-CO1	Mitochondria encoded cytochrome c oxidases, essential components of complex IV, catalyses the reduction of oxygen to water by cytochrome c	
57	MT-CO2		
58	MT-CO3		
59	COX4I1	Nuclear encoded cytochrome c oxidase subunits, essential components of complex IV, catalyses the reduction of oxygen to water by cytochrome c	
60	COX4I2		
61	COX5A		
62	COX5B		

63	COX6A1	Nuclear encoded cytochrome c oxidase subunits, essential components of complex IV, catalyses the reduction of oxygen to water by cytochrome c	[Schaffer & Suleiman, 2010]
64	COX6A2		
65	COX6B1		
66	COX6B2		
67	COX6C		
68	COX7A1		
69	COX7A2		
70	COX7B		
71	COX7B2		
72	COX7C		
73	COX8A		
74	MT-ATP6		
75	MT-ATP8		

76	ATP5A1	Nuclear encoded ATP synthase subunits, essential components of complex V, reversible pump of protons into matrix with formation of ATP	[Schaffer & Suleiman, 2010]
77	ATP5B		
78	ATP5C1		
79	ATP5D		
80	ATP5E		
81	ATP5F1		
82	ATP5G1		
83	ATP5G2		
84	ATP5G3	Nuclear encoded ATP synthase subunits, essential components of complex V, reversible pump of protons into matrix with formation of ATP	[Schaffer & Suleiman, 2010]
85	ATP5H		
86	ATP5I		
87	ATP5J		
88	ATP5J2		

89	ATP5L		
90	ATP5O		
91	ATPIF1	Endogenous inhibitor subunit of ATP synthase, essential component of complex V	
92	ACAD9	Involved in the biogenesis of complex I	[Nouws et al., 2010]
93	FOXRED1	Putative complex I assembly factor	[Formosa et al., 2015]
94	ATPAF1	ATP synthase mitochondrial F1 complex assembly factor 1	[Wang et al., 2001]
95	ATPAF2	ATP synthase mitochondrial F1 complex assembly factor 2	
96	BCS1L	Involved in the assembly of complex III	[Petruzzella et al., 1998]
97	C7orf44	Complex IV assembly factor	[Szklarczyk et al., 2012]
98	CCDC56	Complex IV assembly factor	[Szklarczyk et al., 2012]
99	CHCHD8	Complex IV assembly factor	[Bestwick et al., 2010]

100	COA5	Complex IV assembly factor	[Huigsloot et al., 2011]
101	SELRC1	Complex IV assembly factor	[Kozjak-pavlovic et al., 2014]
102	C1orf31	Required for the stability of complex IV subunit	[Baertling et al., 2015]
103	COX10	Complex IV assembly factor	[Coenen et al., 2004]
104	COX11	Complex IV assembly factor	[Petruzzella et al., 1998]
105	COX14	Complex IV assembly factor	[Szklarczyk et al., 2012]
106	COX15	Complex IV assembly factor	[Petruzzella et al., 1998]
107	COX17	Responsible for providing copper ions to the complex IV	[Banci et al., 2011]
108	COX18	Assembly factors of complex IV	[Sacconi et al., 2005]
109	COX19		

110	COX20	Assembly factor of complex IV	[Szkłarczyk et al., 2013]
111	ECSIT	Assembly factor of complex I	[Vogel et al., 2007]
112	NDUFAF1	Assembly factor of complex I	[Janssen et al., 2002]
113	NDUFAF2	Assembly factor of complex I	[Ogilvie et al., 2005]
114	NDUFAF3	Assembly factors of complex I	[Saada et al., 2009]
115	NDUFAF4		
116	C20orf7	Complex I assembly factor	[Sugiana et al., 2008]
117	C8orf38	Complex I assembly factor	[Mckenzie et al., 2011]
118	C2orf56	Complex I assembly factor	[Zurita rendón et al., 2014]
119	NUBPL	Complex I assembly factor	[Sheftel et al., 2009]
120	SCO1		[Leary et al., 2007]

121	SCO2	Complex I assembly factors	
122	SDHAF1	Complex II specific assembly factor	[Ghezzi et al., 2009]
123	SDHAF2	Complex II specific assembly factor	[Hao et al., 2009]
124	SURF1	Assembly factor of complex IV	[Zhu et al., 1998]
125	TMEM126B	Complex I assembly factor	[Heide et al., 2012]
126	UQCC	Complex III assembly factor	[Tucker et al., 2013]
127	MNF1		
128	TTC19	Complex III assembly factor	[Ghezzi et al., 2011]
129	HCCS	Complex III assembly factor	[Smith et al., 2012]
130	PTCD2	Complex III assembly factor, process RNA transcripts involving cytochrome b	[Xu et al., 2008]
131	TMEM70	Complex V assembly factor	[Torraco et al., 2012]
<i>GLYCOLYSIS</i>			
132	SLC2A1	Basal glucose uptake, present in all mammalian tissues	[Berg et al., 2002]

133	SLC2A2	Glucose uptake in liver and pancreatic β cells	[Berg et al., 2002]
134	SLC2A3	Basal glucose uptake, present in all mammalian tissues	
135	SLC2A4	Glucose transport in the muscle and fat cells	
136	SLC2A5	Fructose transporter, present in the small intestine	
137	HK1	Glucose is phosphorylated to glucose 6-phosphate catalysed by the hexokinase	
138	HK2		
139	HK3		
140	GCK		
141	GPI	Isomerization of glucose 6-phosphate to fructose 6-phosphate by the phosphoglucose isomerase	
142	PFKL	Fructose 6-phosphate is phosphorylated to fructose 1,6-bisphosphate, catalyzed by phosphofructokinase	
143	PFKM		
144	PFKP		
145	ALDOA		

146	ALDOB	Fructose 1,6-bisphosphate converted into glyceraldehyde 3-phosphate and dihydroxyacetone phosphate catalyzed by aldolase	[Berg et al., 2002]
147	ALDOC		
148	TPI1	Dihydroxyacetone phosphate is converted into glyceraldehyde 3-phosphate catalyzed by triose phosphate isomerase	
149	GAPDH	Glyceraldehyde 3-phosphate is converted into 1,3-bisphosphoglycerate catalyzed by glyceraldehyde 3-phosphate dehydrogenase	
150	GAPDHS		
151	PGK1	1,3-bisphosphoglycerate is converted to 3-phosphoglycerate and ATP is released, catalyzed by Phosphoglycerate kinase	
152	PGK2		
153	PGAM1	3-phosphoglycerate is converted into 2-phosphoglycerate catalyzed by phosphoglycerate mutase	
154	PGAM2		
155	ENO1	2-phosphoglycerate is converted into phosphoenolpyruvate catalyzed by enolase	
156	ENO2		
157	ENO3		

158	PKLR	Phosphoenolpyruvate is converted into pyruvate and ATP is produced, catalyzed by pyruvate kinase	[Berg et al., 2002]
159	PKM2		
160	LDHAL6B	Pyruvate is converted to lactate catalyzed by lactate dehydrogenase	
161	LDHC		
162	LDHB		
163	LDHA		
<i>PYRUVATE TRANSFER</i>			
164	BRP44	Involved in the transfer of pyruvate inside mitochondria.	[Bricker et al., 2012]
165	BRP44L		
<i>FORMATION OF ACETYL COA</i>			
166	PDHA1	Pyruvate dehydrogenase complex catalyzes the overall conversion of pyruvate to acetyl CoA	[Berg et al., 2002]
167	PDHA2		
168	PDHB		

169	PDHX	Pyruvate dehydrogenase complex catalyzes the overall conversion of pyruvate to acetyl CoA	[Berg et al., 2002]
170	DLAT		
<i>TRICARBOXYLIC ACID CYCLE</i>			
171	CS	Citrate synthase catalyzes the synthesis of citrate from oxaloacetate and acetyl CoA	[Berg et al., 2002]
172	ACO2	Aconitase catalyzes the interconversion of citrate to isocitrate	
173	IDH1	Isocitrate dehydrogenase catalyze the oxidative decarboxylation of isocitrate to 2-oxoglutarate	
174	IDH2		
175	IDH3A		
176	IDH3B		
177	IDH3G		
178	OGDH	Catalyzes the overall conversion of 2-oxoglutarate to succinyl-CoA and CO ₂	
179	DLST		
180	DLD		

181	SUCLG1	Succinyl CoA synthetase catalyzes the conversion of succinyl CoA to succinate	[Berg et al., 2002]
182	SUCLG2		
183	SUCLA2		
184	SDHA	Part of Succinate dehydrogenase complex in oxidative phosphorylation in TCA cycle it catalyzes the oxidation of succinate to fumarate	
185	SDHB		
186	SDHC		
187	SDHD		
188	FH	Fumarase catalyzes the formation of L-malate from fumarate	
189	MDH2	Malate dehydrogenase catalyzes the reversible oxidation of malate to oxaloacetate	
<i>BETA OXIDATION OF FATTY ACIDS</i>			
190	SLC27A1	Readily converts the transported very long chain fatty acids to acyl-CoAs	[Houten & Wanders, 2010]
191	SLC27A2		
192	SLC27A3		

193	SLC27A4	Readily converts the transported very long chain fatty acids to acyl-CoAs	[Houten & Wanders, 2010]
194	SLC27A5		
195	SLC27A6		
196	ACSL1	Acyl-CoA synthetase activity for long chain free fatty acids and are also involved in the activation of fatty acids	
197	ACSL3		
198	ACSL4		
199	ACSL5		
200	ACSL6		
201	ACSS1	Acyl-CoA synthetase activity for short chain fatty acids	
202	ACSS2		
203	ACSS3		
204	ACSM1		

205	ACSM2A	Acyl-CoA synthetase activity for medium chain fatty acids	[Houten & Wanders, 2010]
206	ACSM2B		
207	ACSM3		
208	ACSM4		
209	ACSM5		
210	C10orf129	ACSM6 Acyl-CoA synthetase activity for medium chain fatty acids	
211	ACSBG1	Acyl-CoA synthetase activity for bubblegum family members	
212	ACSBG2		
213	FABP1	Fatty acid binding proteins involved in the import and export of fatty acids	
214	FABP2		
215	FABP3		
216	FABP4		
217	FABP5		

218	FABP6	Fatty acid binding proteins involved in the import and export of fatty acids	[Houten & Wanders, 2010]
219	FABP7		
220	FABP9		
221	FABP12		
222	CD36	Fatty acid translocase	
223	GOT2	Plasma membrane fatty acid binding protein	
224	CPT1A	Carnitine palmitoyl transferase converts an acyl-CoA into an acylcarnitine	
225	CPT1B		
226	CPT1C		
227	SLC25A20	Carnitine acylcarnitine translocase mediates acylcarnitine entry into mitochondria	
228	CPT2	Acylcarnitines are reconverted to their CoA esters by carnitine palmitoyltransferase 2	
229	CRAT	Free carnitine in the mitochondria can be converted into acyl carnitine by the action of carnitine acetyltransferase	
230	ACAD8	Involved in the catabolism of fatty acids	

231	ACAD10	Involved in the catabolism of fatty acids with significant activity towards branched chains	[Houten & Wanders, 2010]
232	ACAD11	May be involved in the catabolism of long chain fatty acids	
233	ACADL	Long chain hydroxyacyl-CoA dehydrogenase	
234	ACADVL	Very long chain acyl-CoAs are first catalyzed by long chain acyl-CoA dehydrogenase	
235	HADHA	Mitochondrial trifunctional protein catalyzes very long and long chain fatty acids	
236	HADHB		
237	ACADM	Fatty acids are metabolized for 3 to 4 cycles by the medium chain acyl-CoA dehydrogenase	
238	ECHS1	Enoyl-CoA hydratases, short chain, 1, mitochondrial	
239	HADH	Medium and short chain hydroxyacyl-CoA dehydrogenase	
240	ACAA2	Medium chain 3-ketoacyl-CoA thiolase	
241	ACADS	Short chain acyl-CoA dehydrogenase encoded by ACADS catalyzes the final 1 to 2 cycles	
242	ACADSB	Involved in the metabolism of short branched chain fatty acids	
243	DECR1	2,4 dienoyl CoA reductase 1 catalyzes the metabolism of polyunsaturated fatty acids	

ROS DEFENCE			
244	GCLC	Catalyzes the first step reaction which combines cysteine and glutamate to form glutamylcysteine	[Sabharwal & Schumacker, 2014]
245	GCLM	Catalyzes the first step reaction which combines cysteine and glutamate to form glutamylcysteine	
246	GSS	Catalyzes the formation of glutathione from glutamylcysteine by combining it with the glycine	
247	SLC25A11	May be involved in the transport of glutathione into the mitochondria	
248	SLC25A10		
249	SLC25A1		
250	SOD2	Dismutates the superoxide generated in the mitochondrial matrix to hydrogen peroxide	
251	SOD1	May be involved in the removal of superoxides in the inter membrane space of mitochondria	
252	SHC1	Could be involved in the generation of the hydrogen peroxide independent of superoxides in mitochondria	
253	BCKDHA	Involved in the catabolism of amino acids in mitochondria and may also be involved in the production of superoxides and hydrogen peroxide	
254	BCKDHB		
255	GPX1	Reduces hydrogen peroxide to water by using reducing equivalents from glutathione	

256	GSR	Reduces oxidized glutathione which can be re utilized by GPX1	[Sabharwal & Schumacker, 2014]
257	GPX4	Involved in the reduction of the lipid peroxides to their hydroxides	
258	PRDX3	Mitochondrial peroxiredoxin reduces hydrogen peroxide to water	
259	TXN2	Mitochondrial thioredoxin reduces peroxiredoxin to their superoxide scavenging state	
260	TXNRD2	Maintains thioredoxins in their reduced state using NADPH reducing equivalents	
261	MPV17	May have a role in the metabolism of reactive oxygen species	
262	MPV17L		
263	GLRX2	Involved in the control of mitochondrial protein glutathionylation	
264	GSTA1	Mitochondrial glutathione-S-transferases through glutathione conjugation or peroxide reduction detoxify harmful byproducts	
265	GSTA2		
266	GSTA4		
267	GSTP1		

APOPTOSIS			
268	APAF1	Binds CASP9 forming an apoptosome and activates it	[Tait & Green, 2010]
269	CASP3	Executioner caspases leading to apoptosis	
270	MAPK1	Inhibitors of CASP9 activity	
271	CASP7	Executioner caspases leading to apoptosis	
272	DIABLO	Acts as caspase activator by inhibiting the inhibitors of apoptotic proteins	
273	XIAP	X-linked inhibitor of apoptosis protein inhibits caspase activity by directly binding to CASP9, 3 and 7	
274	BCL2	Bcl-2 family member Anti-apoptotic proteins	
275	BCL2L1		
276	MCL1		
277	BAX	Bcl-2 family member propagating apoptosis	
278	BAK1		
279	BAD		

280	BIK	Bcl-2 family member propagating apoptosis	[Tait & Green, 2010]
281	BID		
282	BCL2L11	Bim Bcl-2 family member propagating apoptosis	
283	PMAIP1	Noxa Bcl-2 family member propagating apoptosis	
284	BBC3	Puma Bcl-2 family member propagating apoptosis	
285	TP53	Directly binds both BAK and BAX and activates them	
286	VDAC1	Voltage dependent anion channel forms part of permeability transition pore and is also involved in the takeup of calcium ions from the Endoplasmic reticulum	
287	VDAC2		
288	VDAC3		
289	SLC25A4	Adenine nucleotide translocator forms part of permeability transition pore	
290	SLC25A5		
291	SLC25A6		
292	APOPT1	Localizes to the mitochondria and stimulates the release of cytochrome c	

293	PPIF	Cyclophilin D forms part of permeability transition pore	[Tait & Green, 2010]
294	CYCS	Binds to apoptosis inducing factor 1 (APAF1) forming a structure called apoptosome	
295	ANP32A	Enhances APAF1 function	
296	CASP9	Initiator caspase recruited by Apoptosome	
297	CDK1	Can Inhibit CASP9 activity and also involved in the phosphorylation of DNM1L to increase fission	
298	DNM1	Recruited to mitochondria can induce cristae remodelling to release cytochrome c and subsequent apoptosis	
299	MAPK3	Inhibitors of CASP9 activity	
300	EIF3M	PCI domain containing protein 1 can negatively regulate CASP9 activity	
301	AIFM1	Mitochondria associated apoptosis inducing factor translocates to nucleus and degrades DNA	
302	PPIA	Cyclophilin A might work with ENDOG in a DNA degradation complex	
303	HTRA2	Mitochondrial serine protease induces cell death by inhibiting Inhibitors of apoptotic proteins	
IMPORT & SORTING			
304	TOMM20		

305	TOMM22	Outer membrane translocation, recognize presequences on the mitochondrial outer membrane	[Schmidt et al., 2010] & [Dolezal et al., 2006]
306	TOMM40	Outer membrane translocation, forms the outer membrane channel forming protein	
307	TOMM40L		
308	TOMM5	Outer membrane translocation, transports preprotein to the import pore formed by TOMM40	
309	TOMM70A	Outer membrane translocation, recognizes proteins with internal targeting signals	
310	TOMM6	Outer membrane translocation, required for the assembly and stability of the TOM complex	
311	TOMM7	Outer membrane translocation, required for the assembly and stability of the TOM complex	
312	TIMM50	Inner membrane translocation, guides the pre-proteins to the import channel formed by TIMM23	
313	TIMM17A	Inner membrane translocation, might influence the channel activity formed by the TIMM23	
314	TIMM17B	Inner membrane translocation, might influence the channel activity formed by the TIMM23	
315	TIMM23	Inner membrane translocation, forms the main channel of TIMM23 complex	
316	TIMM21	Inner membrane translocation, connects TOMM and TIMM complex and may assist in the release of preprotein from the TOMM complex	
317	HSPA9	Presequence translocase associated motor, binds to the preprotein and drives it into the matrix in association with other chaperones and also involved in the mediation of the interaction between	

		VDAC1 and Inositol-1,4,5-trisphosphate receptors	[Schmidt et al., 2010] & [Dolezal et al., 2006]
318	TIMM44	Presequence translocase associated motor, gets associated with the HSPA9 to drive proteins into the matrix	
319	DNAJC19	Presequence translocase associated motor, could stimulate the ATPase activity of HSPA9	
320	PAM16	Presequence translocase associated motor, controls the activity of DNAJC19	
321	GRPEL1	Presequence translocase associated motor, acts as a nucleotide exchange factor releasing the ADP from HSPA9	
322	GRPEL2	Presequence translocase associated motor, acts as a nucleotide exchange factor releasing the ADP from HSPA9	
323	TIMM9	Inner membrane carrier pathway, forms complex with TIMM10 and performs chaperone like activity in the intermembrane space	
324	TIMM10	Inner membrane carrier pathway, forms complex with TIMM9 and performs chaperone like activity in the intermembrane space	
325	TIMM8A	Inner membrane carrier pathway, forms complex with TIMM13 and also performs the transfer of inner membrane proteins	
326	TIMM8B	Inner membrane carrier pathway, forms complex with TIMM13 and also performs the transfer of inner membrane proteins	
327	TIMM13	Inner membrane carrier pathway, forms complex with TIMM8 and performs the transfer of inner membrane proteins	
328	TIMM22	Inner membrane carrier pathway, forms the core channel and inserts proteins into inner membrane	

329	CHCHD4	Intermembrane transport and assembly, acts as a receptor at the inter membrane space and recognizes incoming precursor proteins	[Schmidt et al., 2010] & [Dolezal et al., 2006]
330	GFER	Intermembrane transport and assembly, it is known to oxidize CHCHD4 and then the oxidized CHCHD4 acts as a receptor for the pre proteins and it also facilitates assembly of cytosolic Fe-S proteins	
331	SAMM50	Outer membrane sorting and assembly machinery, central component of SAMM complex and inserts beta barrel proteins into the outer membrane	
332	PMPCA	Presequence of pre-proteins are removed by proteolytic enzyme mitochondrial processing peptidase	
333	PMPCB	Presequence of pre-proteins are removed by proteolytic enzyme mitochondrial processing peptidase	
334	MIPEP	Secondary cleavage of the pre proteins processed by the mitochondrial processing peptidase	
335	IMMP1L	Inner membrane peptidase that cleaves hydrophobic sorting signal	
336	IMMP2L	Inner membrane peptidase that cleaves hydrophobic sorting signal	
FE-S CLUSTER BIOSYNTHESIS			
337	FXN	Functions in regulation of mitochondrial iron transport	[Rouault & Tong, 2005] and [Lill, 2009]
338	ISCU	Iron sulfur cluster assembly enzyme, Fe-S cluster intermediate is formed on it	
339	NFS1	The sulfide for Fe-S clusters originates from cysteine via the action of NFS1	

340	LYRM4	Assembles with NFS1	[Rouault & Tong, 2005] and [Lill, 2009]
341	SLC25A37	Functions as an essential iron importer	
342	SLC25A28	Mitochondrial iron transporter	
343	FDXR	Provide reducing equivalents to electron transfer chain and contribute to iron-sulfur cluster biogenesis	
344	FDX1	Small iron-sulfur protein, transfers electrons from NADPH to mitochondrial cytochrome P450	
345	FDX1L	Transfers electrons from NADPH to mitochondrial cytochrome P450	
346	HSCB	Mitochondrial iron-sulfur cluster co-chaperone	
347	GLRX5	Fe-S cluster transfer protein directly to the apoprotein	
348	NFU1	Protein assembles and transfers 4Fe-4S clusters to target apoproteins	
349	BOLA3	Role in the biogenesis of iron-sulfur clusters	
350	FTMT	Shows ferroxidase activity and binds iron	
351	ABCB7	Exports a sulfur product (X) from the mitochondrial iron sulfur cluster system to cytosol	
352	NUBP2	Required for the assembly of cytosolic iron-sulfur proteins	

353	NUBP1	Essential for both cytosolic iron-sulfur protein assembly and iron homeostasis	[Rouault & Tong, 2005] and [Lill, 2009]
354	CIAPIN1	Facilitates NUBP1 and NUBP2 assembly	
355	ISCA1	Involved in the biogenesis and assembly of iron-sulfur clusters	
356	ISCA2	Involved in the maturation of mitochondrial iron-sulfur proteins	
357	IBA57		
358	CIAO1	Cytosolic Fe-S cluster biogenesis and maturation	
359	FAM96A	Components of the cytosolic Fe/S protein assembly (CIA) machinery	
360	FAM96B		
361	MMS19	Cytosolic Fe/S protein assembly targeting factor	
362	NARF	Cytosolic Fe-S protein maturation	
REPLICATION AND TRANSCRIPTION			
363	SSBP1	Promotes helical destabilization for the DNA helicases and Polymerase gamma (POLG) to support mtDNA replication	[Falkenberg et al., 2007]
364	C10orf2	Mitochondrial DNA (mtDNA) helicase (TWINKLE) plays a important role in the maintenance of mtDNA	

365	RNASEH1	May have role in the removal of RNA primers at the origin of replication on heavy and light strands	[Falkenberg et al., 2007]
366	TOP1MT	Suggested to have a role in the removal of positive supercoils created by helicase activity	
367	TOP3A	May also be present in mitochondria with the role in the removal of positive supercoils during replication	
368	LIG3	Involved in the mitochondrial DNA replication and repair	
369	TERT	Role in the protection of mitochondrial integrity with a suggested role in mtDNA replication and/or repair	
370	TFAM	A key activator of mitochondrial transcription and also functions in replication and repair	
371	TFB1M	Regulates the stability of small subunit of mitochondrial ribosome by its methylation activity. It also plays a very important role in transcription	
372	TFB2M	Essential transcription factor involved in the transcription of mitochondrial genes	
373	NRF1	Regulates the expression of TFB1M and TFB2M which are two mitochondrial transcription factors	
374	NFE2L2		
375	PPARGC1A		
376	POLRMT	Provides primers for the initiation of replication of the mitochondria genome	

377	RMRP	RNA component of mitochondrial RNA processing endoribonuclease cleaves mitochondrial RNA at the priming site of mitochondrial DNA replication	[Falkenberg et al., 2007]
378	UNG	Prevent mutagenesis by eliminating uracil from DNA molecules	
379	OGG1	Responsible for the excision of 8-oxoguanine	
380	NTHL1	Involved in the repair of mismatches in DNA	
381	MUTYH	Involved in the mitochondrial DNA base excision repair	
382	APEX1		
383	APEX2		
384	ENDOG	Nuclease which processes the RNA primers for heavy strand replication also has a role in apoptosis where after release from the mitochondria induces nucleosomal DNA fragmentation	
385	POLG	Mitochondrial DNA polymerase, and also shows 3' to 5' exonuclease activity and ensure faithful replication	
386	POLG2	Acts as catalytic subunit of mitochondrial DNA polymerase	
387	MTERF1	Mitochondrial transcription termination factor	
388	MTERF2		

389	MTERF3		[Falkenberg et al., 2007]
390	MTERF4		
391	TRMT10C	Cleaves the 5' terminus of mitochondrial tRNAs	
392	KIAA0391	Human mitochondrial tRNA processing enzyme	
393	HSD17B10		
394	ELAC2	Endolytic processing the 3' end of tRNA	
395	TRNT1	Mitochondrial CCA adding enzyme, adds CCA sequence to the 3' end of tRNA	
396	DGOUK	Involved in the phosphorylation of recycled deoxyribonucleosides in mitochondria specific for guanosine, adenosine and inosine	
397	TK2	Involved in the phosphorylation of recycled deoxyribonucleosides in mitochondria specific for thymidine, cytidine and uridine	
398	NTM5	Pyrimidine 5', 3' deoxyribonucleotidase that dephosphorylates dTMP	
399	AK3	Phosphorylates the deoxyribonucleoside monophosphates specifically on dAMP	
400	AK4		
401	CMPK2		

402	NME4	Shows mitochondrial nucleoside diphosphate kinase activity	[Falkenberg et al., 2007]
403	SLC25A19	Transports thiamine pyrophosphates into mitochondria	
404	SLC25A33	Mitochondrial pyrimidine nucleotide carrier	
405	SLC29A1	Equilibrative nucleoside transporter 1 imports recycled deoxyribonucleosides from cytoplasm into mitochondria	
406	NME3	Shows mitochondrial nucleoside diphosphate kinase activity	
407	NME6		
408	TRMT11	Shows posttranscriptional modifications activity in the human mitochondrial tRNAs	
409	TRMT112		
410	DUS2L		
411	TRMT1		
412	PUS1		
413	RPUSD2		
414	RPUSD4		

415	GTPBP3	Shows posttranscriptional modifications activity in the human mitochondrial tRNAs	[Falkenberg et al., 2007]
416	MTO1		
417	TRMU		
418	QTRT1		
419	QTRTD1		
420	TRMT5		
421	YRDC		
422	OSGEPL1		
423	TRIT1		
424	CDK5RAP1		
425	CDKAL1		
426	PUS3		
427	NSUN2		

428	TRMT2B	Shows posttranscriptional modifications activity in the human mitochondrial tRNAs	[Falkenberg et al., 2007]	
429	TRUB2			
430	TRMT6			
431	TRMT61B			
432	CREB1			Promotes the transcription of mitochondrial genes
433	SLC25A3			Involved in the transport of phosphate into the mitochondrial matrix
434	MTPAP			Involved in the polyadenylation of mitochondrial tRNAs, rRNAs and mRNAs
435	RRM2B	Required for the de novo deoxyribonucleotide synthesis in non-proliferating cells supplying dNTPs to mtDNA synthesis		
TRANSLATION				
436	RARS2	Involved in the specific attachment of arginine amino acid to its cognate tRNA		
437	CARS2	Involved in the specific attachment of cysteine amino acid to its cognate tRNA		
438	EARS2	Involved in the specific attachment of glutamic acid amino acid to its cognate tRNA		

439	IARS2	Involved in the specific attachment of isoleucine amino acid to its cognate tRNA	[Suzuki et al., 2011] [Kenmochi et al., 2001] and [Smits et al., 2010]
440	LARS2	Involved in the specific attachment of leucine amino acid to its cognate tRNA	
441	MARS2	Involved in the specific attachment of methionine amino acid to its cognate tRNA	
442	WARS2	Involved in the specific attachment of tryptophan amino acid to its cognate tRNA	
443	YARS2	Involved in the specific attachment of tyrosine amino acid to its cognate tRNA	
444	VARS2	Involved in the specific attachment of valine amino acid to its cognate tRNA	
445	AARS2	Involved in the specific attachment of alanine amino acid to its cognate tRNA	
446	NARS2	Involved in the specific attachment of asparagine amino acid to its cognate tRNA	
447	DARS2	Involved in the specific attachment of aspartic acid amino acid to its cognate tRNA	
448	GARS	Involved in the specific attachment of glycine amino acid to its cognate tRNA	
449	HARS2	Involved in the specific attachment of histidine amino acid to its cognate tRNA	
450	KARS	Involved in the specific attachment of lysine amino acid to its cognate tRNA	
451	FARS2	Involved in the specific attachment of phenylalanine amino acid to its cognate tRNA	

452	PARS2	Involved in the specific attachment of proline amino acid to its cognate tRNA	<p>[Suzuki et al., 2011]</p> <p>[Kenmochi et al., 2001]</p> <p>and</p> <p>[Smits et al., 2010]</p>
453	SARS2	Involved in the specific attachment of serine amino acid to its cognate tRNA	
454	TARS2	Involved in the specific attachment of threonine amino acid to its cognate tRNA	
455	QRSL1	Involved in the biosynthesis of glutamyl-tRNA	
456	PET112		
457	GATC		
458	MTFMT	Involved in the specific attachment of methionine amino acid to its cognate tRNA	
459	TUFM	Involved in the elongation and termination phases of the translation process	
460	GFM2	Involved in the elongation and termination phases of the translation process may also be involved in the ribosome recycling	
461	GFM1	Involved in the elongation and termination phases of the translation process	
462	TSFM	Involved in the elongation and termination phases of the translation process	
463	MTRF1	Involved in the mitochondrial translation termination, may act as a release factor	
464	MTRF1L		

465	MRRF	Acts as a mitochondrial ribosome recycling factor during translation process	[Suzuki et al., 2011] [Kenmochi et al., 2001] and [Smits et al., 2010]
466	PTCD3	Associates with mitochondrial small ribosomal subunit and regulates translation	
467	MT-TA	mitochondrially encoded tRNA alanine	
468	MT-TC	mitochondrially encoded tRNA cysteine	
469	MT-TD	mitochondrially encoded tRNA aspartic acid	
470	MT-TE	mitochondrially encoded tRNA glutamic acid	
471	MT-TF	mitochondrially encoded tRNA phenylalanine	
472	MT-TG	mitochondrially encoded tRNA glycine	
473	MT-TH	mitochondrially encoded tRNA histidine	
474	MT-TI	mitochondrially encoded tRNA isoleucine	
475	MT-TK	mitochondrially encoded tRNA lysine	
476	MT-TL1	mitochondrially encoded tRNA leucine 1 (UUA/G)	
477	MT-TL2	mitochondrially encoded tRNA leucine 2 (CUN)	

478	MT-TM	mitochondrially encoded tRNA methionine	[Suzuki et al., 2011] [Kenmochi et al., 2001] and [Smits et al., 2010]
479	MT-TN	mitochondrially encoded tRNA asparagine	
480	MT-TP	mitochondrially encoded tRNA proline	
481	MT-TQ	mitochondrially encoded tRNA glutamine	
482	MT-TR	mitochondrially encoded tRNA arginine	
483	MT-TS1	mitochondrially encoded tRNA serine 1 (UCN)	
484	MT-TS2	mitochondrially encoded tRNA serine 2 (AGU/C)	
485	MT-TT	mitochondrially encoded tRNA threonine	
486	MT-TV	mitochondrially encoded tRNA valine	
487	MT-TW	mitochondrially encoded tRNA tryptophan	
488	MT-TY	mitochondrially encoded tRNA tyrosine	
489	MRPL1	Mitoribosome which forms a part of mitochondrial translation machinery	
490	MRPL2		

491	MRPL3	Mitoribosome which forms a part of mitochondrial translation machinery	[Suzuki et al., 2011] [Kenmochi et al., 2001] and [Smits et al., 2010]
492	MRPL4		
493	MRPL9		
494	MRPL10		
495	MRPL11		
496	MRPL12		
497	MRPL13		
498	MRPL14		
499	MRPL15		
500	MRPL16		
501	MRPL17		
502	MRPL18		
503	MRPL19		

504	MRPL20	Mitoribosome which forms a part of mitochondrial translation machinery	[Suzuki et al, 2011] [Kenmochi et al., 2001] and [Smits et al., 2010]
505	MRPL21		
506	MRPL22		
507	MRPL23		
508	MRPL24		
509	MRPL27		
510	MRPL28		
511	MRPL30		
512	MRPL32		
513	MRPL33		
514	MRPL34		
515	MRPL35		
516	MRPL36		

517	MRPL37	Mitoribosome which forms a part of mitochondrial translation machinery	[Suzuki et al, 2011] [Kenmochi et al, 2001] and [Smits et al, 2010]
518	MRPL38		
519	MRPL39		
520	MRPL40		
521	MRPL41		
522	MRPL42		
523	MRPL43		
524	MRPL44		
525	MRPL45		
526	MRPL46		
527	MRPL47		
528	MRPL48		
529	MRPL49		

530	MRPL50	Mitoribosome which forms a part of mitochondrial translation machinery	[Suzuki et al., 2011] [Kenmochi et al., 2001] and [Smits et al., 2010]
531	MRPL51		
532	MRPL52		
533	MRPL53		
534	MRPL54		
535	MRPL55		
536	MRPL57		
537	MRPS10		
538	MRPS11		
539	MRPS12		
540	MRPS14		
541	MRPS15		
542	MRPS16		

543	MRPS17	Mitochondrion which forms a part of mitochondrial translation machinery	[Suzuki et al., 2011] [Kenmochi et al., 2001] and [Smits et al., 2010]
544	MRPS18A		
545	MRPS18B		
546	MRPS18C		
547	MRPS2		
548	MRPS21		
549	MRPS22		
550	MRPS23		
551	MRPS24		
552	MRPS25		
553	MRPS26		
554	MRPS27		
555	MRPS28		

556	DAP3	Mitoribosome which forms a part of mitochondrial translation machinery	[Suzuki et al., 2011] [Kenmochi et al., 2001] and [Smits et al., 2010]
557	MRPS30		
558	MRPS31		
559	MRPS33		
560	MRPS34		
561	MRPS35		
562	MRPS36		
563	MRPS5		
564	MRPS6		
565	MRPS7		
566	MRPS9		
567	MTIF3	Translation initiation factor could assist the mRNA to bind to rRNAs	
568	MTIF2	Translation initiation factor could assist the tRNA to bind to rRNAs	

569	TACO1	Translational activator of complex IV subunit	[Suzuki et al., 2011] [Kenmochi et al., 2001] and [Smits et al., 2010]
570	LRPPRC	Might play a role in the translation and stability of COX subunits	
571	RNASEL	Modulate the stability of mitochondrial mRNAs by interacting with MTIF2	
572	LONP1	Involved in the post translational quality control, has re-solubilization activity of protein aggregates	
573	CLPP		
574	CLPX	Quality control of inner membrane proteins	
575	PHB	Involved in the post translational quality control, stabilizes mitochondrially synthesized proteins	
576	PHB2		
577	OXA1L	May have a role in the insertion of proteins into inner membrane and also a complex V assembly factor	
578	ATAD3A	May interact with mitochondrial proteins and is required mitochondrial protein synthesis	
579	ATAD3B		
580	MPV17L2	May be involved in the biogenesis of mitochondrial ribosomes	
581	DHX30		

582	DDX28		
MITOCHONDRIAL DYNAMICS			
583	MFN1	Involved in the mitochondrial fusion, mitofusins dimerize resulting in the tethering of the outer membranes of the fusing mitochondria.	[Palmer et al., 2011], [Hales, 2010] and [Ranieri et al., 2013]
584	MFN2		
585	OPA1	Involved in the mitochondrial fusion, initiates inner membrane fusion	
586	PHB2	Involved in the mitochondrial fusion, scaffold proteins coordinate stability of the OPA1	
587	STOML2		
588	PINK1	Involved in the mitochondrial fusion, PINK1 phosphorylates PARK2 and consequently PARK2 induced ubiquitination of mitofusins	
589	PARK2	Involved in the mitochondrial fusion, PARK2 induces ubiquitination of mitofusins	
590	OPA3	Involved in the mitochondrial fusion, interacts with MFN1 and involved in mitochondrial fragmentation	
591	PARL	Involved in the mitochondrial fusion, regulates the cleavage of OPA1	
592	SPG7		

593	AFG3L2	Involved in the mitochondrial fusion, known to maintain the OPA1 isoforms	[Palmer et al., 2011], [Hales, 2010] and [Ranieri et al., 2013]
594	OMA1	Involved in the mitochondrial fusion, known to induce proteolytic inactivation of OPA1	
595	YME1L1	Involved in the mitochondrial fusion, known to cleave OPA1	
596	PLD6	Involved in the mitochondrial fusion, promotes mitofusin-mediated fusion	
597	MARCH5	Involved in the mitochondrial fusion and fission, control of mitochondrial morphology by regulating MFN2 and DNM1L	
598	TRAP1	Involved in the mitochondrial fission, known to regulate fission proteins DNM1L and MFF	
599	DNM1L	Involved in the mitochondrial fission, mediates the division of mitochondria	
600	MFF	Involved in the mitochondrial fission, suggested to have roles in recruiting DNM1L	
601	MIEF1		
602	MIEF2		
603	FIS1	Involved in the mitochondrial fission, facilitates binding and assembly of DNM1L	
604	MTFP1	Involved in the mitochondrial fission, role in mitochondrial fragmentation and is dependent on DNM1L expression	
605	GDAP1	Involved in the mitochondrial fission, know to have a role in the mitochondrial fragmentation	

606	SH3GLB1	Involved in the mitochondrial fission, proposed to be involved in the lipid remodeling of the outer membrane during fission	
607	PKIA	Involved in the mitochondrial fission, is known to inhibit GTPase activity of DNM1L	
608	BECN1	Involved in the mitophagy, involved in the initiation of autophagy	[Thomas & Gustafsson, 2013]
609	AMBRA1	Involved in the mitophagy, translocates to the mitochondria and facilitate phagophore formation	
610	BNIP3	Involved in the mitophagy, cause permeabilization of the mitochondrial membrane and also acts as a proapoptotic factor	
611	BNIP3L	Involved in the mitophagy, cause permeabilization of the mitochondrial membrane and also regulate mitophagy	
612	MAP1LC3A	Involved in the mitophagy, interacts with BNIP3 and BNIP3L to remove mitochondria via autophagy	
613	GABARAP	Involved in the mitophagy, interacts with BNIP3 and BNIP3L to remove mitochondria via autophagy	
614	SQSTM1	Involved in the mitophagy, recruited to mitochondria and binds mitochondrial substrates on the autophagosomes	
615	RHOT1	Involved in the mitophagy, tethers mitochondria to the tubulin network but phosphorylation by PINK1 results in the detachment of mitochondria	
616	RHOT2		
617	KIF5B	Involved in the mitochondrial movement, have role in the mitochondrial distribution in neurons	

618	KIF1B	Involved in the mitochondrial movement, have role in the mitochondrial distribution in neurons	[Chen & Chan, 2009]
619	DYNLL1	Involved in the mitochondrial movement, have role in the retrograde mitochondrial movement	
620	SYBU	Involved in the mitochondrial movement, have a role in linking the mitochondria to KIF5B	
621	TRAK1	Involved in the mitochondrial movement, acts as an adapter linking kinesin-1 to mitochondria	
622	TRAK2		
623	MSTO1	Involved in the regulation of mitochondrial distribution and morphology	
CALCIUM TRAFFICKING			
624	MCU	Involved in the accumulation of calcium ions in the matrix through ion impermeable inner mitochondrial membrane	[Rizzuto et al., 2012]
625	SLC24A6	Involved in the calcium homeostasis by counteracting the calcium accumulation in the mitochondria	
626	LETM1	Might act as calcium ion and hydrogen ion antiporter exchanging hydrogen for calcium	
627	MICU1	Regulates the mitochondrial calcium uniporter by inhibiting and permitting the calcium depending upon the cytosolic calcium concentrations	
628	EFHA1		

629	CCDC90A	Mitochondrial calcium uniporter regulator 1 required for the MCU dependent calcium uptake by the mitochondria	
630	EFHA2	Regulates the mitochondrial calcium uniporter by inhibiting and permitting the calcium depending upon the cytosolic calcium concentrations	
631	CCDC109B	Forms an important component of mitochondrial calcium uniporter with MCU	
632	C22orf32		
633	ITPR3	Component of the Inositol-1,4,5-trisphosphate receptors channels used for the fluxes of Ca ²⁺ from ER to mitochondria	
634	ITPR2		
635	ITPR1		
636	TCHP	Involved in the regulation of ER mitochondria juxtaposition	
637	SIGMAR1	Stabilises the Inositol-1,4,5-trisphosphate receptors and ensures proper Ca ²⁺ fluxes	
638	PACS2	Involved in the control of ER mitochondria appositions	
639	PML	Regulates Inositol-1,4,5-trisphosphate receptor mediated Ca ²⁺ release from the ER	
HEME BIOSYNTHESIS			
640	ALAS2		

641	ALAS1	Catalyzes the reaction in which glycine and succinyl CoA from TCA cycle condenses to form aminolevulinatate (ALA) and CO ₂	[Dailey, 1997]
642	ALAD	ALA dehydratase catalyzes the reaction where two molecules of ALA condenses to form monopyrrole porphobilinogen (PBG)	
643	HMBS	Hydroxymethylbilane synthase catalyzes head to tail condensation of four PBG and subsequent deamination to form a linear tetrapyrrole, Hydroxymethylbilane	
644	UROS	Uroporphyrinogen III synthase catalyzes the linear tetrapyrrole molecule is cyclized or rearranged	
645	UROD	Uroporphyrinogen III decarboxylase catalyzes stepwise decarboxylation of the Uroporphyrinogen III forming Coproporphyrinogen III	
646	CPOX	Coproporphyrinogen III is transported to mitochondria and in the presence of coproporphyrinogen III oxidase it is oxidatively decarboxylated	
647	PPOX	Protoporphyrinogen oxidase converts Protoporphyrinogen IX to Protoporphyrin IX	
648	FECH	Ferrochelatase catalyzes the step involving the addition of Ferrous iron into the protoporphyrin IX to form the protoheme IX	
CARDIOLIPIN BIOSYNTHESIS			
649	CDS1	Converts phosphatidic acid to cytidine diphosphate diacylglycerol	[Houtkooper & Vaz, 2008]
650	PGS1	Phosphatidylglycerol synthase converts cytidine diphosphate diacylglycerol to phosphatidylglycerol phosphate	
651	PTPMT1	Phosphatidylglycerophosphatase activity removes phosphate from phosphatidylglycerol phosphate to	

		form phosphatidylglycerol	[Houtkooper & Vaz, 2008]
652	CRLS1	Catalyzes the condensation of cytidine diphosphate diacylglycerol and phosphatidylglycerol forming a nascent cardiolipin	
653	TAZ	Converts the nascent cardiolipin to mature cardiolipin	
UREA CYCLE			
654	CPS1	Carbamoyl phosphate synthetase catalyzes the formation of carbamoyl phosphate	[Berg et al., 2002]
655	OTC	Ornithine transcarbamoylase catalyzes the formation of citrulline, carbamoyl phosphate combines with ornithine to form citrulline	
656	ASS1	Argininosuccinate synthetase catalyzes the formation of argininosuccinate	
657	ASL	Argininosuccinate lyase catalyzes the formation of arginine and fumarate	
658	ARG1	Arginase catalyzes the formation of Urea	
659	ARG2		